95-02

NATIONAL WATER RESEARCH INSTITUTE

INSTITUT NATIONAL de RECHERCHE sur les EAUX

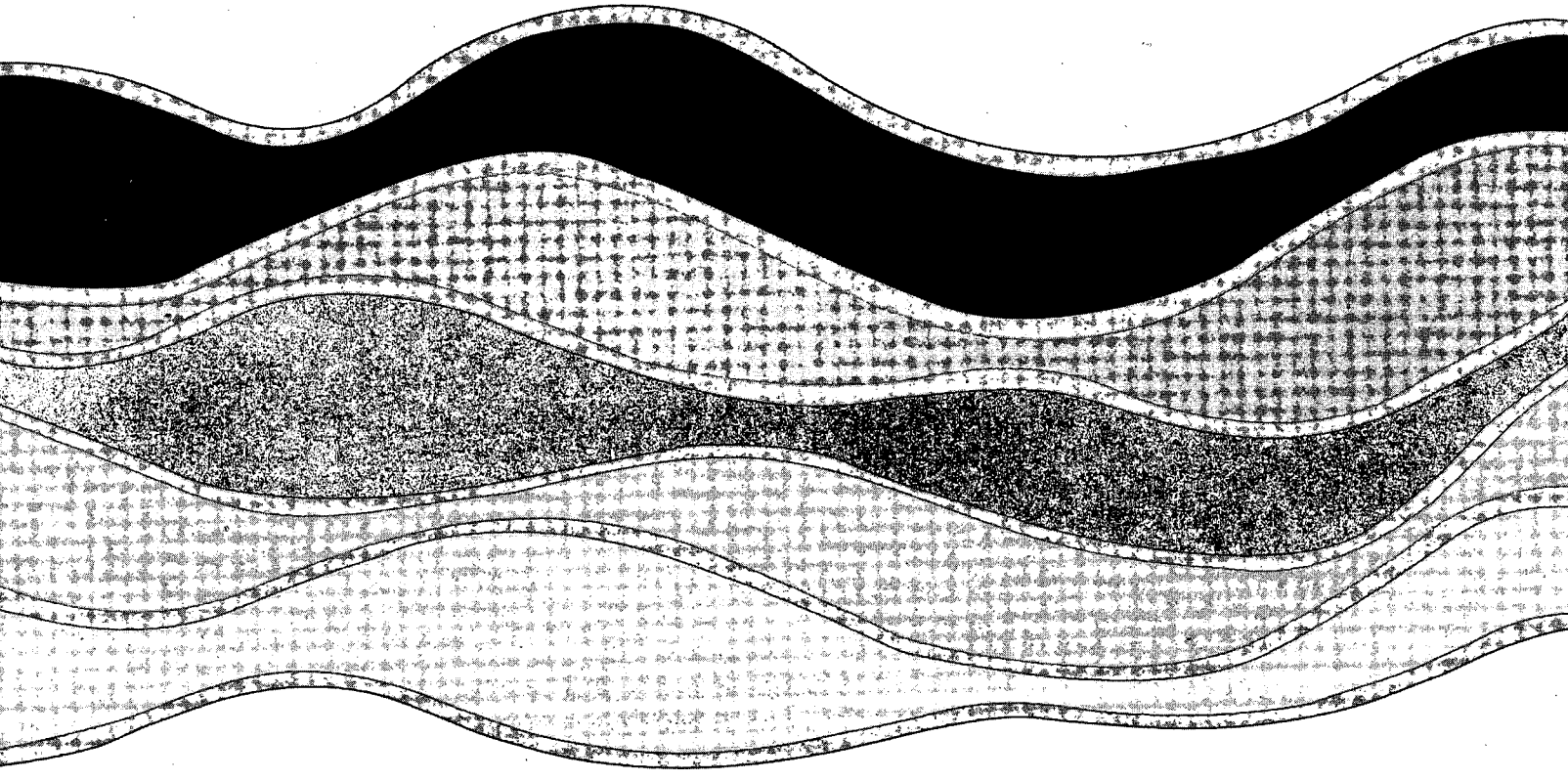

EVALUATION OF PRIMARY AND SECONDARY CONSOLIDATION OF HAMILTON HARBOUR AND LAKE ONTARIO SEDIMENTS DUE TO *IN-SITU* CAPPING

A.J. Zeman and T.S. Patterson

NWRI Contribution No. 95-02

EVALUATION OF PRIMARY AND SECONDARY CONSOLIDATION OF HAMILTON HARBOUR AND LAKE ONTARIO SEDIMENTS DUE TO *IN-SITU* CAPPING

A.J. Zeman and T.S. Patterson

Aquatic Ecosystem Restoration Branch
National Water Research Institute
867 Lakeshore Road, P.O. Box 5050
Burlington, Ontario L7R 4A6

NWRI Contribution No. 95-02

ABSTRACT

The magnitudes and rates of primary consolidation due to the load applied by a 0.5-m thick sand cap, which rests on a very compressible fine-grained sediment substratum, have been analyzed for the proposed capping site in Hamilton Harbour, for two other locations in the Harbour, and for an adjacent location in Lake Ontario. Large oedometer tests with pore pressure measurements were used to determine void ratio-effective stress and void ratio-permeability relationships. Primary consolidation due to the dissipation of excess pore pressure has been analyzed using the classical (Terzaghi) consolidation analysis, the finite strain analysis, and a numerical analysis, using a computer code CONSOL, in which the governing (Terzaghi's) differential equation is approximated by a finite-difference discretization. It is shown that both the Terzaghi and the finite strain methods predict identical ultimate settlements of about 0.2 m at the proposed capping site. In general, substantially faster rates of consolidation are predicted by the finite strain theory than by the classical theory. The results obtained by CONSOL are in a reasonable agreement with the two other methods. The predicted time to reach 95% of primary consolidation at the capping site ranges from about 8 to 11 days.

The effect of secondary consolidation was investigated by examining the dial deflection vs. time consolidation curves from standard consolidation tests and from the results of a creep test carried out at stresses of 5 and 10 kPa. Although the determination of the coefficient of secondary compression was found highly variable, the results indicate that the sediments are of very high secondary compressibility and, for this reason, the amount of secondary consolidation could amount up to an additional 0.2 m over the period of 20 years.

This secondary settlement and associated pore water extrusion will be, however, significantly reduced due to the gradual formation of a low-permeability layer of fresh sediment deposited onto the top of the cap.

Field monitoring by a set of settlement gauges is proposed for the capping demonstration project in order to obtain an empirical control on the laboratory and analytical results presented in this report.

TABLE OF CONTENTS

LIST OF FIGURES

15 Dial deflection vs. time
Sample LO-90
a. 5 kPa
b. 10 kPa
c. 20 kPa
d. 40 kPa
e. 80 kPa
f. 160 kPa
g. 320 kPa

16 Sample HH-1-90
a. 5 kPa
b. 10 kPa
c. 20 kPa
d. 40 kPa
e. 80 kPa
f. 160 kPa

17 Sample HH-2-90
a. 5 kPa
b. 10 kPa
c. 20 kPa
d. 40 kPa
e. 80 kPa
f. 160 kPa
g. 320 kPa

18 Sample HH-1-93
a. 5 kPa
b. 10 kPa
c. 20 kPa
d. 40 kPa
e. 80 kPa
f. 160 kPa
g. 320 kPa

19 Coefficient of consolidation vs. pressure
a. Sample LO-90
b. Sample HH-1-90
c. Sample HH-2-90
d. Sample HH-1-93

20 Degree of consolidation vs. time, Sample HH-1-93, Terzaghi's theory
a. H = 1 m
b. H = 2 m

21 Degree of consolidation vs. time, Sample HH-1-93, finite strain theory
a. H = 1 m
b. H = 2 m

Part B: Secondary Consolidation

22 Coefficient of secondary compression vs. consolidation pressure
   a. Sample LO-90
   b. Sample HH-1-90
   c. Sample HH-2-90
   d. Sample HH-1-93

23 Rowe Cell creep test, applied pressure 5 kPa
   a. Void ratio vs. elapsed time
   b. Void ratio vs. elapsed time (log scale)
   c. Void ratio vs. log of elapsed time

24 Rowe Cell creep test, applied pressure 10 kPa
   a. Void ratio vs. elapsed time
   b. Void ratio vs. elapsed time (log scale)
   c. Void ratio vs. log of elapsed time

LIST OF TABLES

1.0 INTRODUCTION

The purpose of this report is to evaluate the relative importance of primary and secondary consolidation that may occur in recently deposited offshore sediments as a result of subaqueous capping. The magnitude and rate of primary consolidation of Hamilton Harbour and Lake Ontario samples due to subaqueous capping have previously been analyzed (Zeman, 1992). In the present report, the consolidation test data for the same samples, as well as the data for two samples taken in 1993 at the proposed capping site in Hamilton Harbour, are examined.

Primary consolidation is due to the extrusion of water in sediment voids and associated dissipation of excess pore pressure, u. The end of primary consolidation is reached when u becomes zero. Secondary consolidation is due to the continued readjustment of sediment particles under sustained loading at the end of primary consolidation. As pointed out by Das (1983), primary and secondary consolidation are in fact continuous processes that can be jointly investigated by various viscoelastic models. This approach has not been attempted within the scope of this report.

Consolidation behaviour of very soft contaminated sediments due to subaqueous capping is investigated in connection with the proposed pilot-scale project in Hamilton Harbour (Zeman, 1993). Results of consolidation analysis are used for estimates of pore water released from the sediment into the cap. Reliable estimates of both the primary and secondary consolidation of very soft contaminated sediments are also desirable for the evaluation of long-term cap stability against major storm events and the effects of ship traffic over the cap. The surface elevation of the cap will reflect not only sediment erosion or deposition but also the settlement of the underlying highly-compressible sediments. Thus it is important to distinguish elevation changes due to any possible sand transport, accumulation of any new fine-grained sediment on the cap, and cap surface settlements occurring as a result of primary and secondary consolidation.

2.0 SAMPLING AND TESTING METHODS

Previous investigations (Mudroch and Zeman, 1975) have shown that fine-grained sediments in Hamilton Harbour have anomalous geotechnical properties probably due to the presence of large amounts of iron. For this reason, consolidation behaviour was investigated not only for Hamilton Harbour

sediments, but also for Lake Ontario basin sediments. Large box cores were collected at sites HH-1-90, HH-2-90 and HH-1-93 (Fig. 1) in Hamilton Harbour, and at site LO-90 (Fig. 2) in Lake Ontario. In addition, a gravity sediment core was collected at each site for logging and subsequent geotechnical laboratory testing, including six gravity sediment cores taken in and around the proposed capping site, which were collected with a modified Kajak-Brinkhurst (K-B) corer with a 3-in. (7.6-cm) dia. plastic liner.

Consolidation behaviour of the sediments was investigated by large oedometer tests carried out in the Rowe Cell test apparatus (Rowe and Barden, 1966). Each specimen was saturated under back pressure equivalent in magnitude to the water depth at the respective sample location. Back pressures of 130 kPa, 176 kPa, 206 kPa, and 313 kPa were used for samples HH-1-93, HH-1-90, HH-2-90 and LO-90 respectively. After saturation, the consolidation stage of the test was carried out. Load increments of 5, 10, 20, 40, 80, 160 and 320 kPa were used, followed by unloading to 80 and 10 kPa. The oedometer creep test was carried out at stresses of 5 and 10 kPa. The test procedures are described in detail in reports by Golder Associates (1991 and 1994). Particle size analyses were performed using the sieve and Sedigraph method (Duncan and Lahaie 1979), with detailed results to be found in Dalton (1991) and Patterson (1993). Undrained shear strength of the sediments was determined by the fall-cone method (Hansbo, 1957). Water content determinations were carried out according to the ASTM D2216-80 Standard. Specific gravity determinations were carried out according to the ASTM D8854-83 Standard using de-aired kerosene as the liquid.

3.0 SITE (SAMPLE) CONDITIONS

Locations of the Hamilton Harbour sites are shown in Fig. 1. The Lake Ontario sample site for LO-90 is shown in Fig. 2. The proposed capping site, including contours and sample locations, is shown in Fig. 3.

3.1 Site LO-90

This site is at the same location as Moses Station No. 14, which was previously sampled and tested by Vanderpost (1972). On the basis of particle distribution measured at 10-cm intervals on subsamples (Fig. 4a), the sediment is clayey silt throughout, with the silt fraction varying from about 60% to 80%, and the clay fraction varying from about 20% to 40%. The natural water content, w, decreases in a parabolic fashion within the upper 30 cm from about 250% to 75%, and further below decreases slightly with depth to about 60% towards the end of the core (Fig. 6a). Fall-cone shear strength values,

s_u, increase with depth from the near zero value to about 5 kPa at the end of the core (Fig. 12a). The sediment is of very soft consistency throughout (s_u < 12 kPa).

3.2 Site HH-1-90

The sediment is texturally clayey silt to silty clay. The silty fraction predominates in the upper 10 cm and below the depth of 60 cm (Fig. 4b). The natural water content measurements (Fig. 5b) decrease in a parabolic fashion from about 360% to about 145% at 40 cm below the surface. Further below, the w values increase with depth in the interval 45 cm to 60 cm from about 145% to 250%, and then decrease slightly to about 225% at 75 cm. The s_u measurements (Fig. 6b) increase linearly with depth, having some variability, from near zero values to about 3 kPa. Somewhat lower s_u values measured toward the bottom of the core may be due to sediment disturbance during sampling.

3.3 Site HH-2-90

The vertical trend of particle size distribution (Fig. 4c) is quite similar to Site HH-1-90. The sediment is clayey silt within the uppermost 15 cm of the core, silty clay from 15 to 70 cm and clayey silt from 70 to 80 cm. Natural water content at the sediment-water interface is about 430%, decreases rapidly with depth to about 200% at 20 cm, remains approximately constant from 20 cm to 65 cm, and increases to about 275% toward the end of the core (Fig. 5c). The overall trend of w values is similar to Core HH-1-90, with the exception of higher values near the sediment-water interface. The shear strength profile (Fig. 6c) is also quite similar to Core HH-1-90, with values ranging from near zero at the sediment-water interface, increasing irregularly with depth to about 3 kPa at 65 cm. Lower s_u values obtained between 65 cm and 80 cm are likely caused by sediment disturbance during sampling.

3.4 Sample HH-1-93

Sample HH-1-93 was collected within the proposed capping site. Specific gravity and moisture content measurements for the sample are available in Golder Associates (1994). Grain size, shear strength and moisture content data were measured on subsamples from six gravity cores taken in and around the capping site within about 100 m from Sample HH-1-93 (Fig. 3 and Figs. 7a to f). Although all cores differ somewhat from each other, the top 30 cm interval for all cores is generally silty clay, changing to clayey silt below this approximate depth. Sand pockets appear without any apparent pattern in a total of three cores, between 40 cm and 100 cm. Natural water content ranges from about 480% at the top layer (Fig. 7c -

Core 2X) to as low as 25% at sand pockets (Figs. 7a and 7d). Shear strength profiles were also quite consistent for all cores, ranging from close to zero values to about 2 kPa. Sand pockets were the exception, where shear strength rose as high as 32.7 kPa (Fig. 7d).

PART A: PRIMARY CONSOLIDATION

4.0 THEORY

4.1 Terzaghi's Governing Equation

The usual form of Terzaghi's governing equation (Terzaghi and Peck, 1968) is

$$\frac{\delta u}{\delta t} = C_v \frac{\delta^2 u}{\delta x^2} \tag{1}$$

where u is the excess pore pressure and C_v is the coefficient of consolidation. The independent variables are time, t, and the vertical space coordinate, x. The relationship between the degree of consolidation, U, and the length of time, t, elapsed from the application of load is

$$U\,\% = f(T_v) \tag{2}$$

$$t = \frac{H^2\, T_v}{C_v} \tag{3}$$

where H is the thickness of a singly-drained layer and T_v is the dimensionless time factor. The relationship between U and T_v has been tabulated and plotted for principal practical situations (Terzaghi and Peck, 1968; Das, 1983).

Expected ultimate settlement due to primary consolidation, S (∞), can be computed from the piecewise relationship for individual sublayers (Terzaghi and Peck, 1968)

$$S(\infty) \approx \sum_{i=1}^{n} m_{vi}\, \Delta\sigma'_i\, \Delta x_i \tag{4}$$

where m_v is the coefficient of volume compressibility, $\Delta\sigma'$ is the change in vertical effective stress due to applied load, Δx_i is the sublayer height and n is the number of sublayers used during summation.

4.2 Finite-Difference Solution of Terzaghi's Governing Equation

A computer code CONSOL Version 2.0 (Duncan et al. 1988) was used to calculate magnitudes and rates of consolidation settlement. In the program, $S(\infty)$ is computed by applying Eq. (4). An implicit finite-difference approximation is used to calculate the rate of consolidation settlement and the rate of dissipation of excess pore pressures. In comparison with a chart solution, a numerical solution permits variations in the changes of stress with depth, and variations in sediment properties with depth to be taken into account as input parameters. The finite-difference equations used by CONSOL to approximate Eq. (1) are given in Duncan et al. (1988) and they are not repeated here. The required input parameters: total unit weight, γ, void ratio, e, compression index, C_c, and coefficient of consolidation, C_v, were obtained from the available consolidation test results and core geotechnical profiles.

4.3 Finite Strain Governing Equation

The governing equation for finite strain consolidation (Gibson et al., 1967; Gibson et al., 1981) is

$$\left(\frac{\gamma_s}{\gamma_w}-1\right)\frac{d}{de}\left[\frac{k}{(1+e)}\right]\frac{\partial e}{\partial z}+\frac{\partial}{\partial z}\left[\frac{k}{\gamma_w(1+e)}\frac{d\sigma'}{de}\frac{\partial e}{\partial z}\right]+\frac{\partial e}{\partial t}=0 \quad (5)$$

where γ_s is the unit weight of solids, γ_w is the unit weight of water, e is the void ratio, z is the strain-invariant material coordinate and k is the coefficient of permeability. The relationship between the degree of consolidation for finite strain, $U_{f.s.}$, and t can can be determined from solution charts developed from a finite-difference solution of Eq. 5 (Cargill, 1984). The charts provide $U_{f.s.}$ as a function of the dimensionless time factor for finite strain, $T_{f.s.}$, defined as

$$T_{f.s.}=\frac{gt}{l^2} \quad (6)$$

where g is the coefficient of consolidation for finite strain and l is the thickness of a singly-drained layer in material coordinates.

The ultimate settlement, S(∞), can be computed from the relationship (Gibson et al., 1981)

$$S(\infty) = \int_0^l [e(z,0) - e(z,\infty)]\, dz \approx \sum_{i=1}^{n} (e_{i,0} - e_{i,\infty})\, l_i \qquad (7)$$

where l_i is the total height of material solids calculated for each sublayer from

$$l_i = \frac{\Delta x_i}{1+e_i} \qquad (8)$$

where e_i is the average initial void ratio in a sublayer.

As m_{vi} in Eq. 4 is equal to

$$m_{vi} = \frac{a_{vi}}{1+e_i} \approx \frac{\Delta e_i}{\Delta \sigma'_i (1+e_i)} \qquad (9)$$

where a_v is the coefficient of compressibility, it is apparent that Eqs. 4 and 7 are mathematically equivalent.

5.0 RESULTS

5.1 Ultimate Settlement, S(∞)

The results obtained for Samples LO-90, HH-1-90 and HH-2-90 are presented in Zeman (1992). The void ratio, e, vs. effective stress, σ′ (kPa), and void ratio vs. coefficient of permeability, k (m/day), relationships for Sample HH-1-93 are presented in Figs. 8 and 9. These results are compared with other samples tested in Figs. 10 and 11. The logarithmic and power regression coefficients, for the two relationships and the four samples tested, are presented in Tables 1 and 2.

As can be seen from Fig. 10, the initial void ratio for Sample HH-1-93 is somewhat lower than that for Sample HH-2-90, but it is higher than the corresponding values for the two remaining samples. Using the relationship for the compression index, C_c:

$$C_c = \frac{\Delta e}{\log(\frac{\sigma'_2}{\sigma'_1})} \qquad (10)$$

the C_c values are obtained from the regression curves presented in Fig. 12. These values are 0.940, 1.343, 2.068 and 2.054 for Samples LO-90, HH-1-90, HH-2-90 and HH-1-93 respectively. It can thus be concluded that the compressibility of Sample HH-1-93 is very close to that of Sample HH-2-92. The k values for Sample HH-1-93 range from about $1*10^{-1}$ m/day to about $1*10^{-5}$ m/day and they are within the general range obtained for the two other samples taken in the Harbour (Fig. 11).

Further data on primary consolidation characteristics at Site HH-1-93 were obtained from the results of the creep test carried out to estimate the coefficient of secondary compressibility, C_α (Section 7.2 following). The C_c value obtained from the creep test, taken as the straight line from end of saturation (2 kPa) to 10 kPa stress, is 1.4. The reason for the difference in the C_c values between the standard test and the creep test at Site HH-1-93 is not known.

Geotechnical data measured on six gravity sediment cores from the capping site were used to compute the effective vertical stress, σ', as a function of depth below the bottom (Fig. 13). Using the settlement formulas (Eqs. 4 and 7) and the e-σ' relationship obtained from the consolidation test, the ultimate settlement, $S(\infty)$, can then be computed as the function of the depth below the bottom. The $S(\infty)$ values obtained are somewhat larger than corresponding values for Sample HH-2-90 (Zeman, 1992), i.e., about 22 cm and 35 cm for the upper 1 m (H = 1 m) and the upper 2 m (H = 2 m) below the sediment-water interface respectively (Fig. 14). The result for H = 2 m should be regarded as a gross estimate, as the stratigraphy below the one-metre depth is presently unknown. The computed $S(\infty)$ values for all four samples are summarized in Table 3.

5.2 Determination of Time for 100% Primary Consolidation, t_{100}

The t_{100} values are required for the determination of the coefficient of secondary compression, c_α (Section 7.0). The end of primary consolidation is usually determined from deformation-log time curves of a consolidation test using the Casagrande method (Terzaghi and Peck, 1968). However, the time for 100% primary consolidation, t_{100}, is often not well-defined on deformation-log time curves for colloidal and organic clays (Yong and Warkentin, 1971, Sridharan et al., 1987). For this reason, the rectangular hyperbola method (Sridharan et al., 1987) is also used in the present report, in order to determine t_{100} and the magnitude of primary consolidation, δ_{100}, for each loading stage.

The Casagrande (t_{100C}) and the rectangular hyperbola methods (t_{100R}) were both plotted on deformation-log time curves in Figs. 15a to 18g for varying applied pressures (effective stresses, σ') ranging from 5 kPa to 320 kPa.

Typical deformation-log time curves have a lower gradient toward the end of the curve (e.g. Fig. 16f), allowing t_{100} to be measured. Many unusual curves were encountered (e.g. Fig. 16e), which often made it difficult or impossible to determine t_{100C}. Dial deflections were no more than 1 mm for each of the samples measured at 5 kPa, but rose to as much as 8 mm as higher pressure was applied. Irregular deformation-log time curves were obtained especially for low applied pressures.

In general, all samples required more time to reach t_{100} as a higher load was applied. Between 7 and 25 minutes were required at 5 kPa, increasing to about 500 to 1,000 minutes at 160 kPa and 320 kPa. The t_{100C} for 160 kPa could only be recorded for Samples HH-1-90, HH-2-90 and HH-1-93, and these times were more than the times required for 320 kPa for these same samples.

There was no consistent difference in t_{100C} and t_{100R} values, except for the fact that t_{100C} values were generally lower than t_{100R} values for the same consolidation pressure (Table 4).

5.2.1 Casagrande's method

The deformation-log time curves were used to obtain time required to reach the end of primary consolidation, t_{100C}. In some cases, the point of intersection could not be determined due to insufficient time allowed in testing of the sample, or simply due to an obscurely shaped curve. Three determinations were possible for Samples LO-90, HH-1-90, and HH-1-93. Four determinations were possible for Sample HH-2-90. The values range from 20 to 280 min for Sample LO-90, from 25 to 390 min for Sample HH-1-90, from 120 to 410 min for Sample HH-2-90, and from 220 to 1040 min for Sample HH-1-93 (Table 4). Apart

from low values obtained for 5-kPa plots for Samples LO-90 and HH-1-90, no trend was found between t_{100C} values and consolidation pressure.

5.2.2 Rectangular hyperbola method

The time required for primary consolidation, t_{100R}, was determined from the compression corresponding to 100 % primary consolidation, δ_{100}, using the equation (Sridharan et al., 1987)

$$\delta_{100} = \frac{0.859}{m} \qquad (11)$$

where m is the slope of the linear portion of the hyperbolic plot of t/δ vs. t (Sridharan et al., 1987). The point of intersection on the deflection vs. log-of-time plots was then determined (Figs. 15a to 18g). For seven curves (Figs. 15b, 16b, 16c, 17d, 18a, 18f and 18g), δ_{100} are below the end of experimental curves and, consequently, no t_{100R} values were obtained. The results for the four samples and different consolidation pressures are summarized in Table 4. The results are comparable to Casagrande's method (Section 5.2.1) in that low values were obtained for the consolidation pressure of 5 kPa and no obvious relationship was established for higher consolidation pressures. Values are both higher and lower than t_{100C} for those curves where both estimates were obtained.

5.3 Determination of Coefficient of Consolidation

5.3.1 Taylor's method

The c_{vT} values were computed from the equation (Das, 1983)

$$c_{vT} = \frac{0.848\ H^2}{t_{90}} \qquad (12)$$

where H = the length of the drainage path in the sample and t_{90} = time required to reach 90% primary consolidation (which is obtained from dial readings vs. square-root-of-time plots). The values are presented in Table 5.

The c_{vT} values obtained for Sample LO-90 are relatively constant for stresses greater than 10 kPa (Table 5, Fig. 19a). The values obtained for Samples HH-1-90 and HH-2-90 slightly decrease with pressure within the range of about 1.7×10^{-1} to

about 7.3 x 10^{-4} cm^2 s^{-1} (Table 5, Figs. 19b and 19c). For Sample HH-1-93, c_{vT} values generally decrease with consolidation pressure from about 3.7 x 10^{-2} at 5 kPa to about 1.1 x 10^{-3} cm^2 s^{-1} at 80 kPa (Table 5, Fig. 19d).

5.3.2 Casagrande's method

The c_{vC} values were computed from the equation (Das, 1983)

$$c_{vC} = \frac{0.197\ H^2}{t_{50}} \qquad (13)$$

where t_{50} = time required to reach 50% primary consolidation obtained from deflection - logarithm-of-time plots. These values were obtained for only those curves that allowed the deflection reading to correspond to 100% primary consolidation. For Sample LO-90, three values were obtained in the range of about 2.5 x 10^{-3} to about 2.3 x 10^{-4} cm^2 s^{-1} (Table 5, Fig. 19a). Three c_{vC} values obtained for Sample HH-1-90 (Table 5, Fig. 19b), four values obtained for Sample HH-2-90 (Table 5, Fig. 19c) and three values determined for Sample HH-1-93 are generally lower than c_{vT} values discussed in Section 5.3.1 preceding. The values obtained for Sample HH-1-93, at the three highest consolidation pressures, were in the range from 2.7 x 10^{-4} to 4.1 x 10^{-5} cm^2 s^{-1} (Table 5, Fig. 19d). The empirical $c_{vC} < \text{or} = c_{vT}$ relationship, reported by Sridharan et al. (1987) who used a large amount of experimental data, holds for all comparisons.

5.3.3 Rectangular hyperbola method

The c_{vR} values were computed from the equation (Sridharan et al., 1987)

$$c_{vR} = \frac{0.24 m H^2}{c} \qquad (14)$$

where m = slope of the linear portion of the t/δ versus t plot, δ = observed compression at any time (t), and c = intercept made by the linear portion of the t/δ versus t plot on the t/δ axis. The c_{vR} values for the three samples are, except for two values obtained for Sample LO-90 and three values obtained for Sample HH-2-90, somewhat lower than those

calculated from Taylor's and Casagrande's methods (Table 5, Figs. 19a to 19d), with noticeably lower c_{vR} values in Sample HH-1-93 (Fig. 19d). This is contrary to empirical findings reported by Sridharan et al. (1987) who reported the general relationship

$$c_{vC} \leq c_{vR} \leq c_{vT} \qquad (15)$$

A possible reason for this deviation between expected and obtained results can be due to very high compressibility of the four samples tested. Due to relatively large deflection values of δ at the beginning of a loading stage, t/δ vs t plots are linear only toward the end of a loading stage, which introduces appreciable uncertainties in determining both m and c in Eq. 14.

5.4 Degree of Consolidation

5.4.1 Terzaghi's theory

The degree of consolidation, U, as a function of time, t, has been computed for Sample HH-1-93 using the average coefficient of consolidation, c_{vT}, obtained from the consolidation test. The results for H = 1 m and H = 2 m are presented in Figs. 20a and 20b respectively. For the 1-m thick layer, the time required to reach 95 % primary consolidation is about 11.3 days and for the 2-m thick layer 45.1 days. These values are somewhat lower than those obtained for Samples LO-90, HH-1-90 and HH-2-90 (Zeman, 1992).

5.4.2 Finite strain theory

The degree of consolidation for finite strain has been determined by means of the solution charts for Eq. 5 (Cargill, 1984) and the results for H = 1 m and H = 2 m are presented in Figs. 21a and 21b respectively. The average coefficients of consolidation for finite strain, g, were determined using the relation (Gibson et al., 1981):

$$g = \frac{c_v}{(1+e_a)^2} \qquad (16)$$

The values of g are functions of the average void ratio, e_a, and the average effective stress, σ_a', are therefore influenced by the selected value of H. The computed times for 95% primary consolidation are 8.8 days and 29.6 days for H = 1 m and H = 2 m respectively (Figs. 21a and 21b). These

results, i.e. faster finite-strain consolidation rates, are consistent with the previous comparisons between the Terzaghi theory and the finite strain theory obtained for Samples LO-90, HH-1-90 and HH-2-90 (Table 6).

5.5 Results Obtained with Computer Code CONSOL

A brief description of the computer code CONSOL Version 2.0 (Duncan et al., 1988) was given in Section 4.2. All computations using the code were made for the upppermost one metre of the sediment (subdivided into ten 10-cm thick sublayers) at the four locations (Figs. 1 and 2). One of the required input parameters, the void ratio e, can be derived from available geotechnical data either from the measured moisture profiles and the measured specific gravity values (referred to below as the "e derivation no. 1"). The alternative approach is to use e values obtained from the void ratio-effective stress relationships (Fig. 10). This procedure is referred to below as the "e derivation no. 2". The remaining input parameters were the same for both types of computations. The coefficients of consolidation values used were the average values obtained by the Taylor method, c_{vT}, for each sample (Section 5.3.1).

5.5.1 Ultimate settlement, S(∞)

The results using CONSOL (Table 7) are in general agreement with the S(∞) values described in Section 5.1. As can be seen from this table, selection of void ratio values influences the results to a certain degree.

5.5.2 Degree of Consolidation

The estimated number of days required for 95 % primary consolidation to occur using CONSOL are presented in Table 7. The t_{95} values obtained are considered to be in a reasonable agreement with those obtained by other procedures and they are closer to the results obtained by the finite strain theory (Section 5.4.2) than to those obtained by the Terzaghi theory (Section 5.4.1).

PART B: SECONDARY CONSOLIDATION

6.0 THEORY

The mechanism of secondary consolidation is due to the continuation of volume change initiated during primary consolidation including deformation of individual particles and particle flocs, and the relative movement of these with respect to each other (Mesri, 1973). The volumetric changes during secondary consolidation occur under constant effective stress. The coefficient of secondary compression, C_α, appears to be the most useful parameter for evaluating the magnitude of secondary consolidation. In the present report, C_α is defined following Das (1983) as

$$C_\alpha = \frac{\frac{\Delta H}{H_{tp}}}{\log(t_2 - t_1)} \qquad (17)$$

where ΔH = sample height change between times t_1 and t_2, and H_{tp} = sample height at the beginning of the linear portion of a deformation-log time curve.

Note that in this definition, C_α corresponds to $\epsilon_{\alpha p}$ of Mesri (1973) while Mesri's C_α, referred to also as the coefficient of secondary compression, is defined as

$$C_\alpha[Mesri] = \frac{\Delta e}{\log(t_2 - t_1)} \qquad (18)$$

where Δe = sample void ratio change between times t_1 and t_2.

The relationship between Eqs. (17) and (18) is

$$C_\alpha = \epsilon_{\alpha p} = \frac{C_\alpha\,[Mesri]}{1+e_p} \qquad (19)$$

where e_p = sample void ratio at the beginning of the linear portion of a deformation-log time curve.

7.0 RESULTS

7.1 Determination of Coefficient of Secondary Compression, (C_α)

C_α was plotted against consolidation pressure (Figs. 22a to 22d) for each of the four samples.

7.1.1 Casagrande method ($C_{\alpha C}$ using t_{100C})

The determination of coefficient of secondary compression using the Casagrande method ($C_{\alpha C}$) could only be found where the proper shaped curve existed on the dial deflection vs. time graph.

$C_{\alpha C}$ remained below 10% in all of the samples, for all loadings, ranging from 0.17% in Sample HH-1-90 to 8.02% in Sample HH-1-93 (Figs. 22a to 22d and Table 7). It can be concluded that $C_{\alpha C}$ values are highly variable and they fall within all categories of secondary compressibility proposed by Mesri (1973), ranging from "very low" (<0.2%) to "extremely high" (>6.4%)

7.1.2 Rectangular hyperbola method ($C_{\alpha R}$ using t_{100R})

The coefficient of secondary compression using t_{100} determined by the rectangular hyperbola method, $C_{\alpha R}$, could only be found where the dial deflection readings on the ordinate were within the range of the curve. The coefficient was found in the same way as in Section 7.1.1.

$C_{\alpha R}$ peaked at 80 kPa for Samples HH-1-90 and HH-2-90 (5.61% and 10.31% respectively), but peaked at 10 kPa for HH-1-93 (Sample LO-90 at 80 kPa was undetermined). Percentages for $C_{\alpha R}$ remained below 10.5% for all samples and loadings, ranging from 0.15% for Sample HH-2-90 at 5 kPa to 10.31% for Sample HH-2-90 at 80 kPa (Table 7). The $C_{\alpha R}$ values are also highly variable and they range from "very low" to "extremely high" according the classification proposed by Mesri (Mesri, 1973).

7.2 Creep Test

The oedometer creep test was carried out at stresses of 5 and 10 kPa and the results pertaining to primary consolidation are reported in Section 5.1 preceding. Testing was first conducted at 5 kPa for 47 days, and then tested at 10 kPa for 52 days on the same sample (Golder Associates, 1994). Porewater pressure, volume (inflow and outflow) changes, back pressure, applied pressure and dial deflection readings against elapsed time were measured and recorded

periodically. After approximately 37 days of testing, gas bubble build-up in the outflow (volume change) line was observed, in contrast to the standard consolidation test (using the same Rowe cell), which was completed within a much shorter time duration. The volume change inflow line for the cell (applied pressure) was not observed to contain gas bubbles and it was therefore used to determine the dial deflection (void ratio) vs. elapsed time relationship. The gas bubble generation had apparently little influence on this relationship (Golder Associates, private communication).

7.2.1 Evaluation of C_α from creep test

The void ratio-time relationships obtained at applied pressures of 5 and 10 kPa are plotted in Figs. 23a and 24a respectively. Figs 23b and 24b show the same relationships with time plotted on the logarithmic scale. The steeper portions of e-log t curves were used to obtain estimates for C_α (Equations 18 and 19). The values of C_α [Mesri] were found to be 0.302 and 0.338 for applied pressures of 5 and 10 kPa respectively. Assuming e_p values to be 4.741 at 5 kPa (Fig. 23c) and 4.541 at 10 kPa (Fig. 24c), the corresponding values for C_α from Eq. 19 are 5.268% and 6.104%. Both values are in reasonable agreement with estimates obtained in Sections 7.1.1 and 7.1.2 preceding, and the sediment can be classified as being of very high secondary compressibility (C_α between 3.2% and 6.4%) according to the classification proposed by Mesri (1973).

7.3 Secondary Consolidation Settlement, S_s

Secondary consolidation settlement, S_s, can be estimated from (Das, 1983)

$$S_s = C_\alpha H_{ts} \log\left(\frac{t}{t_p}\right) \qquad (20)$$

where H_{ts} is a thickness of sediment layer at the beginning of secondary consolidation (i.e. $H_t - S(\infty)$), t is time at which secondary consolidation is required and t_p is time at the end of primary consolidation.

As can be seen from Eq. 20, which is derived from Eq. 17, S_s depends both on the magnitude and the rate of primary consolidation. Consequently, computations of S_s, which have to be regarded as pure estimates only, were carried out for four cases: A. Terzaghi's theory, H = 1 m; B. Terzaghi's theory, H

H = 2 m; C. finite strain theory, H = 1 m; and D. finite strain theory, H = 2 m (Table 8). Three values of C_α selected were 1%, 2.5% and 5%, which are in reasonable agreement with the C_α values obtained for low presures in Sections 7.1 and 7.2 preceding. The secondary consolidation settlements were computed for times ranging from 1 to 20 years. In all cases, the highest S_s values were obtained for Site HH-1-93 and the lowest ones were obtained for Site LO-90. The finite strain theory (Tables 8C and 8D) yielded slightly higher estimates than Terzaghi's theory (Tables 8A and 8B) due to faster rates of primary consolidation. The estimates for Case A (Table 8A) for C_α = 5% and t = 20 years range from 9.5 cm for Sample LO-90 to 11.9 cm for Sample HH-1-93. The corresponding ranges for Cases B, C and D are 14.2 to 19.8 cm, 10.1 to 12.2 cm and 17.3 to 21.4 cm respectively (Tables 8B, 8C and 8D). The results are linearly proportional, and therefore highly sensitive, to pre-selected values of C_α. Although actual measurements of S_s are relatively scarce, good agreement of measured and estimated values have been reported by several observers (Das, 1983).

The estimates of S_s presented in Table 7 are likely high for the following reason. Following placement of the sand cap, a new layer of fine-grained sediment will be gradually formed on the top of the cap. Existing information indicates that this layer will be deposited at a sedimentation rate of about 0.3 cm per year. Thus in 20 years a fine-grained layer of about 6 cm will form. This layer will seal the cap and slow down the expulsion of water caused by secondary consolidation.

7.4 Amount of Pore Water Released During Primary and Secondary consolidation

Based on the results presented in Section 5.1 preceding, it is assumed that primary consolidation will displace about 140-350 l/m^2 of pore water into the 0.5 m thick sand cap with the porosity of the cap in the range of 40-45% (Kezdi, 1974). Out of this amount, about 70-100 l/m^2 will be squeezed from the uppermost 30-cm thick contaminated layer. The total volume of pore water in the cap will be in the range of 200-225 l/m^2. Consequently, it is expected that all displaced water due to primary consolidation of the 30-cm thick contaminated layer will be confined within the cap. Additional amounts of pore water will be released during secondary compression evaluated in Sections 7. 2 and 7.3 preceding. Although the secondary consolidation settlement could theoretically be up to about 20 cm within the 20-year time period, and therefore release additional 200 l/m^2 into the cap, it is concluded that this settlement and associated pore water extrusion will be significantly reduced by the gradual formation of a new fine-grained layer of low permeability at the top of the cap. In

the Hamilton Harbour demonstration project, the composition of sediment pore water in the cap will be monitored by collecting pore water samples in situ, using several dialysis chambers called "peepers" (Rosa nad Azcue, 1993). Based on the results of long-term monitoring of capping projects by three different US Army Corps of Engineers offices (Sumeri et al., 1991), which lasted from three to 11 years following the placement of caps, long-term transport of metals and organic contaminants up and through the caps appears unlikely.

PART C: CONCLUSIONS

The present report summarizes available knowledge on consolidation behaviour of very soft fine-grained sediments from three sites, including the proposed capping site, in Hamilton Harbour and from one site in western Lake Ontario. The expected magnitudes and rates of primary consolidation due to surcharge of a sand cap 0.5 m in thickness were determined using large diameter consolidation tests with pore pressure measurements. In addition, gravity cores were collected at each of these sites to establish vertical geotechnical trends.

Three different approaches were used to determine the magnitudes and rates associated with primary consolidation; i. the classical (Terzaghi) theory; ii. the finite strain theory (Gibson et al., 1967; Gibson et al., 1981 and Cargill, 1984); and iii. the computer code CONSOL (Duncan et al., 1981) that uses numerical analysis procedures to calculate magnitudes and rates of consolidation settlement. The ultimate settlements, $S(\infty)$, determined by approaches i. and ii. were identical, ranging from 0.11 cm at Site LO-90 to 0.22 cm at Site HH-1-93 for the uppermost one-m thick sediment layer. Similar or somewhat larger estimates were obtained from the analyses using CONSOL. The rates of primary consolidation were significantly faster (from 20 days at Site LO-90 to 9 days at Site HH-1-93) using the finite strain method than the classical method (from 54 days at Site LO-90 to 11 days at Site HH-1-93). The rates of primary consolidation using CONSOL were in general similar to the results obtained by the finite strain method. Furthermore, extrapolations for both the magnitudes and rates of primary consolidation were made for a 2-m thick sediment layer.

The magnitudes and rates of secondary consolidation were evaluated using the coefficient of secondary consolidation, C_α, obtained from the dial deflection vs. time curves. The Casagrande method (Terzaghi and Peck, 1968) and the rectangular hyperbola method (Sridharan et al., 1987) were used to determine time for 100% primary consolidation, t_{100}, for individual dial deflection vs. time consolidation curves. Both of these methods resulted in highly variable values of C_α, falling within all categories of secondary compressibility proposed by Mesri (1973). The results of the oedometer creep test, using a sample from the proposed capping site, yielded values of C_α of 5.3% and 6.1% for applied stresses 5 kPa and 10 kPa respectively, thus indicating that the sediments at the proposed capping site are of very high secondary compressibility according to the Mesri classification. The predicted settlements associated with secondary consolidation were calculated, but they are expected to be too high in view of the gradual formation of a low-permeability new-sediment

layer on the top of the cap. Amounts of pore water released from the sediment due to primary and secondary consolidation were also computed. Potential migration of contamimnants contained in the pore water through the cap appears unlikely in view of the amounts predicted and the existing experience from other capping projects.

ACKNOWLEDGEMENTS

The work undertaken in connection with the preparation of the capping demonstration project in Hamilton Harbour has been sponsored by the Great Lakes Cleanup Fund of Environment Canada. Field sampling was carried out by the Technical Operations Section of the NWRI under the supervision of Pat Healey and Henk Don. The consolidation testing of Hamilton Harbour and Lake Ontario sediments was carried out by Golder Associates Ltd., Mississauga, Ont.

REFERENCES

Cargill, K.W. 1984. Prediction of consolidation of very soft soil. J. Geotech. Eng., ASCE, 110(6): 775-795.

Dalton, J.A. 1991. Particle size report, Lake Ontario and Hamilton Harbour cores. NWRI report no. RAB-90-03J.

Das, B.M. 1983. Advanced Soil Mechanics, New York: McGraw-Hill Book Comp., 511 p.

Duncan, J.M., Smith, R.W., Brandon, T.L. and Wong, K.S. 1988. CONSOL Version 2.0: A computer program for 1-D consolidation analysis of layered soil masses. Manual, Dept. Civ. Eng., Virginia Polytechnic Institute and State University, Blacksburg, VA, 67 p.

Gibson, R.E., England, G.L. and Hussey, M.J.L. 1967. The theory of one-dimensional consolidation of saturated clays. 1. Finite non-linear consolidation of thin homogeneous layers. Géotechnique, 17:261-273.

Gibson, R.E., Schiffman, R.L. and Cargill, K.W. 1981. The theory of one-dimensional consolidation of saturated clays. II. Finite nonlinear consolidation of thick homogeneous layers. Can. Geotech. J., 18: 280-293.

Golder Associated Ltd. 1990. Geotechnical laboratory testing very soft cohesive sediments, Lake Ontario and Hamilton Harbour. Mississauga, Ont.

Golder Associates Ltd. 1994. Consolidation testing of very soft Hamilton Harbour sediment. Mississauga, Ont.

Hansbo, S. 1957. A new approach to the determination of the shear strength of clay by the fall-cone test. Proceedings Royal Swedish Geotechnical Institute, No. 14, 46 p.

Mesri, G. 1973. Coefficient of secondary compression. Journal of the Soil Mechanics and Foundations Division, ASCE, 99(SMI):123-137.

Mudroch, A., and Zeman, A.J. 1975. Physicochemical properties of dredge spoil. Journal of the Waterways Harbors, and Coastal Engineering Division, ASCE, 101 (WWE): 201-216.

Patterson, T.S. 1993. Hamilton Harbour sediments particle data report. NWRI report no. RAB-TN-93-46.

Rosa, F., and Azcue, J. M. 1993. "Peeper methodology" - A detailed procedure from field experience. NWRI Contribution No. 93-33.

Rowe, P.W., and Barden, L. 1966. A new consolidation cell. Géotechnique, XVI (2): 162-170.

Sridharan, A., Murthy, N. S. and Prakash, K. 1987. Rectangular hyperbola method of consolidation analysis. Géotechnique 37, 3:355-368.

Sumeri, A., Fredette, T. J., Kullberg, P. G., Germano, J. D., Carey, D. A., and Pechko, P. 1991. Sediment chemistry profiles of capped in-situ and dredged sediment deposits: Results from three US Army Corps of Engineers offices. Proc. 24th Annual Dredging Seminar, The Center for Dredging Studies (Texas A&M Univ.) and The Western Dredging Assoc., Las Vegas, Nevada, May 1991: 161-188.

Terzaghi, K., and Peck, R.B. 1968. Soil Mechanics in Engineering Practice. New York: John Wiley and Sons, 720 p.

Vanderpost, J.M. 1972. Bacterial and physical characteristics of Lake Ontario sediment during several months. Proc. 15th Conf. Great Lakes Res., Intern. Assoc. Great Lakes Res., 198-213.

Yong, R.N., and Warkentin, B.P. 1971. Introduction to Soil Behaviour. The Macmillan Company, New York and Collier Macmillan Ltd., London, 451 p.

Zeman, A.J. 1992. Consolidation of very soft sediments due to subaqueous capping. NWRI Contribution No., 92-67.

Zeman, A.J. 1993. Subaqueous capping of very soft contaminated sediments. Proc. 4th Canadian Conference on Marine Geotechnical Engineering, St. John's, Newfoundland, V.2, pp. 598-609.

TABLES

Table 1: Logarithmic regression coefficients for e-σ′ and e-k relationships

CONSTITUTIVE EQUATIONS FROM ROWE CELL CONSOLIDATION TESTS; LOGARITHMIC REGRESSION: y = a + b*ln(x); r^2 = coefficient of determination						
Sample No.	a (e-σ′)	b (e-σ′)	r^2	a (e-k)	b (e-k)	r^2
LO-90	3.346	-0.408	0.985	3.789	0.272	0.831
HH-1-90	4.775	-0.583	0.994	4.544	0.274	0.955
HH-2-90	7.139	-0.907	0.995	7.019	0.539	0.858
HH-1-93	6.551	-0.892	0.986	5.092	0.291	0.978

Table 2: Power regression coefficients for e-σ′ and e-k relationships

CONSTITUTIVE EQUATIONS FROM ROWE CELL CONSOLIDATION TESTS; POWER REGRESSION: $y = a*x^b$; r^2 = coefficient of determination						
Sample No.	a (e-σ′)	b (e-σ′)	r^2	a (e-k)	b (e-k)	r^2
LO-90	4.100	-0.231	0.976	5.399	0.157	0.860
HH-1-90	5.574	-0.213	0.990	5.060	0.098	0.914
HH-2-90	9.110	-0.254	0.983	9.607	0.162	0.843
HH-1-93	8.701	-0.287	0.997	5.903	0.102	0.965

Table 3: Ultimate settlements (primary consolidation only), computed for four sites investigated, due to capping with a 0.5-m thick sand layer (Eqs. 4 and 7)

Sample (Site) No.	S(∞), m H = 1 m	S(∞), m H = 2 m
LO-90	0.11	0.14
HH-1-90	0.14	0.18
HH-2-90	0.16	0.21
HH-1-93	0.22	0.35

Table 4: Time for primary compression

Sample	Consolid. Pressure	t_{100C}	t_{100R}
	kPa	min.	min.
LO-90	5	20	16
	10	-----	-----
	20	60	1,000
	40	280	505
	80	-----	1,040
	160	-----	3,000
	320	-----	810
HH-1-90	5	25	21
	10	-----	-----
	20	-----	-----
	40	390	1,000
	80	-----	300
	160	130	1,030
HH-2-90	5	-----	7
	10	-----	405
	20	160	125
	40	410	-----
	80	-----	310
	160	170	210
	320	120	320
HH-1-93	5	-----	-----
	10	-----	75
	20	-----	70
	40	-----	180
	80	220	1040
	160	1040	-----
	320	310	-----

Table 5: Coefficients of consolidation

Sample	Consolid. Pressure	c_{vT}	c_{vC}	c_{vR}
	kPa	cm^2/s	cm^2/s	cm^2/s
LO-90	5	9.7×10^{-2}	2.46×10^{-3}	2.54×10^{-2}
	10	2.81×10^{-3}	---------	1.01×10^{-3}
	20	3.31×10^{-3}	2.31×10^{-3}	1.74×10^{-3}
	40	2.35×10^{-3}	2.34×10^{-4}	8.02×10^{-4}
	80	2.56×10^{-3}	---------	3.16×10^{-4}
	160	1.56×10^{-3}	---------	8.58×10^{-5}
	320	1.98×10^{-3}	---------	6.74×10^{-4}
HH-1-90	5	1.67×10^{-1}	3.40×10^{-3}	2.64×10^{-3}
	10	1.20×10^{-2}	---------	1.37×10^{-4}
	20	3.39×10^{-3}	---------	1.47×10^{-5}
	40	7.30×10^{-4}	1.15×10^{-4}	4.76×10^{-5}
	80	1.33×10^{-3}	---------	1.42×10^{-4}
	160	8.60×10^{-4}	1.30×10^{-4}	3.42×10^{-5}
HH-2-90	5	1.30×10^{-2}	---------	9.14×10^{-1}
	10	2.00×10^{-2}	---------	1.45×10^{-4}
	20	3.04×10^{-3}	4.63×10^{-4}	1.82×10^{-3}
	40	3.31×10^{-3}	1.88×10^{-4}	1.54×10^{-4}
	80	4.67×10^{-3}	---------	3.16×10^{-4}
	160	2.13×10^{-3}	3.05×10^{-4}	2.61×10^{-4}
	320	1.57×10^{-3}	1.62×10^{-4}	1.41×10^{-4}
HH-1-93	5	---------	---------	3.03×10^{-5}
	10	3.72×10^{-2}	---------	5.25×10^{-6}
	20	2.94×10^{-2}	---------	1.81×10^{-6}
	40	1.30×10^{-3}	---------	2.24×10^{-6}
	80	1.11×10^{-3}	2.74×10^{-4}	9.71×10^{-7}
	160	4.12×10^{-3}	4.11×10^{-5}	4.20×10^{-7}
	320	2.48×10^{-3}	4.26×10^{-5}	1.35×10^{-7}

Note: c_{vT} = coefficient of consolidation obtained from Taylor's method (from Golder Associates); c_{vC} = coefficient of consolidation obtained from Casagrande's method; c_{vR} = coefficient of consolidation obtained from the rectangular hyperbola method.

Table 6: Ninety-five % degree of primary consolidation, $U_{95\%}$ (days), computed for four sites investigated

Sample (Site) No.	Terzaghi's Theory		Finite Strain Theory	
	H = 1 m	H = 2 m	H = 1 m	H = 2 m
LO-90	54	216	20	100
HH-1-90	36	143	15	50
HH-2-90	19	77	10	40
HH-1-93	11	45	9	30

Table 7: Primary consolidation results obtained with finite-difference computer code CONSOL in comparison to other results

Sample No.	Ultimate Settlement, S(∞) (m) H = 1 m			Ninety-five % Degree of Primary Consolidation (days) H = 1 m			
	Table 3	e deriv. no. 1 * CONSOL	e deriv. no. 2 * CONSOL	Table 6, Terz. Theory	Table 6, Fin. Strain	e deriv. no. 1 * CONSOL	e deriv. no. 2 * CONSOL
LO-90	0.11	0.16	0.12	54	20	32	16
HH-1-90	0.14	0.17	0.15	36	15	16	16
HH-2-90	0.16	0.24	0.29	19	10	8	8
HH-1-93	0.22	0.27	0.22	11	9	8	8

* For explanation of the e derivations nos. 1 and 2 see Section 5.5

Table 8: Coefficients of secondary compression

Sample	Consolid. Pressure	$C_{\alpha C}$	$C_{\alpha R}$
	kPa	%	%
LO-90	5	-----	0.82
	10	-----	-----
	20	0.69	-----
	40	2.39	2.39
	80	-----	-----
	160	-----	5.34
	320	-----	1.77
HH-1-90	5	0.17	1.81
	10	-----	-----
	20	-----	-----
	40	2.54	2.54
	80	-----	5.61
	160	1.01	1.17
HH-2-90	5	-----	0.15
	10	-----	-----
	20	0.29	4.81
	40	1.59	-----
	80	-----	10.31
	160	5.06	5.06
	320	1.01	1.51
HH-1-93	5		
	10		10.29
	20		4.60
	40		7.08
	80	8.02	8.02
	160	3.20	
	320	3.74	

Table 9: Secondary consolidation settlements, S_s

A. Terzaghi's theory, H = 1 m				
Sample No.	Time (yrs)	C_α = 1% (m)	C_α = 2.5% (m)	C_α = 5% (m)
LO-90	1	0.007	0.018	0.037
	2	0.010	0.025	0.050
	5	0.014	0.034	0.068
	10	0.016	0.041	0.081
	20	0.019	0.047	0.095
HH-1-90	1	0.009	0.022	0.043
	2	0.011	0.028	0.056
	5	0.015	0.037	0.073
	10	0.017	0.043	0.086
	20	0.020	0.050	0.099
HH-2-90	1	0.011	0.027	0.054
	2	0.013	0.033	0.067
	5	0.017	0.042	0.083
	10	0.019	0.048	0.096
	20	0.022	0.054	0.109
HH-1-93	1	0.013	0.032	0.064
	2	0.015	0.038	0.077
	5	0.019	0.047	0.093
	10	0.021	0.053	0.106
	20	0.024	0.059	0.119

Table 9, cont'd.: Secondary consolidation settlements, S_s

B. Terzaghi's theory, H = 2 m				
Sample No.	Time (yrs)	C_α = 1% (m)	C_α = 2.5% (m)	C_α = 5% (m)
LO-90	1	0.004	0.011	0.021
	2	0.010	0.025	0.049
	5	0.017	0.043	0.086
	10	0.023	0.057	0.114
	20	0.028	0.071	0.142
HH-1-90	1	0.007	0.019	0.037
	2	0.013	0.032	0.064
	5	0.020	0.050	0.101
	10	0.026	0.064	0.128
	20	0.031	0.078	0.155
HH-2-90	1	0.012	0.030	0.060
	2	0.017	0.044	0.087
	5	0.025	0.062	0.123
	10	0.030	0.075	0.150
	20	0.035	0.088	0.177
HH-1-93	1	0.016	0.041	0.081
	2	0.022	0.054	0.108
	5	0.029	0.072	0.144
	10	0.034	0.085	0.171
	20	0.040	0.099	0.198

Table 9, cont'd.: Secondary consolidation settlements, S_s

C. Finite strain theory, H = 1 m				
Sample No.	Time (yrs)	C_α = 1% (m)	C_α = 2.5% (m)	C_α = 5% (m)
LO-90	1	0.011	0.028	0.056
	2	0.014	0.035	0.070
	5	0.017	0.044	0.087
	10	0.020	0.050	0.101
	20	0.023	0.057	0.114
HH-1-90	1	0.012	0.030	0.060
	2	0.015	0.036	0.073
	5	0.018	0.045	0.090
	10	0.021	0.051	0.103
	20	0.023	0.058	0.116
HH-2-90	1	0.013	0.033	0.066
	2	0.016	0.039	0.078
	5	0.019	0.047	0.095
	10	0.022	0.054	0.108
	20	0.024	0.060	0.120
HH-1-93	1	0.014	0.034	0.068
	2	0.016	0.040	0.080
	5	0.019	0.048	0.097
	10	0.022	0.055	0.110
	20	0.024	0.061	0.122

Table 9, cont'd.: Secondary consolidation settlements, S_s

D. Finite strain theory, H = 2 m				
Sample No.	Time (yrs)	C_α = 1% (m)	C_α = 2.5% (m)	C_α = 5% (m)
LO-90	1	0.010	0.026	0.052
	2	0.016	0.040	0.080
	5	0.023	0.059	0.117
	10	0.029	0.073	0.145
	20	0.035	0.087	0.173
HH-1-90	1	0.016	0.039	0.079
	2	0.021	0.053	0.106
	5	0.028	0.071	0.142
	10	0.034	0.085	0.170
	20	0.039	0.098	0.197
HH-2-90	1	0.017	0.043	0.086
	2	0.023	0.056	0.113
	5	0.030	0.074	0.148
	10	0.035	0.088	0.175
	20	0.040	0.101	0.202
HH-1-93	1	0.019	0.049	0.097
	2	0.025	0.062	0.124
	5	0.032	0.080	0.160
	10	0.037	0.093	0.187
	20	0.043	0.107	0.214

SAMPLE LOCATIONS IN HAMILTON HARBOUR

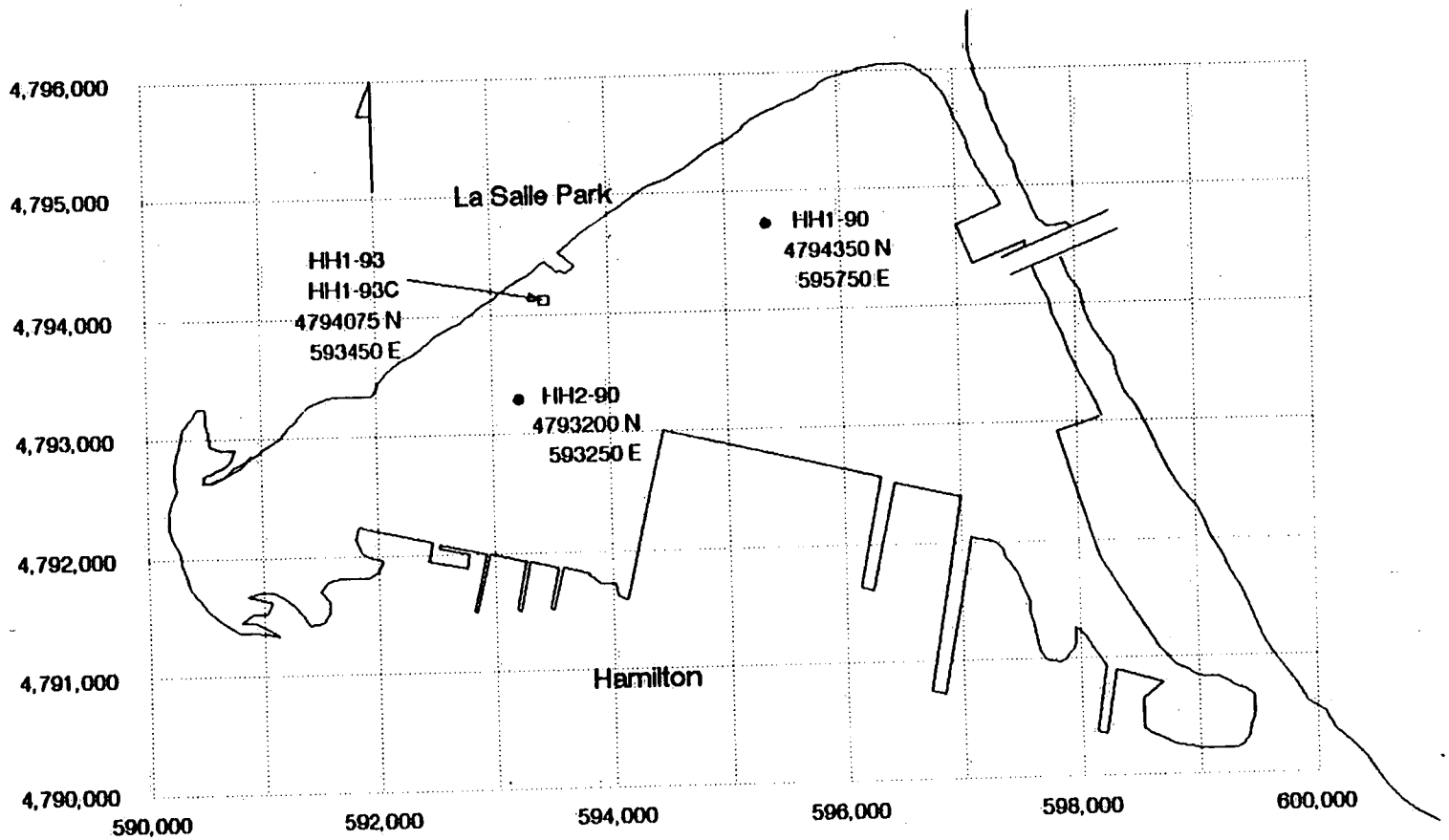

UTM in NAD 27

Figure 1

SAMPLE LOCATION FOR LO-90

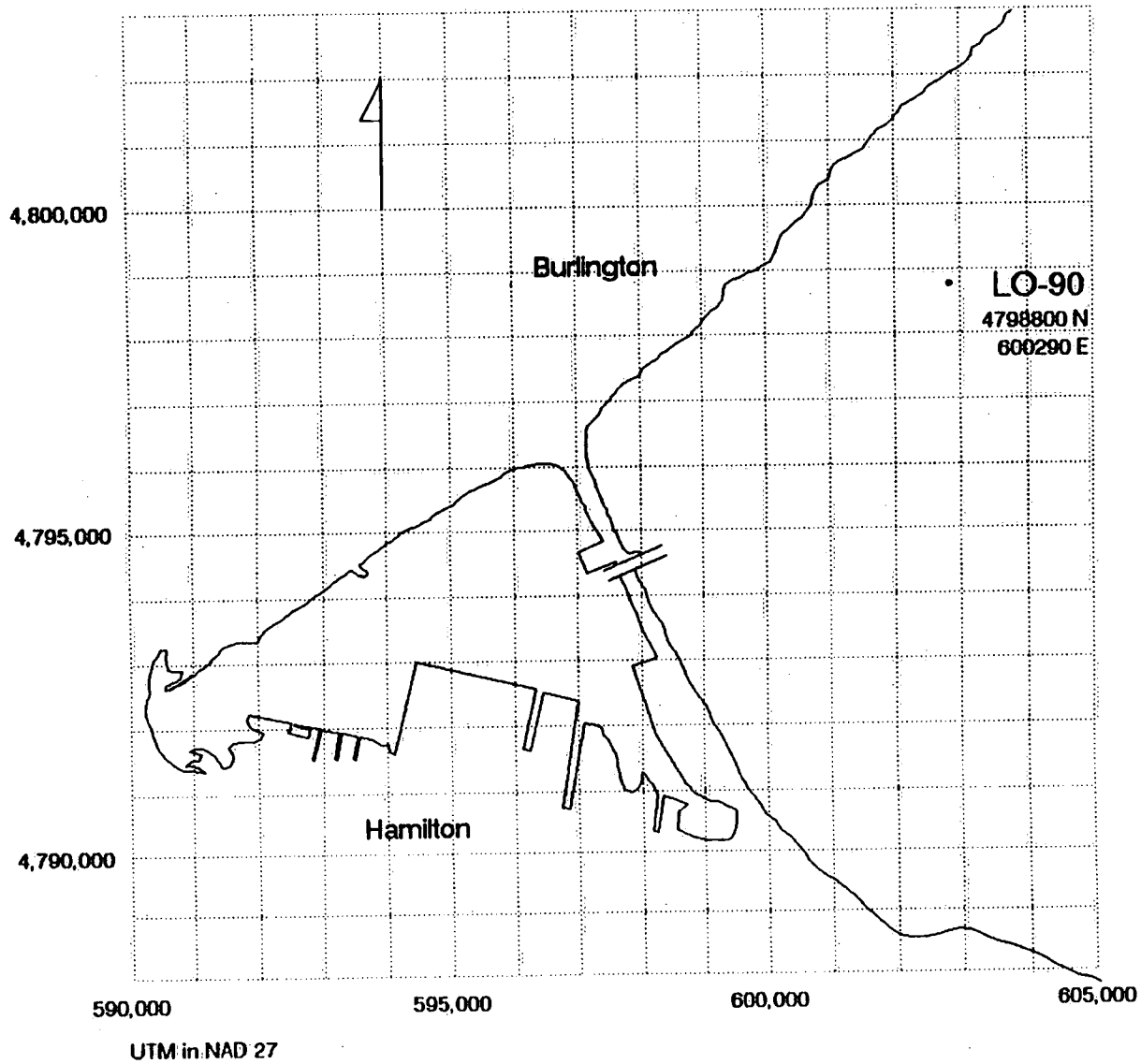

Figure 2

SEDIMENT CORES TAKEN AT PROPOSED CAPPING SITE

SEDIMENT GEOTECHNIQUE

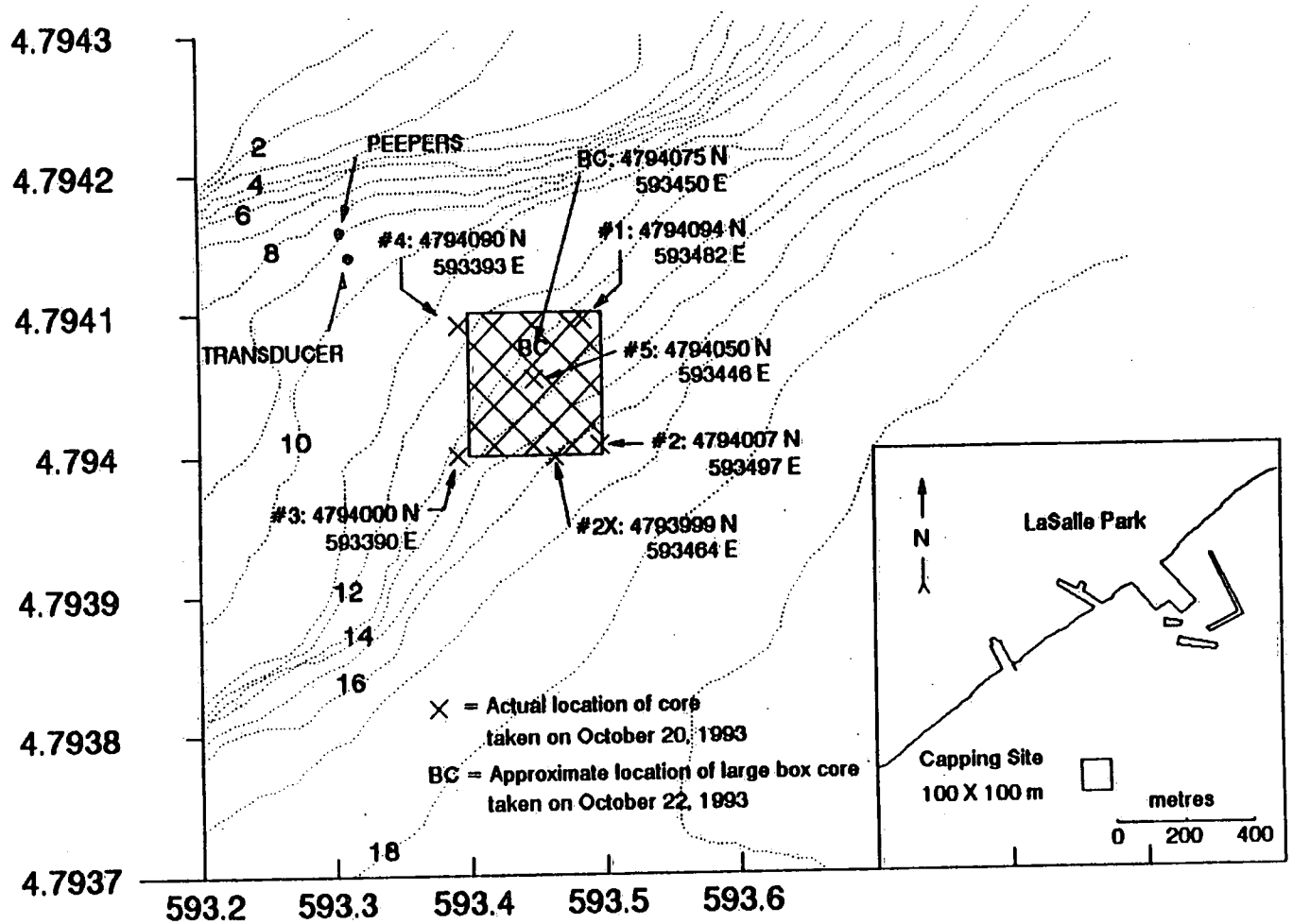

Depths are in metres

IGLD 1985

UTM coordinates are measured by NAD 27

Figure 3

LO-90

PARTICLE SIZE DISTRIBUTION (%)

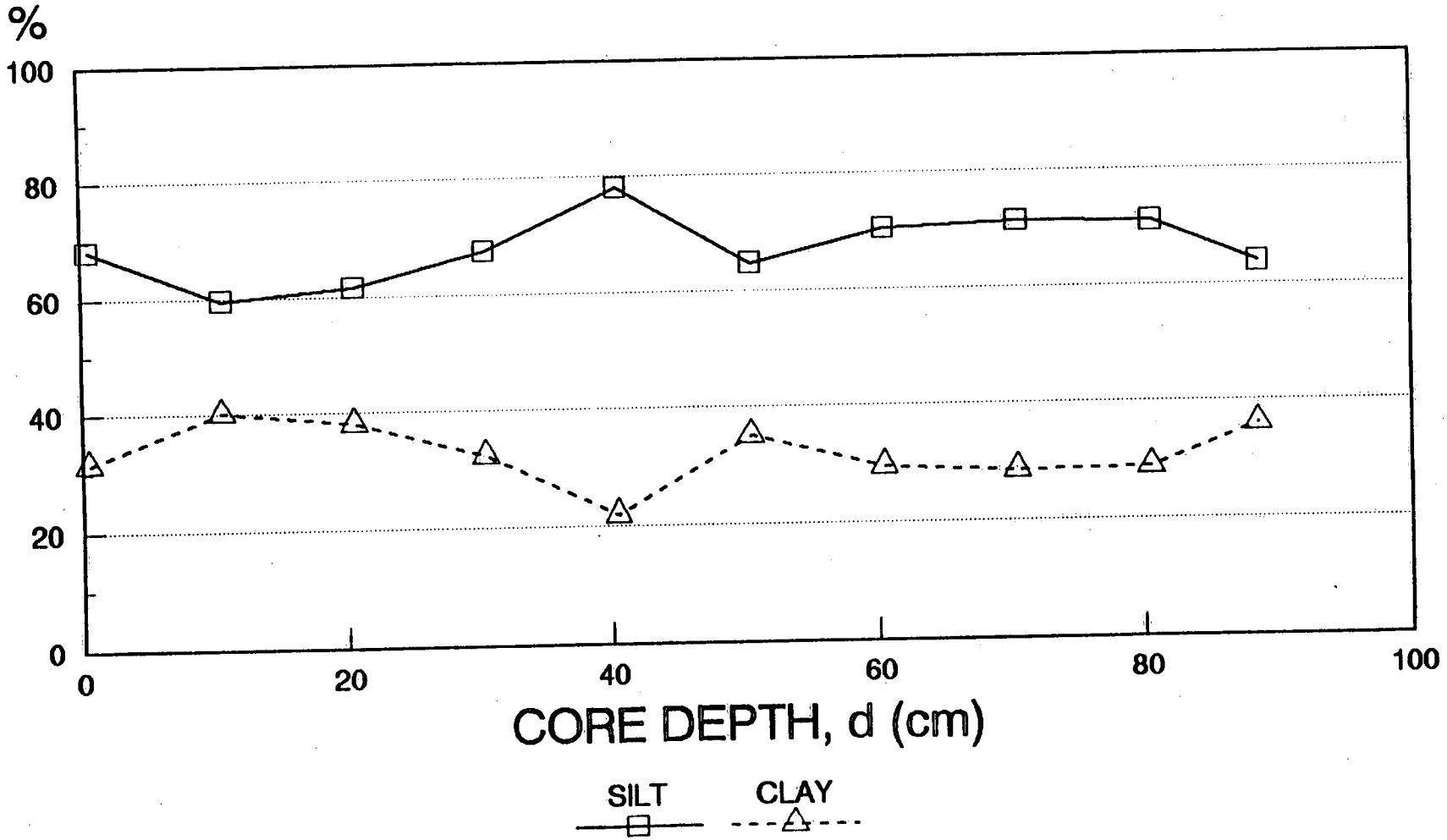

Figure 4a

No gravel or sand was found.

HH-1-90

PARTICLE SIZE DISTRIBUTION (%)

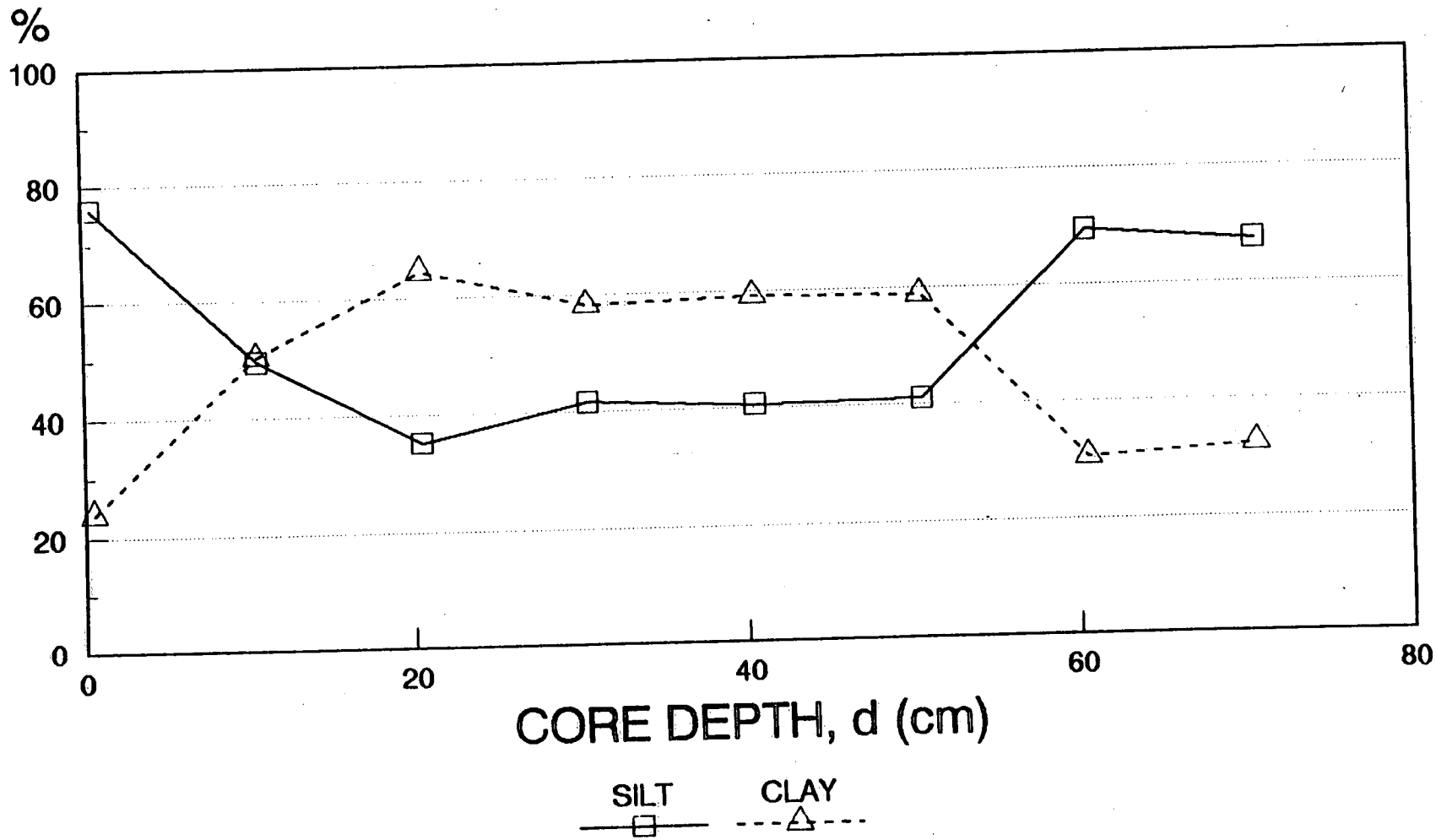

Figure 4b

No gravel or sand was found.

HH-2-90

PARTICLE SIZE DISTRIBUTION (%)

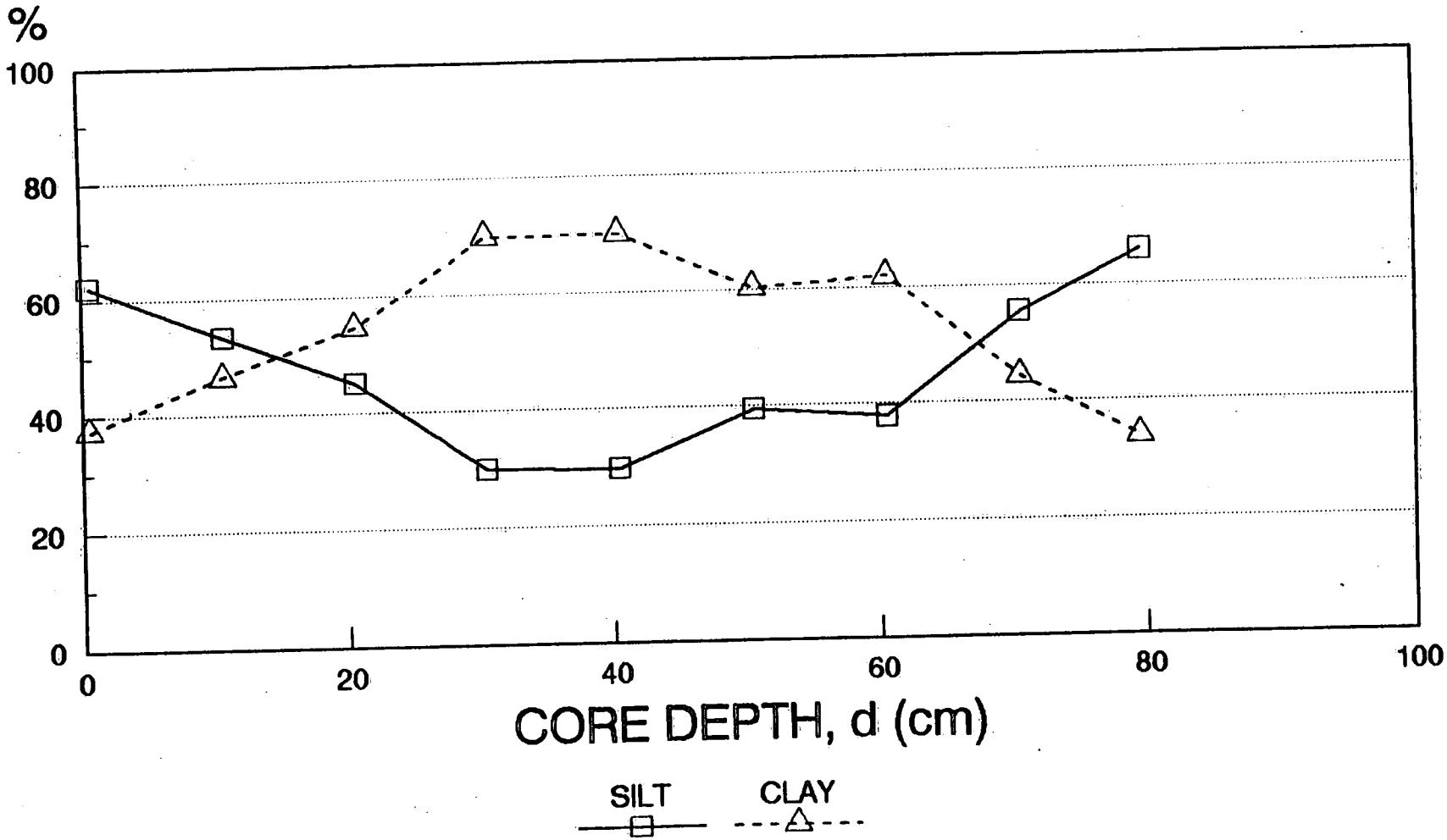

Figure 4c

No gravel or sand was found.

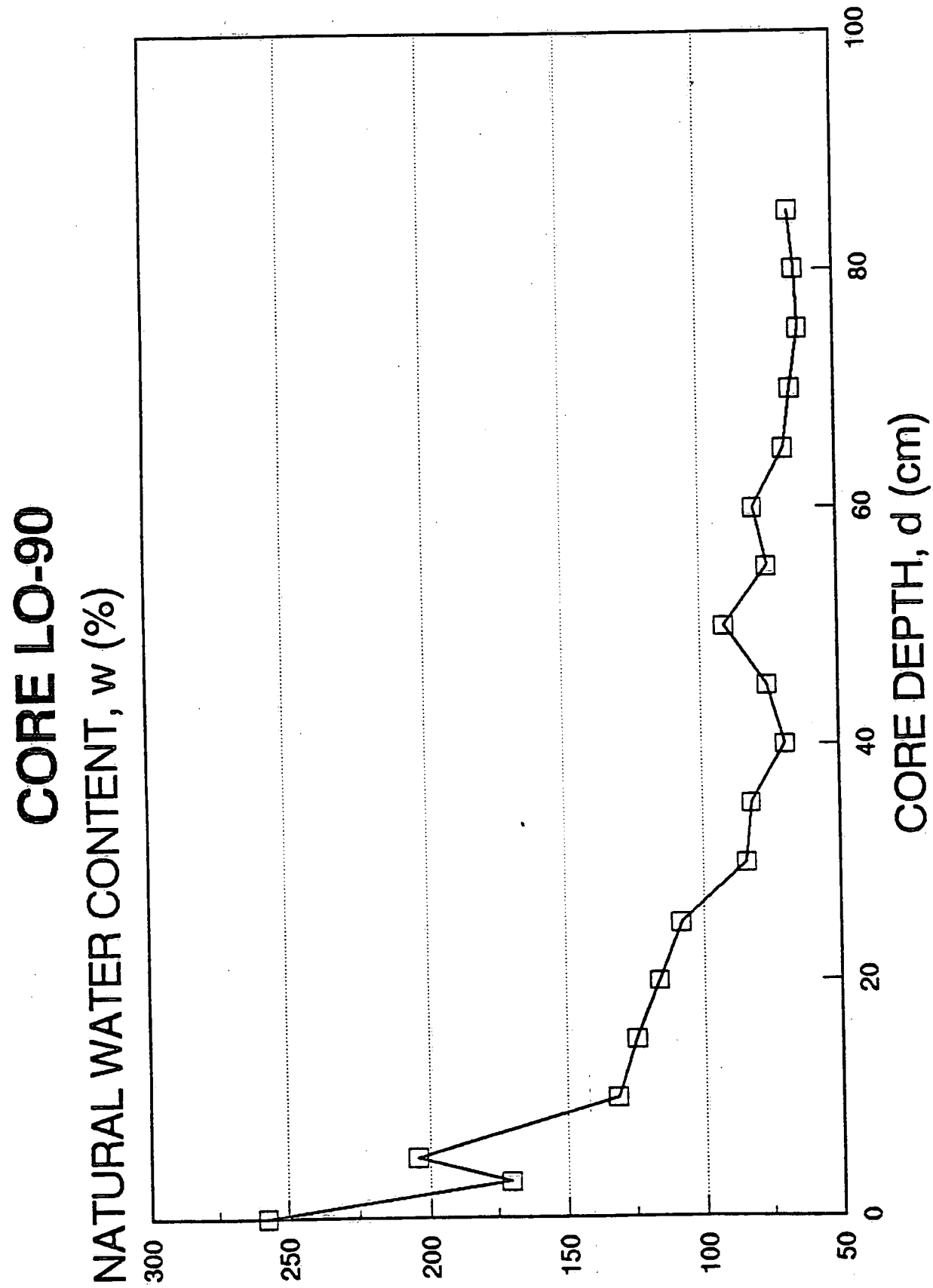
CORE LO-90
NATURAL WATER CONTENT, w (%)
300
250
200
150
100
50
0
20
40
60
80
100
CORE DEPTH, d (cm)

Figure 5a

CORE HH1-90

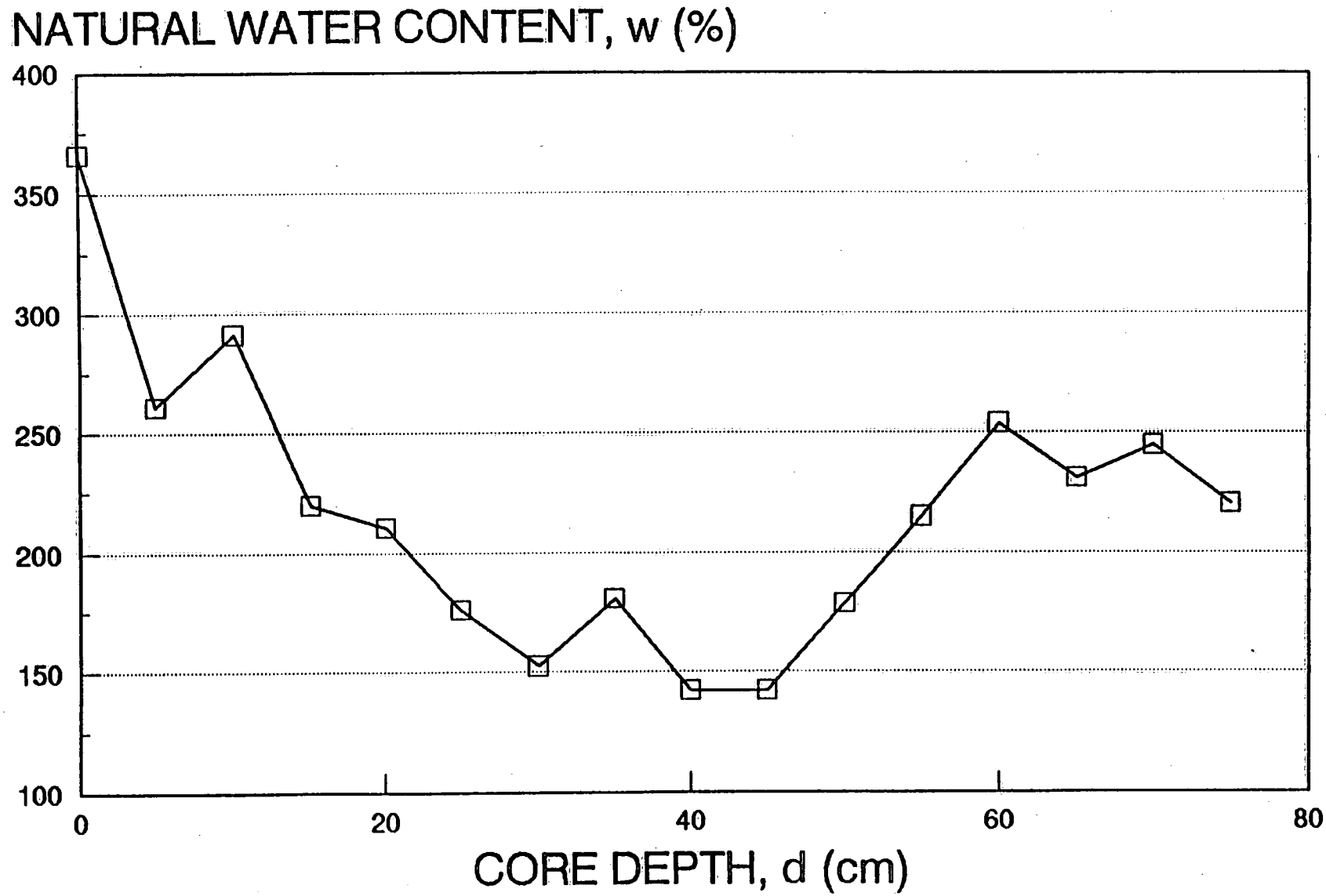

Figure 5b

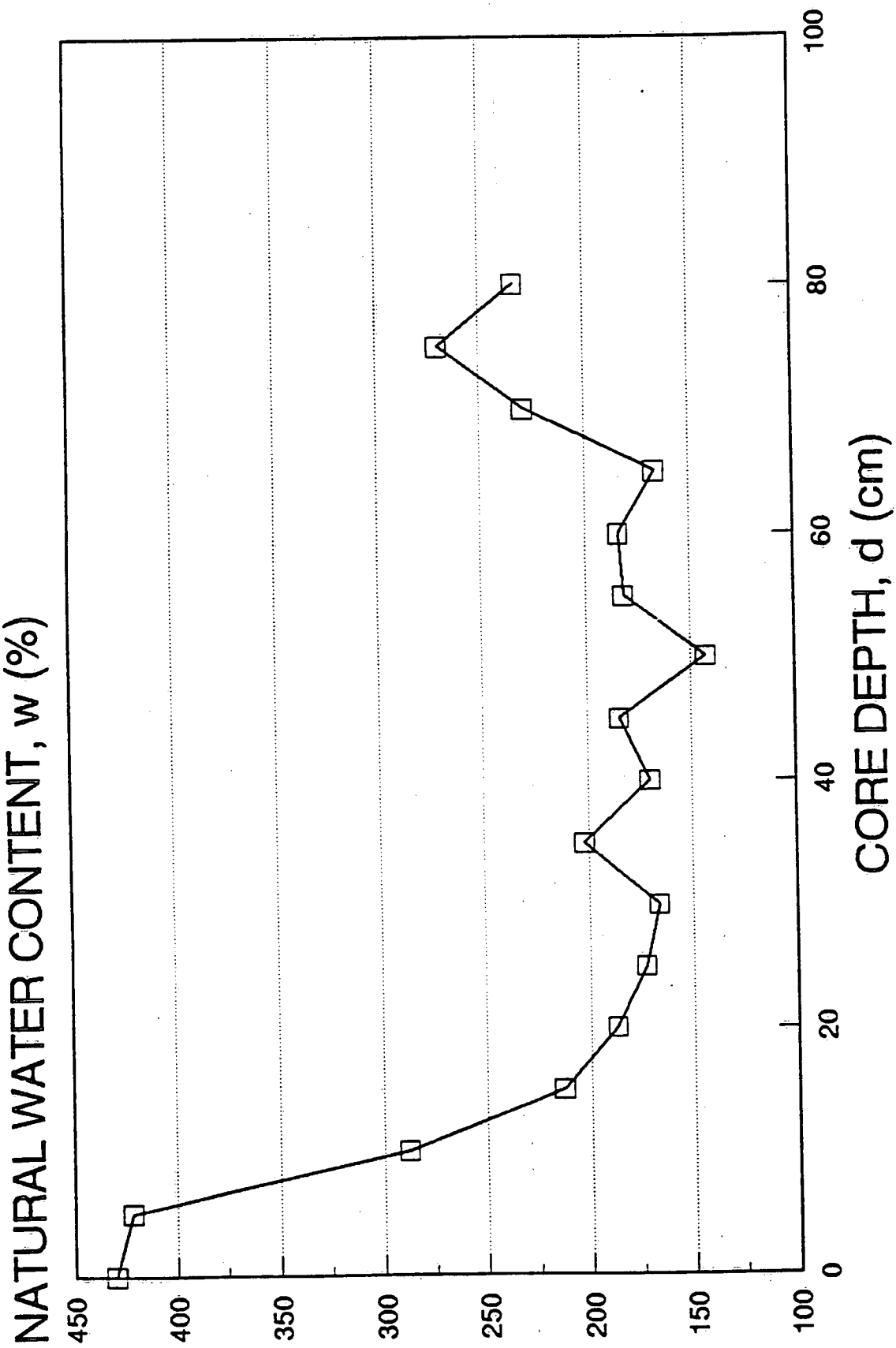
CORE HH2-90
NATURAL WATER CONTENT, w (%)
450
400
350
300
250
200
150
100
0
20
40
60
80
100
CORE DEPTH, d (cm)

Figure 5c

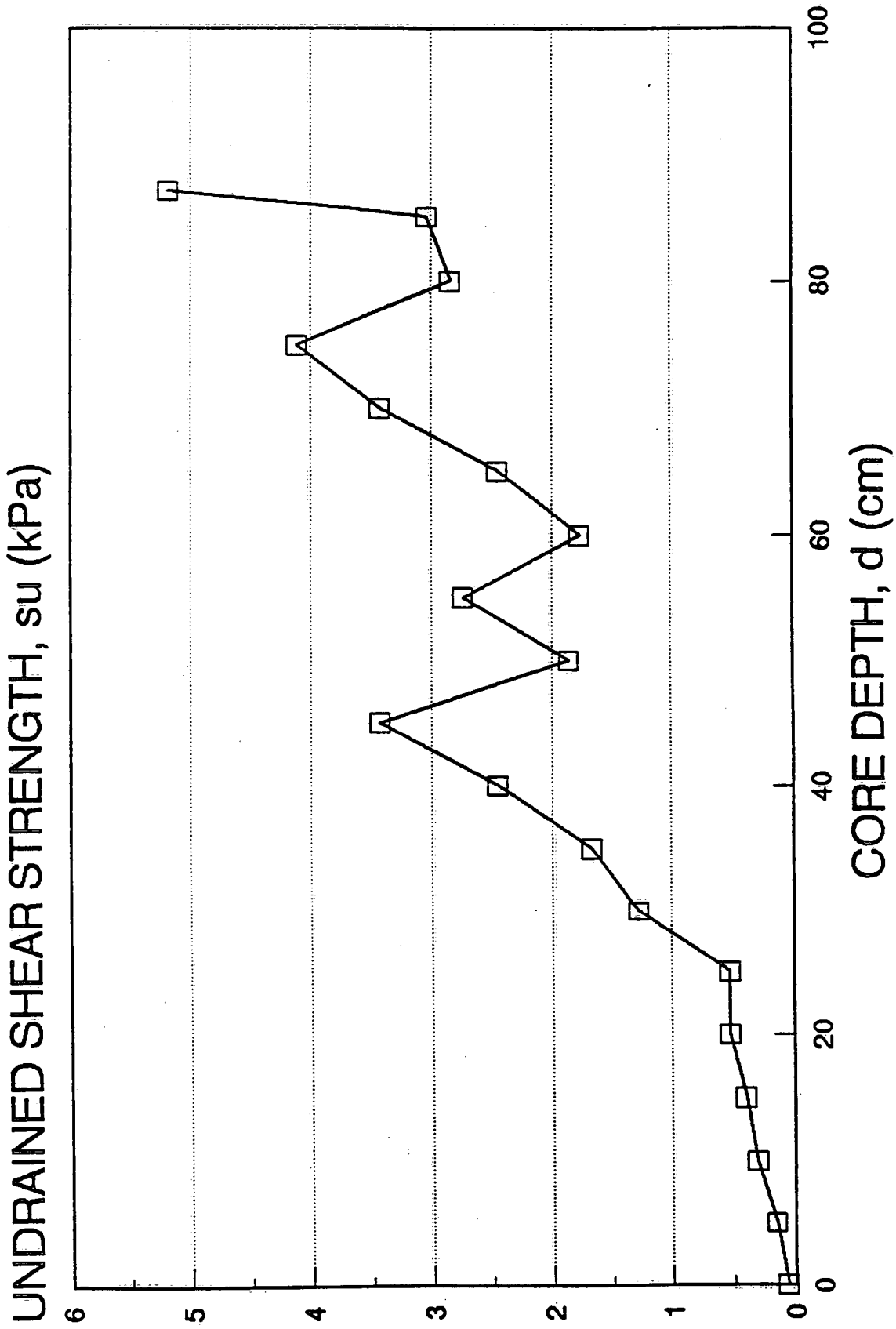
CORE LO-90
UNDRAINED SHEAR STRENGTH, su (kPa)
CORE DEPTH, d (cm)
0
1
2
3
4
5
6
0
20
40
60
80
100

Figure 6a

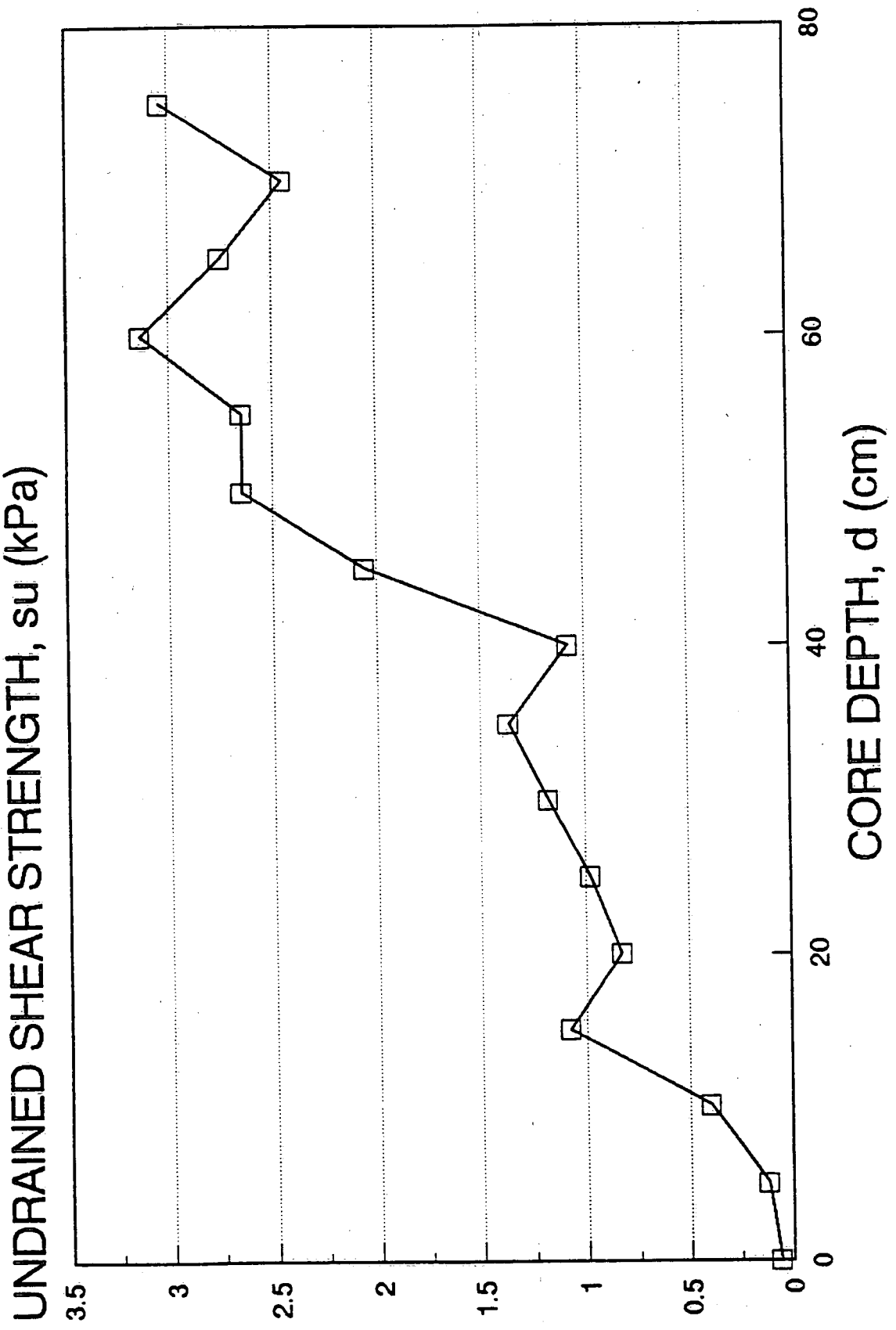
CORE HH1-90
UNDRAINED SHEAR STRENGTH, su (kPa)
3.5
3
2.5
2
1.5
1
0.5
0
0
20
40
60
80
CORE DEPTH, d (cm)

Figure 6b

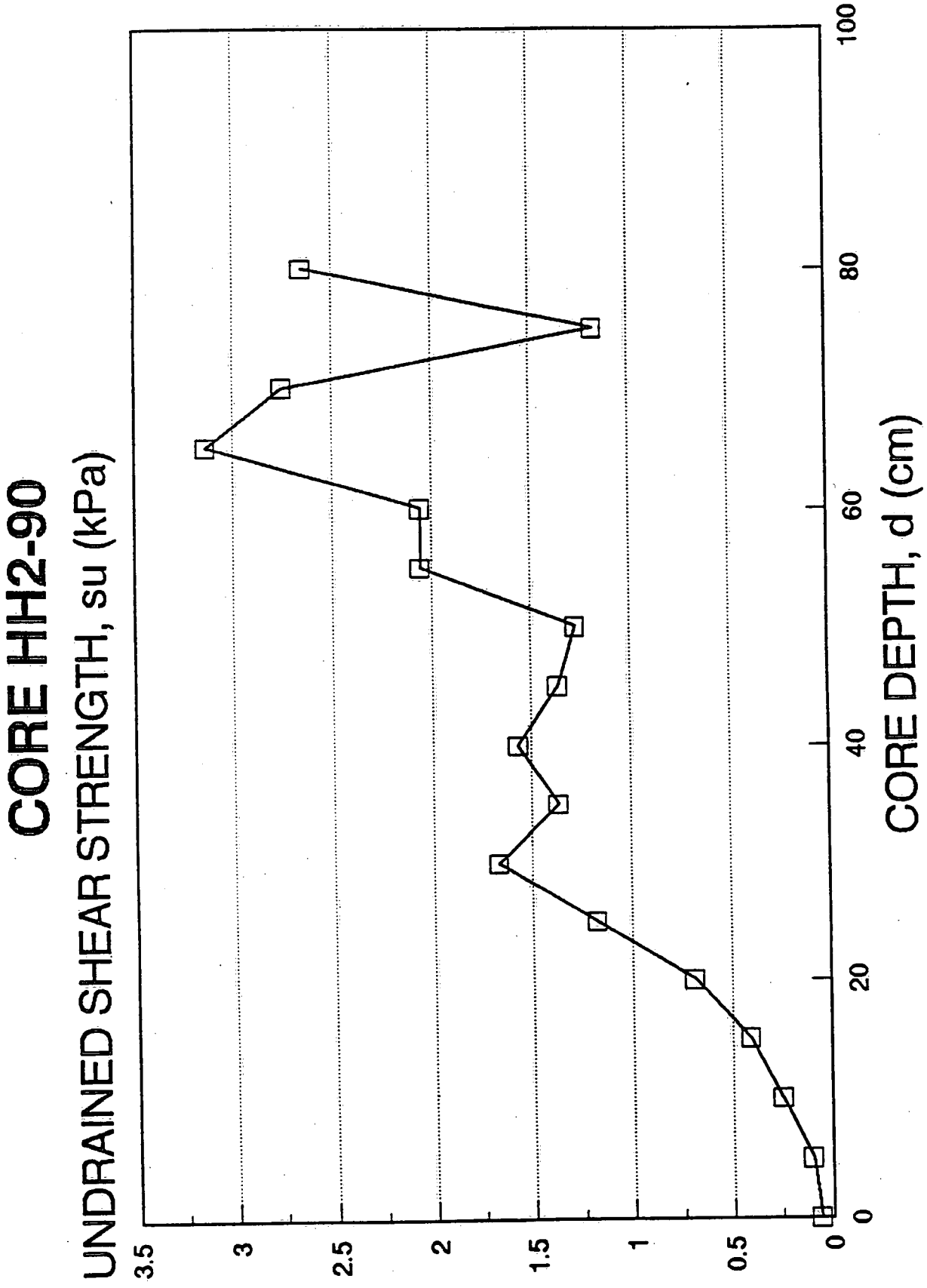
CORE HH2-90
UNDRAINED SHEAR STRENGTH, su (kPa)
CORE DEPTH, d (cm)
0
0.5
1
1.5
2
2.5
3
3.5
0
20
40
60
80
100

Figure 6c

CORE 1

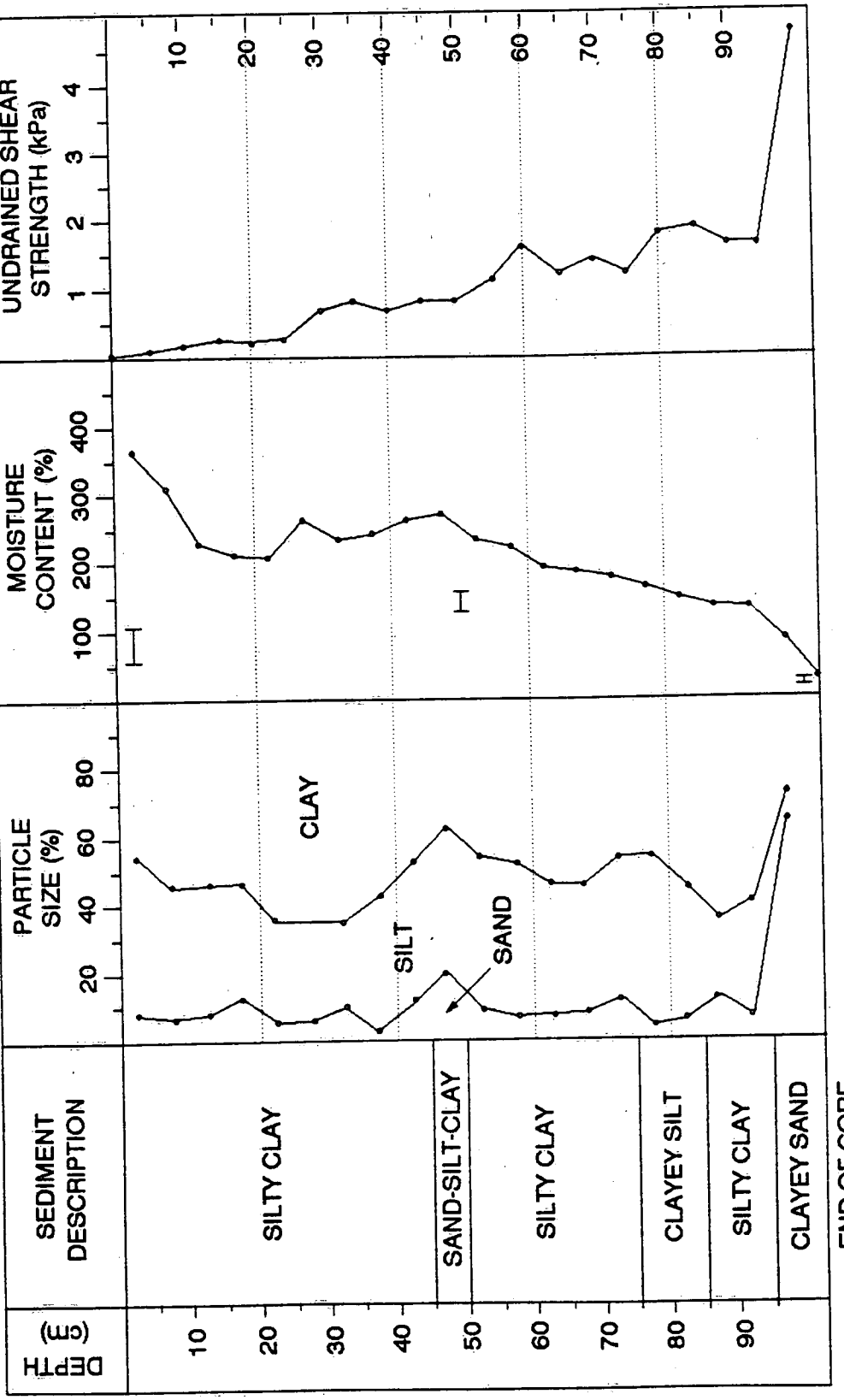

Figure 7a

CORE 2

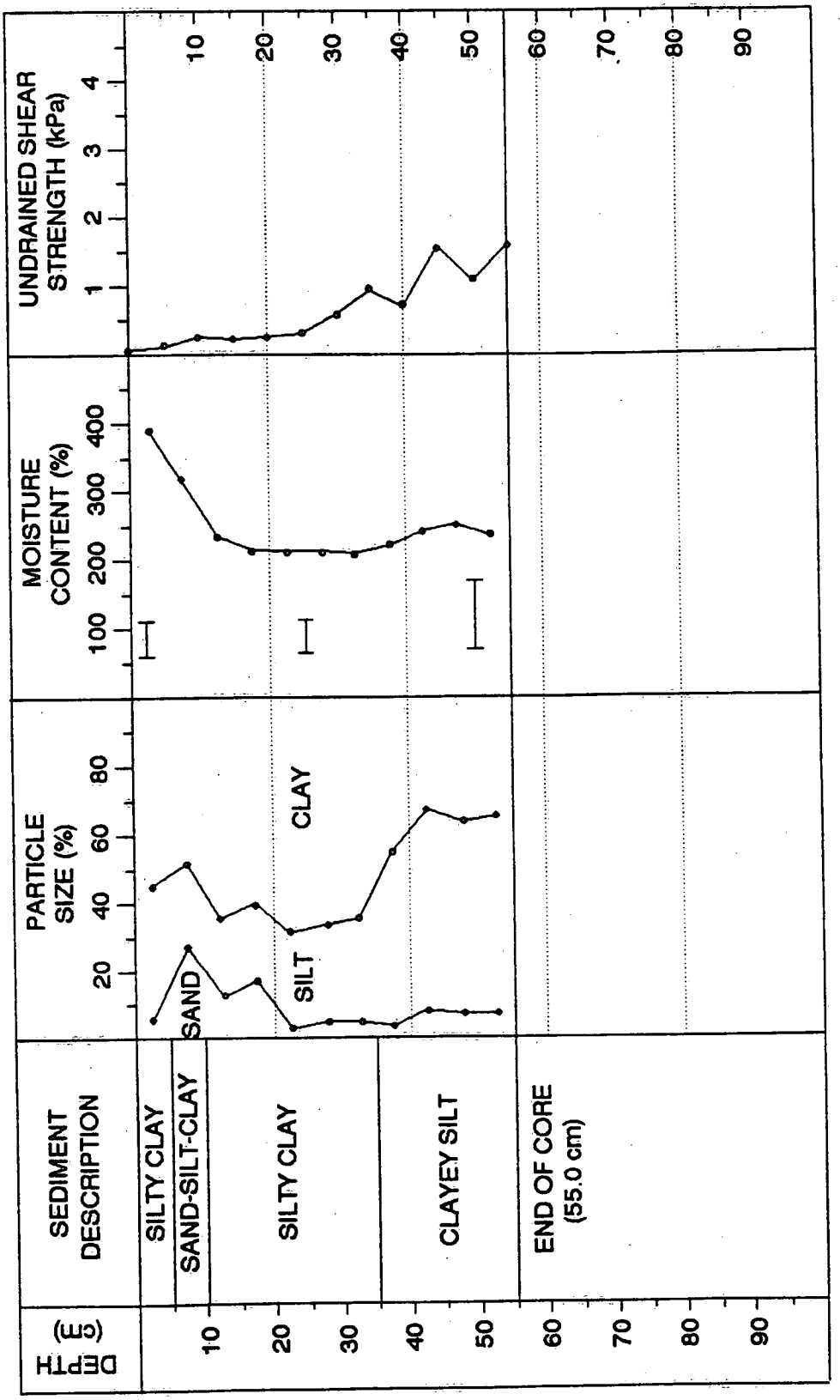

Figure 7b

CORE 2X

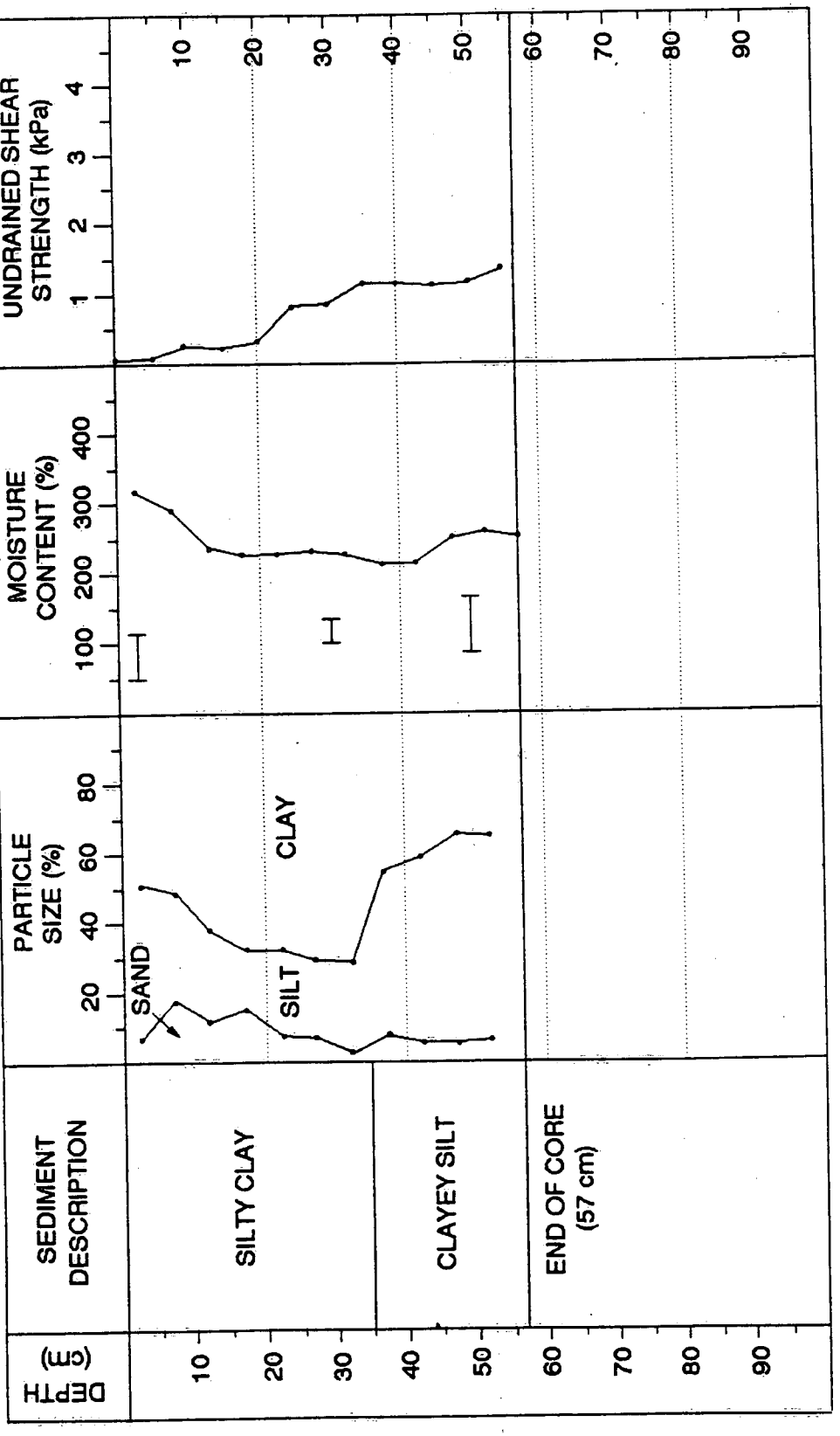

Figure 7c

CORE 3

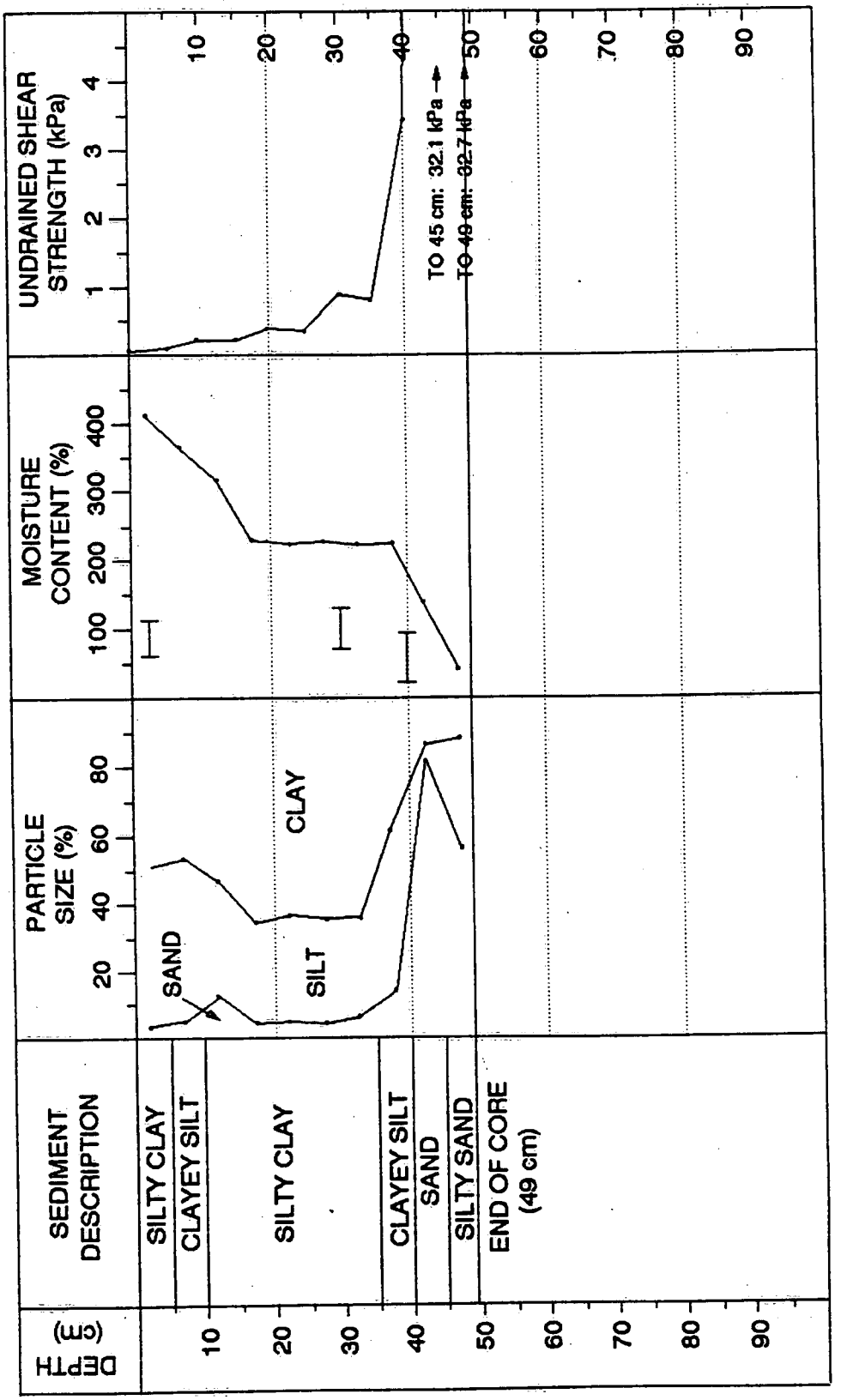

Figure 7d

CORE 4

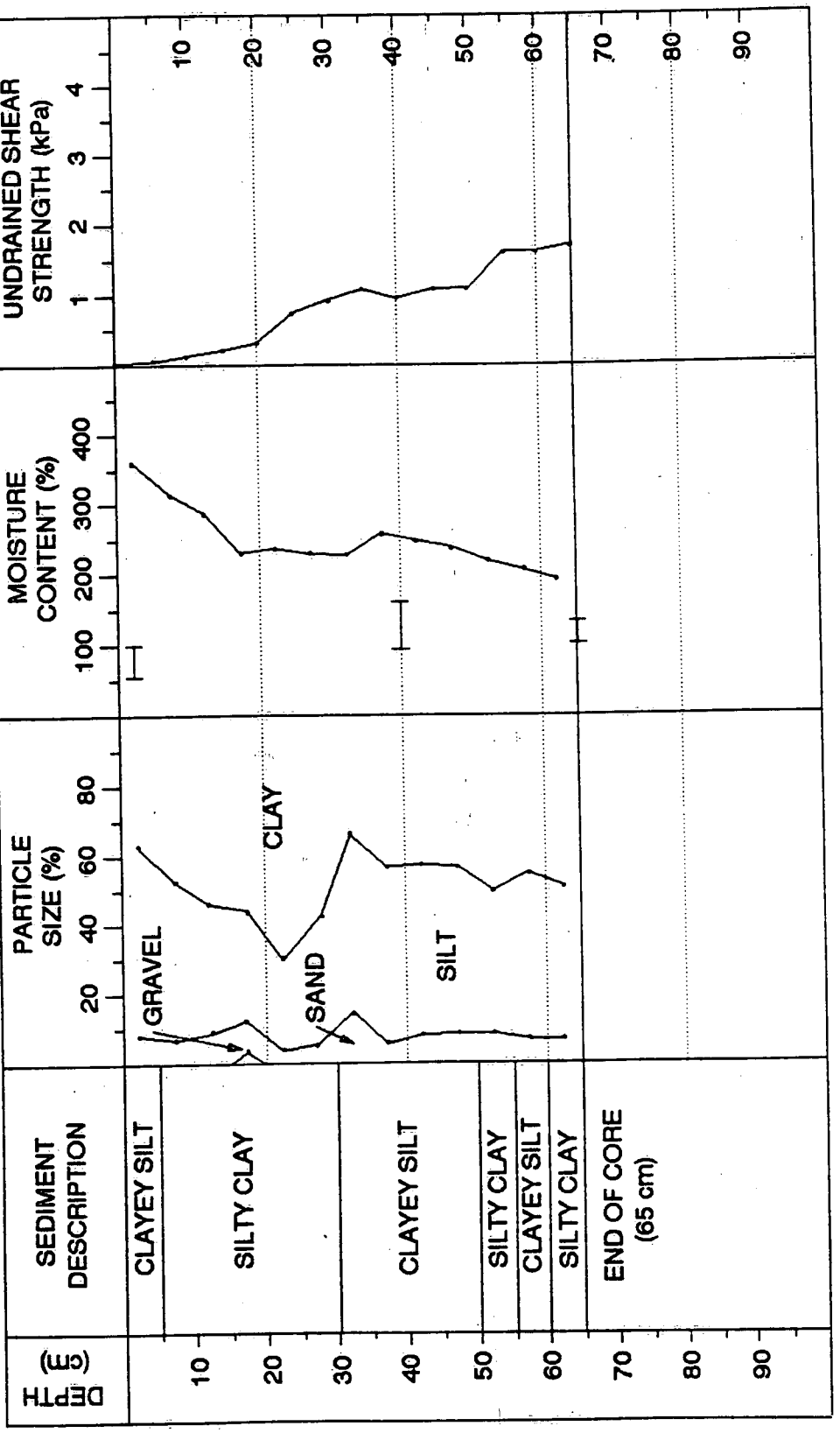

Figure 7e

CORE 5

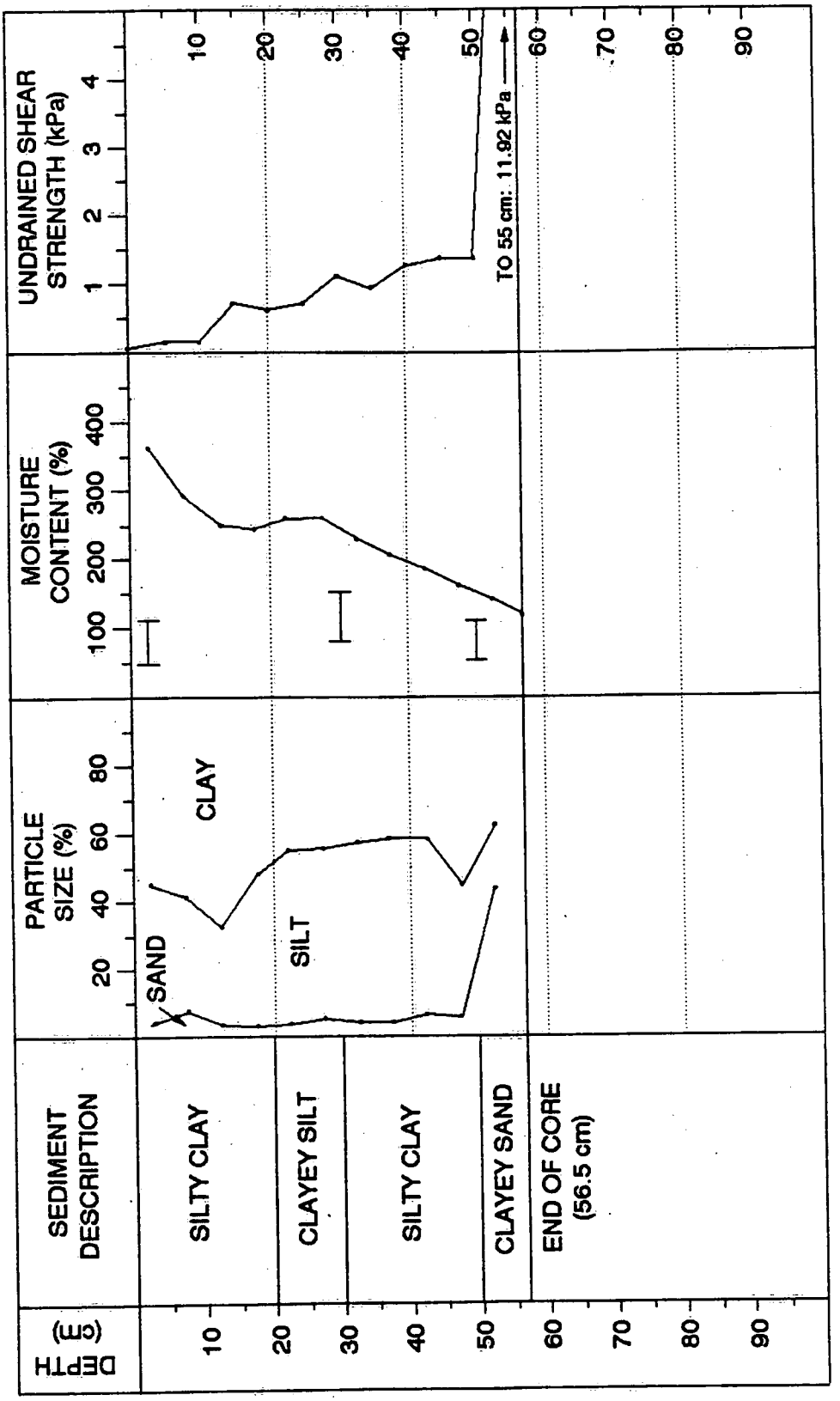

Figure 7f

VOID RATIO VS. EFFECTIVE STRESS

SAMPLE HH1-93

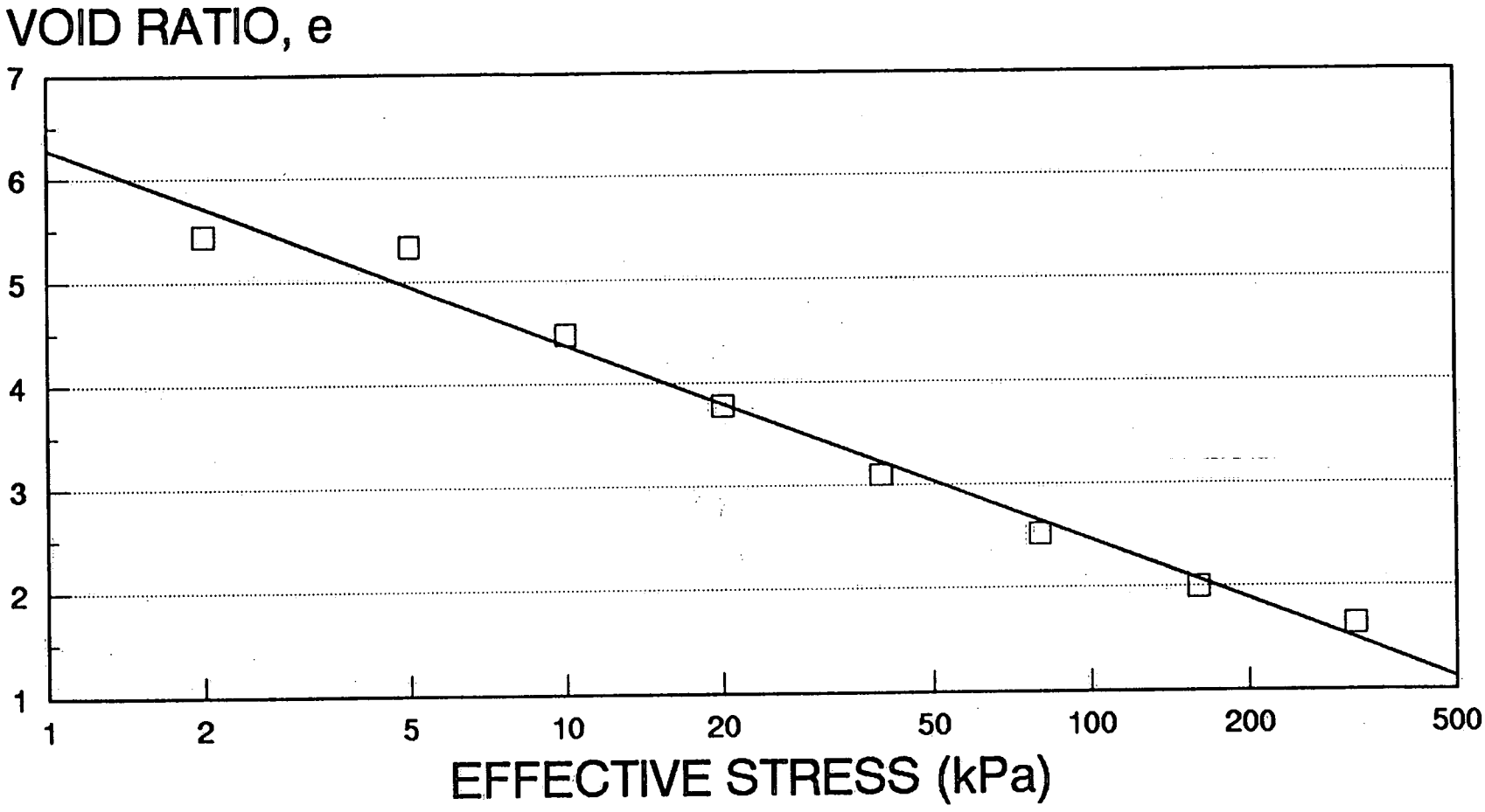

a = 6.2892585
b = -0.831560
r^2 = 0.9807552

Figure 8

VOID RATIO VS. PERMEABILITY

SAMPLE HH1-93

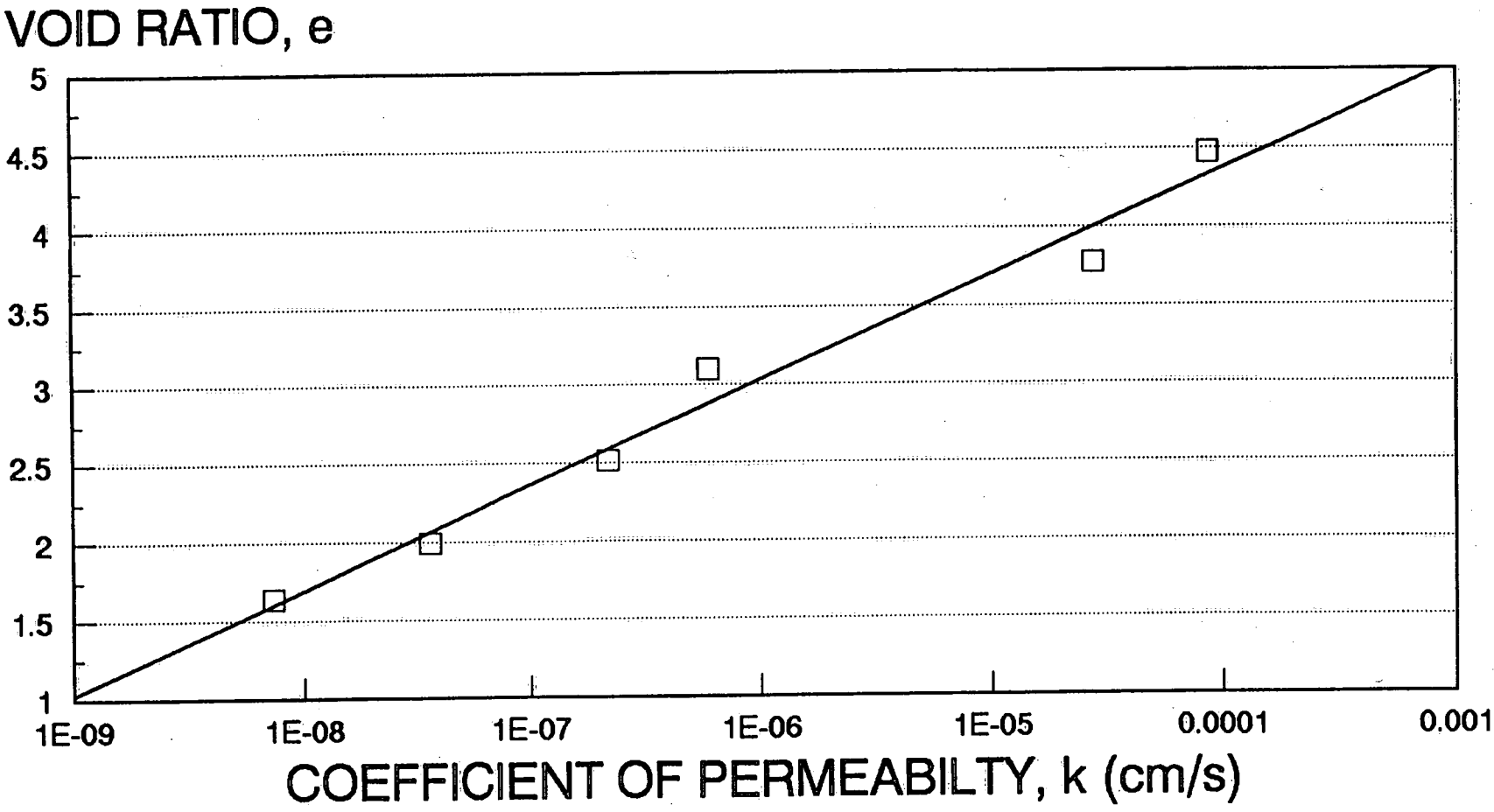

a = 7.0619328
b = 0.2912742
r^2 = 0.9776647

Figure 9

VOID RATIO - EFFECTIVE STRESS RELATIONSHIP

E - LN SIGMA CURVES (TEST DATA)

SAMPLES LO-90, HH-1-90, HH-2-90, HH-1-93

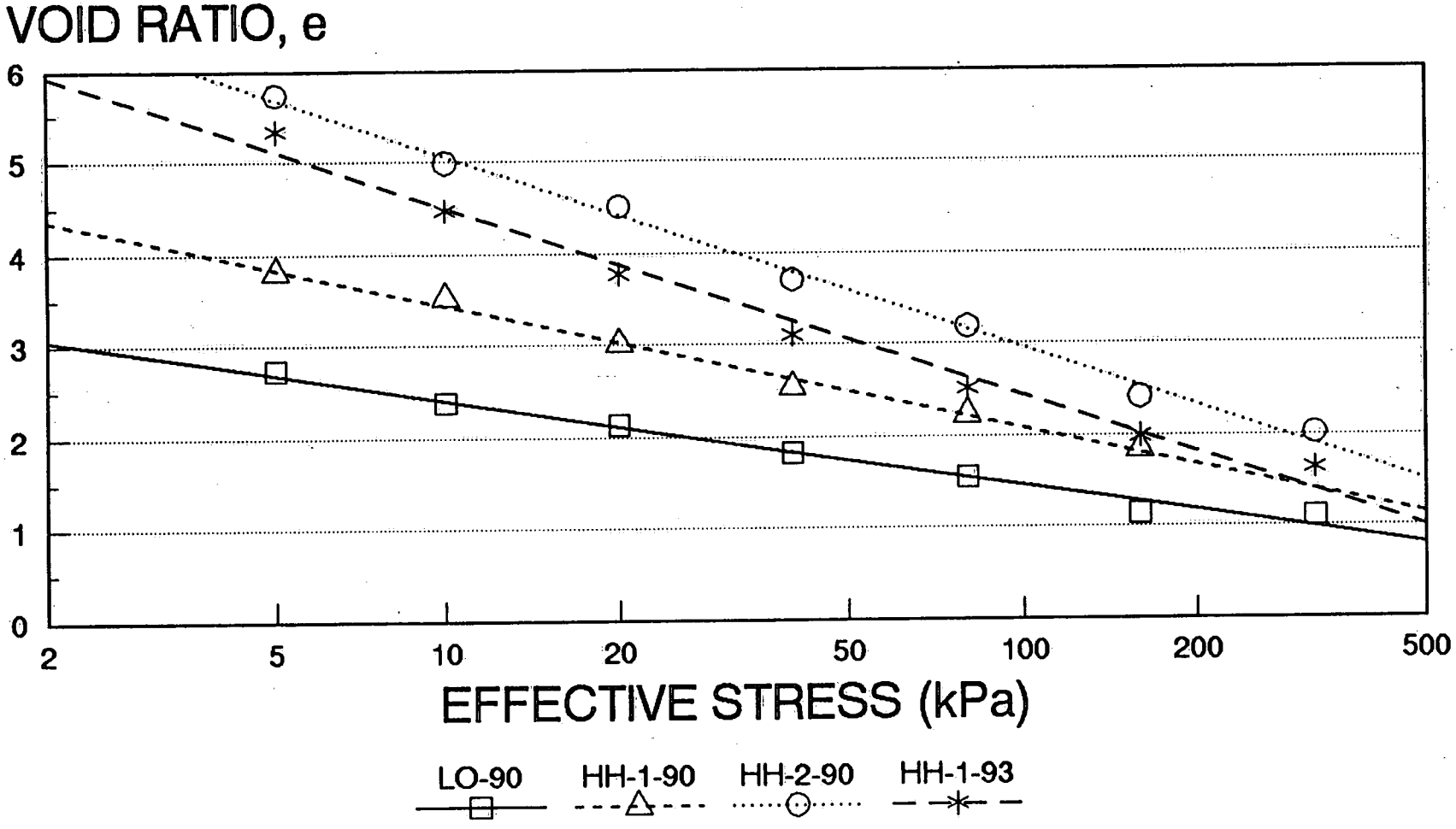

Figure 10

VOID RATIO - COEF. OF PERMEABILITY RELATIONSHIP

E - LN K CURVES (TEST DATA)

SAMPLES LO-90, HH-1-90, HH-2-90, HH-1-93

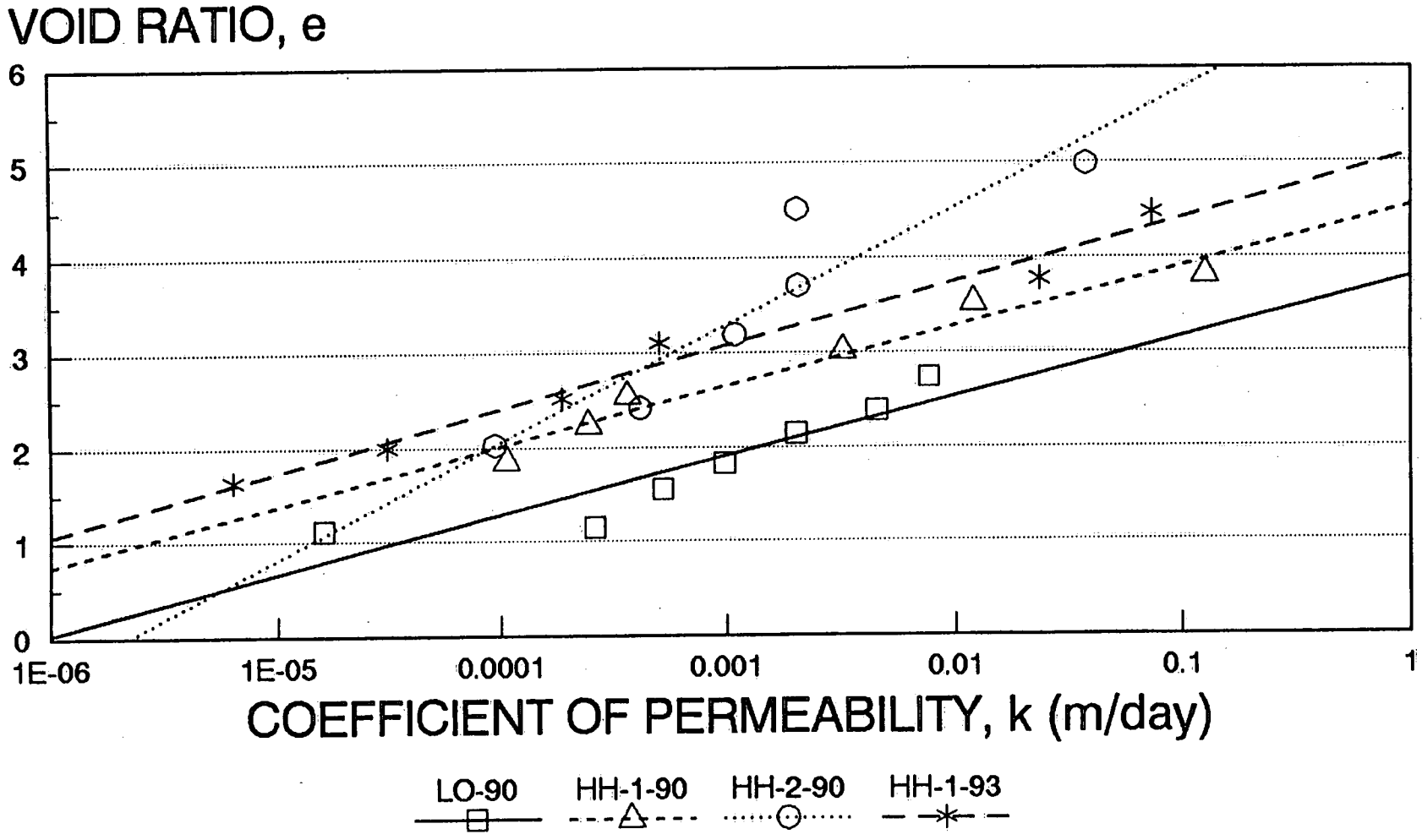

Figure 11

COMPRESSION INDEX VALUES

SAMPLES LO-90, HH-1-90, HH-2-90, HH-1-93

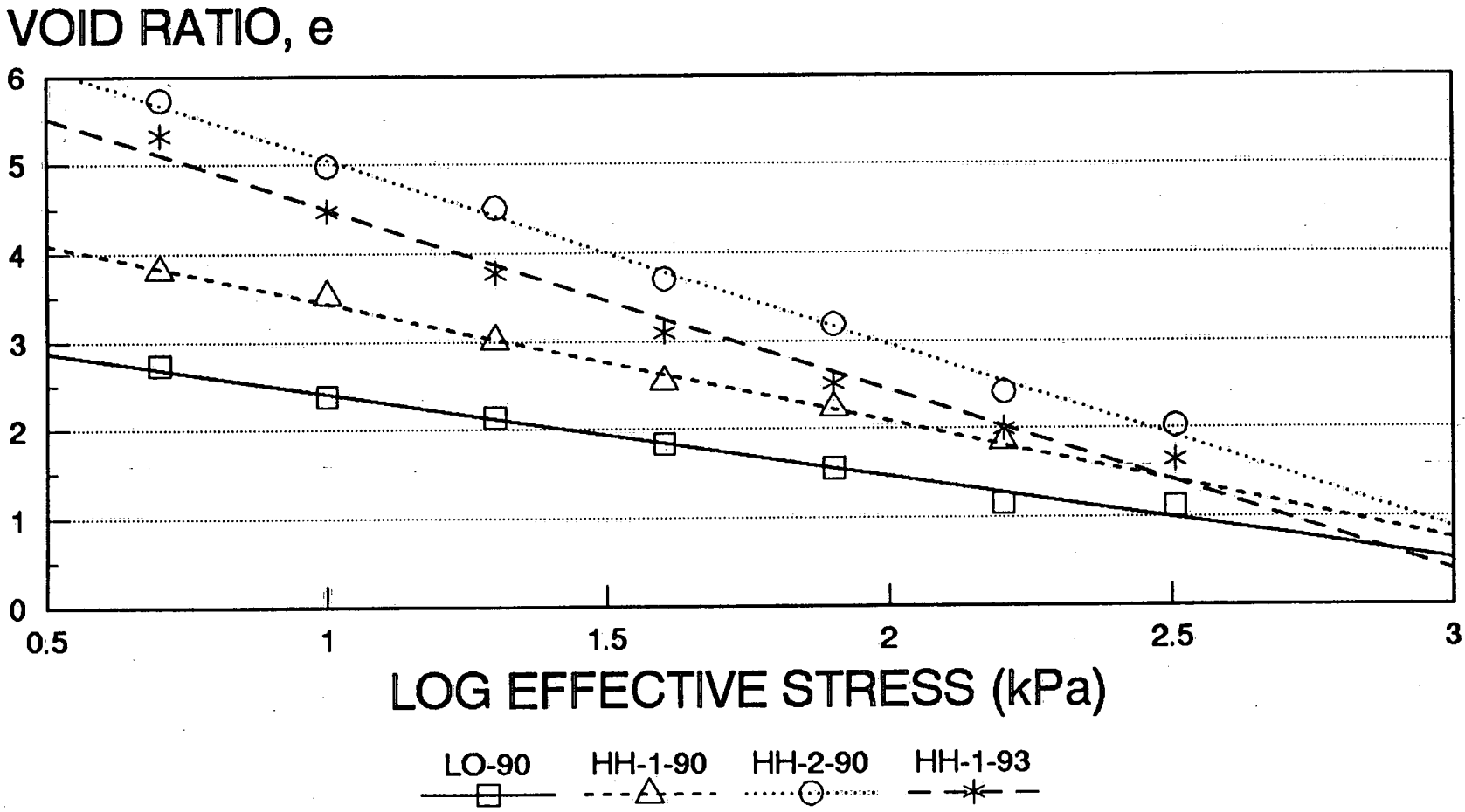

COMPRESSION INDEX VALUES:
LO-90: 0.940; HH-1-90: 1.343; HH-2-90: 2.088;
HH-1-93: 2.054

Figure 12

EFFECTIVE VERTICAL STRESS

CAPPING SITE CORES NOS. 1 TO 5

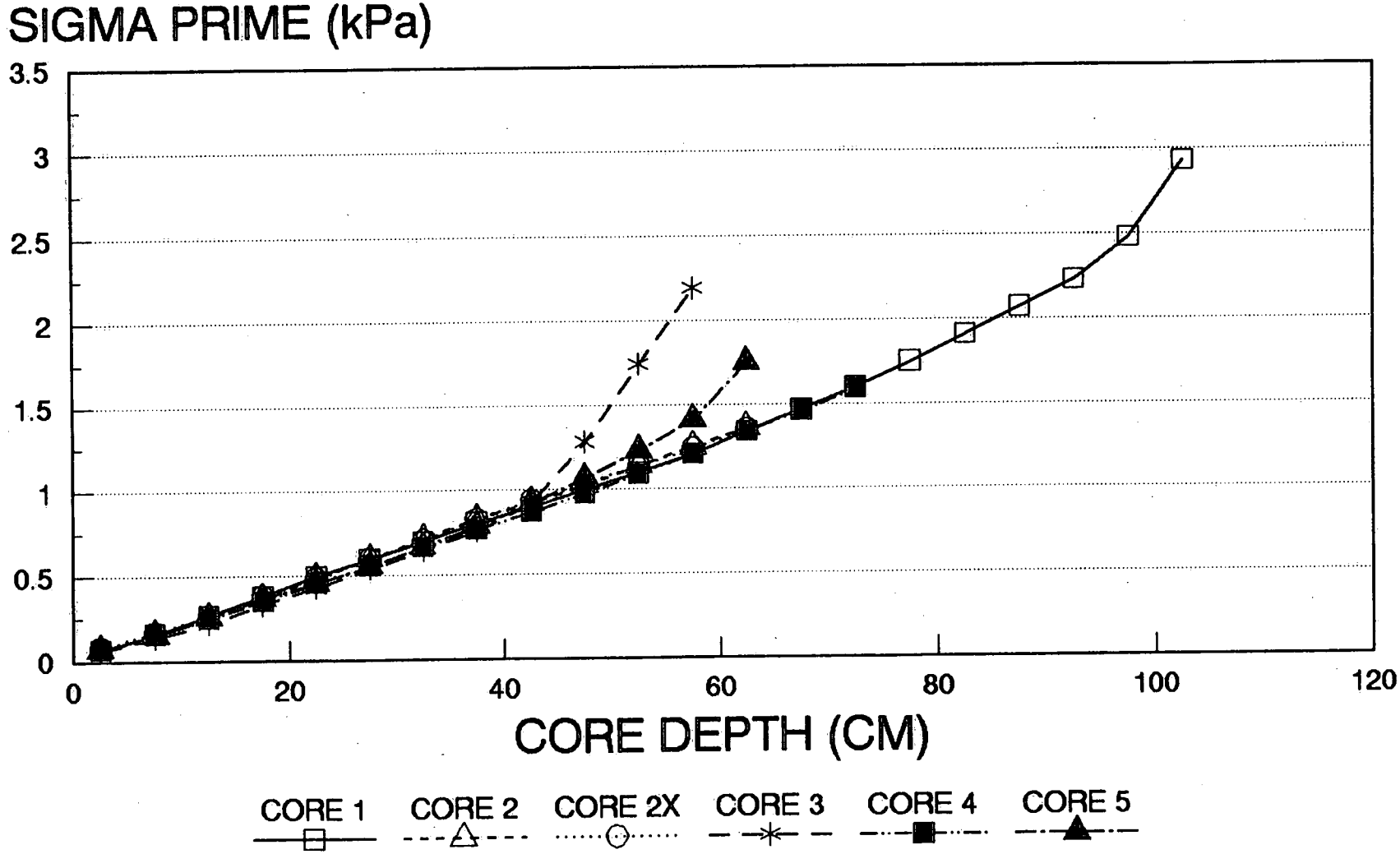

Figure 13

SETTLEMENT - FINITE STRAIN

CORES 1-5; HH CAPPING SITE

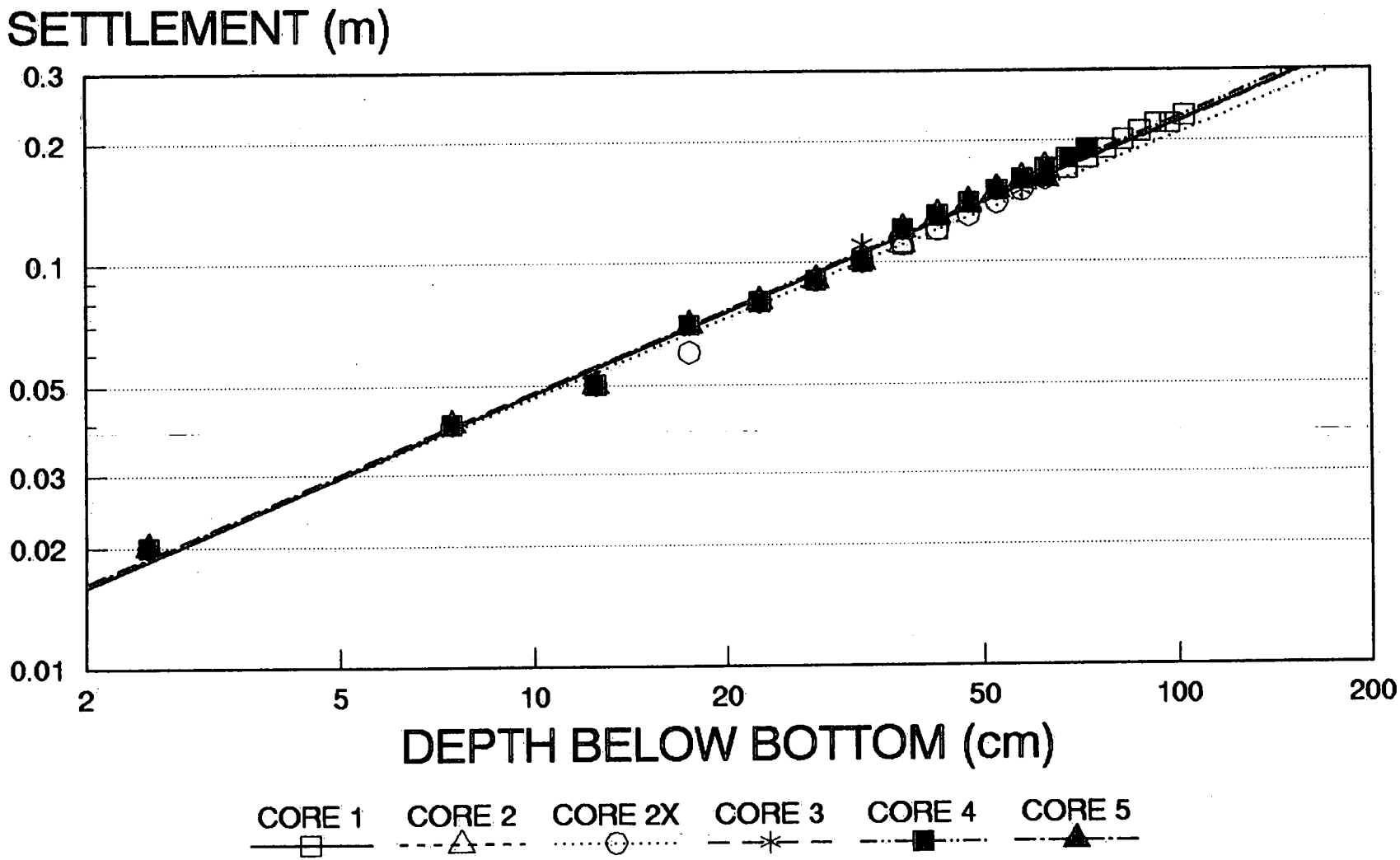

Figure 14

SAMPLE LO-90 (5 kPa)

DIAL DEFLECTION VS. TIME

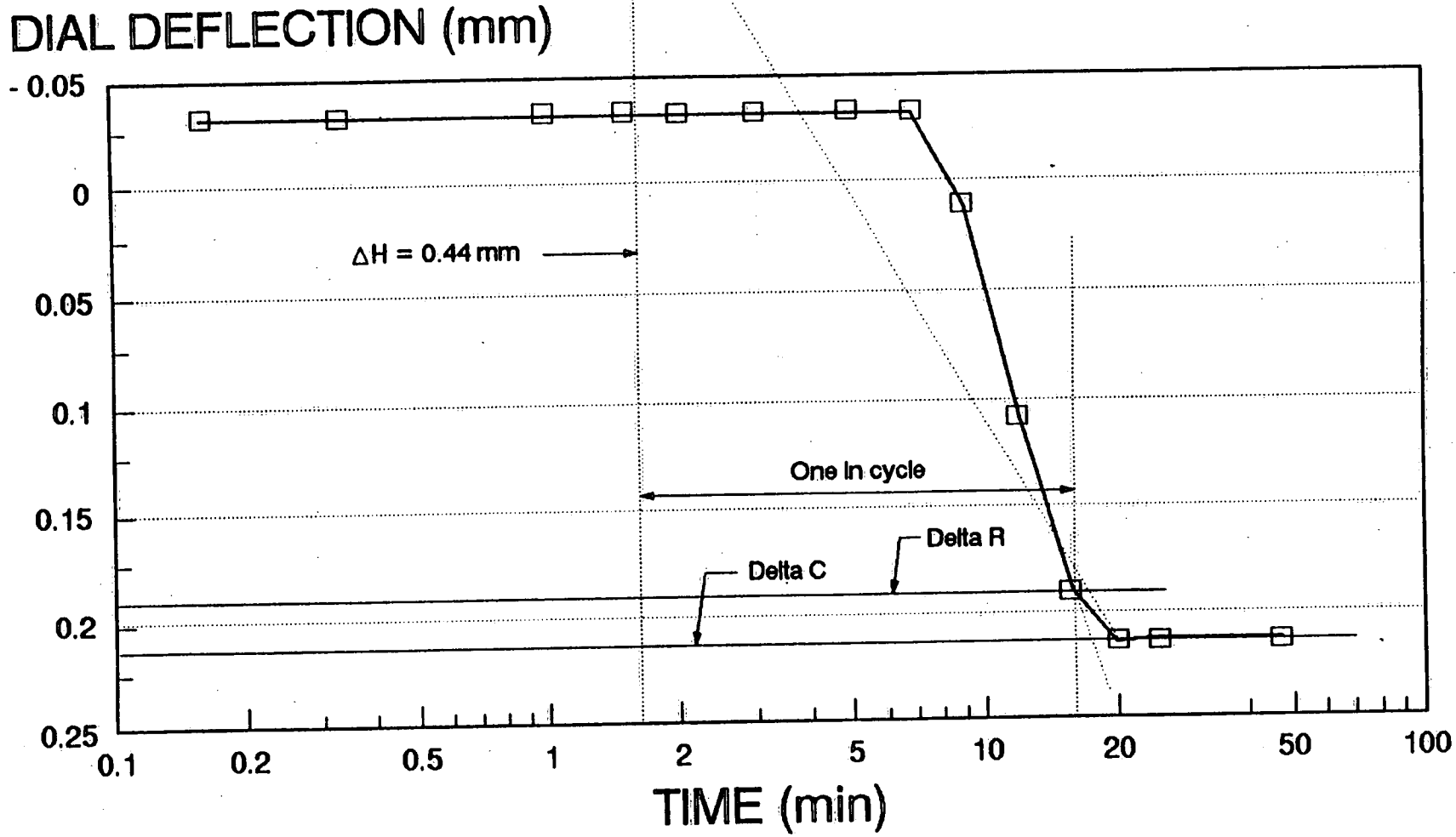

Delta R = 0.191 mm
Delta C = 0.214 mm

Figure 15a

SAMPLE LO-90 (10 kPa)

DIAL DEFLECTION VS. TIME

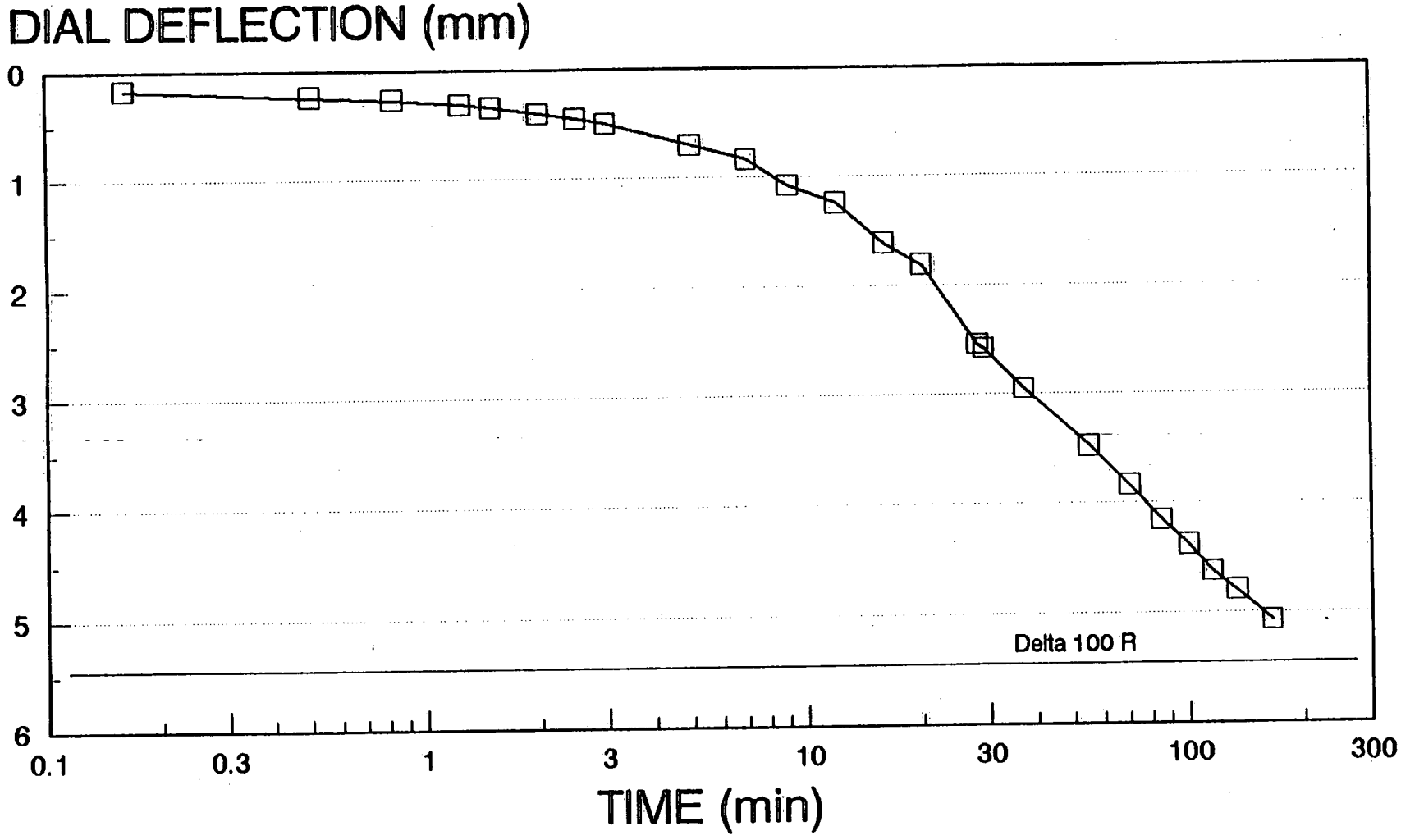

Delta 100 R = 5.47 mm

Figure 15b

SAMPLE LO-90 (20 kPa)

DIAL DEFLECTION VS. TIME

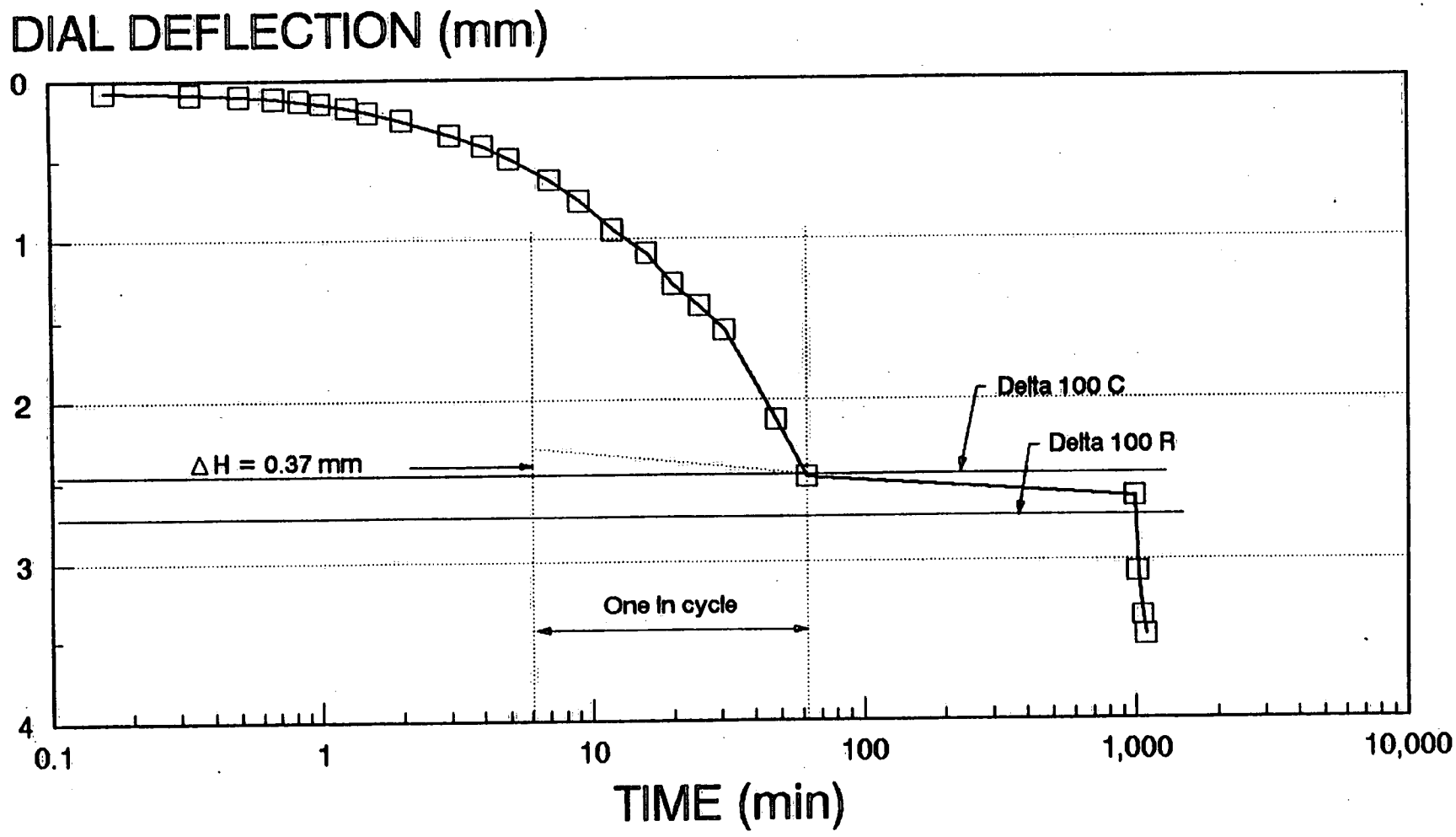

Delta R = 2.75 mm (ΔH undetermined)
Delta C = 2.47 mm

Figure 15c

SAMPLE LO-90 (40 kPa)

DIAL DEFLECTION VS. TIME

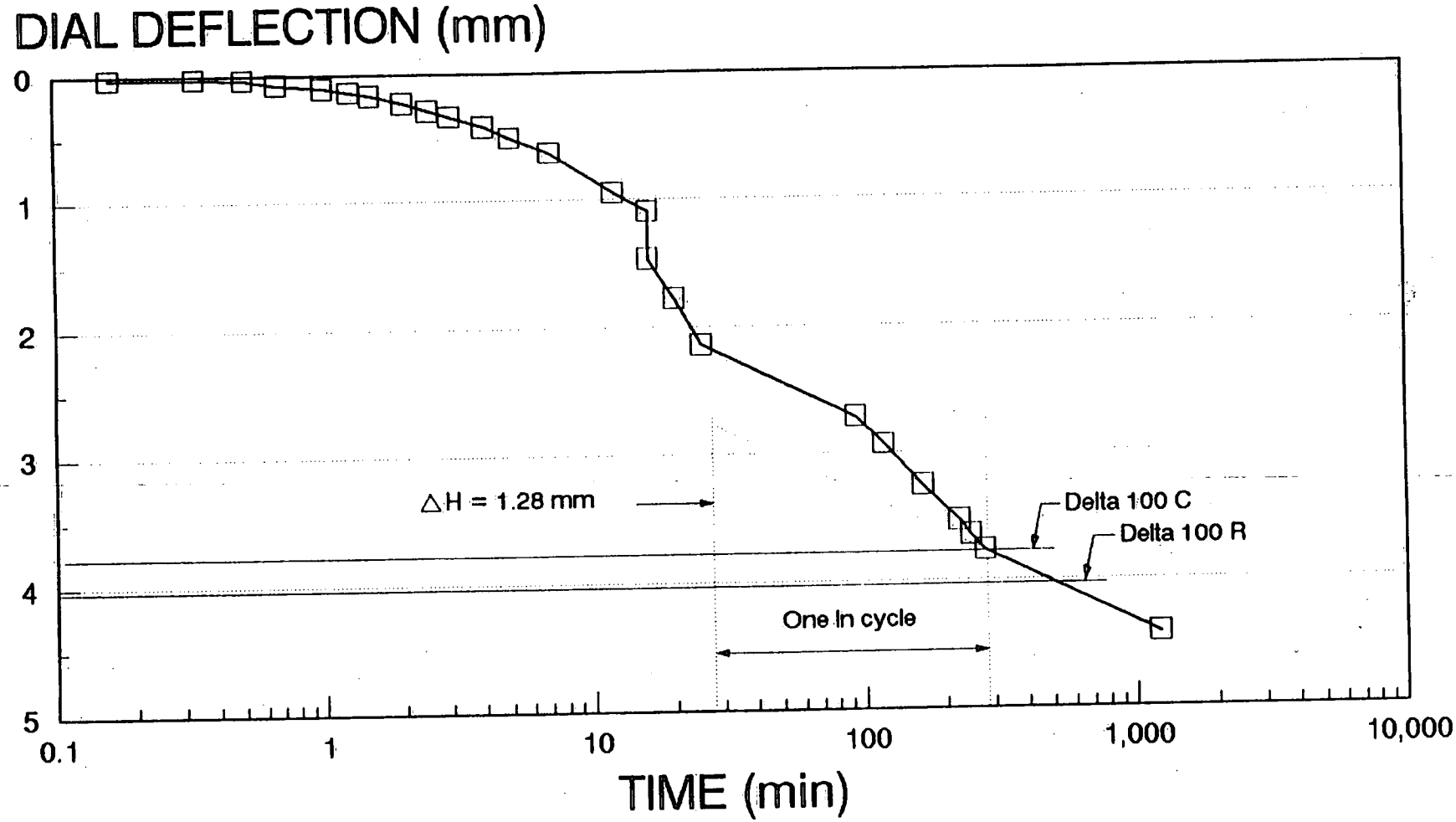

Figure 15d

Delta 100 R = 4.02 mm
Delta 100 C = 3.80 mm

SAMPLE LO-90 (80 kPa)

DIAL DEFLECTION VS. TIME

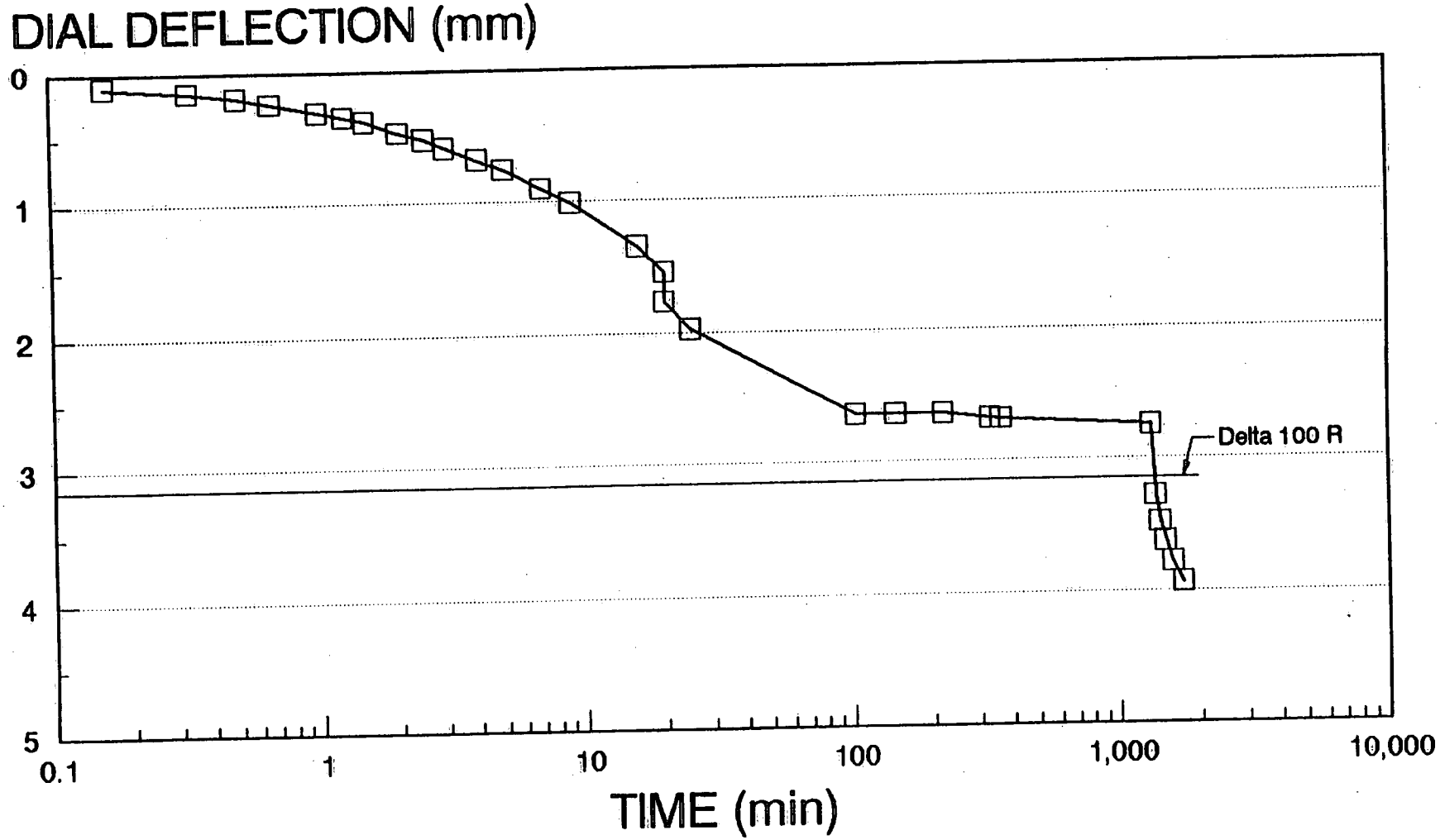

Delta 100 R = 3.18 mm (ΔH undetermined)

Figure 15e

SAMPLE LO-90 (160 kPa)

DIAL DEFLECTION VS. TIME

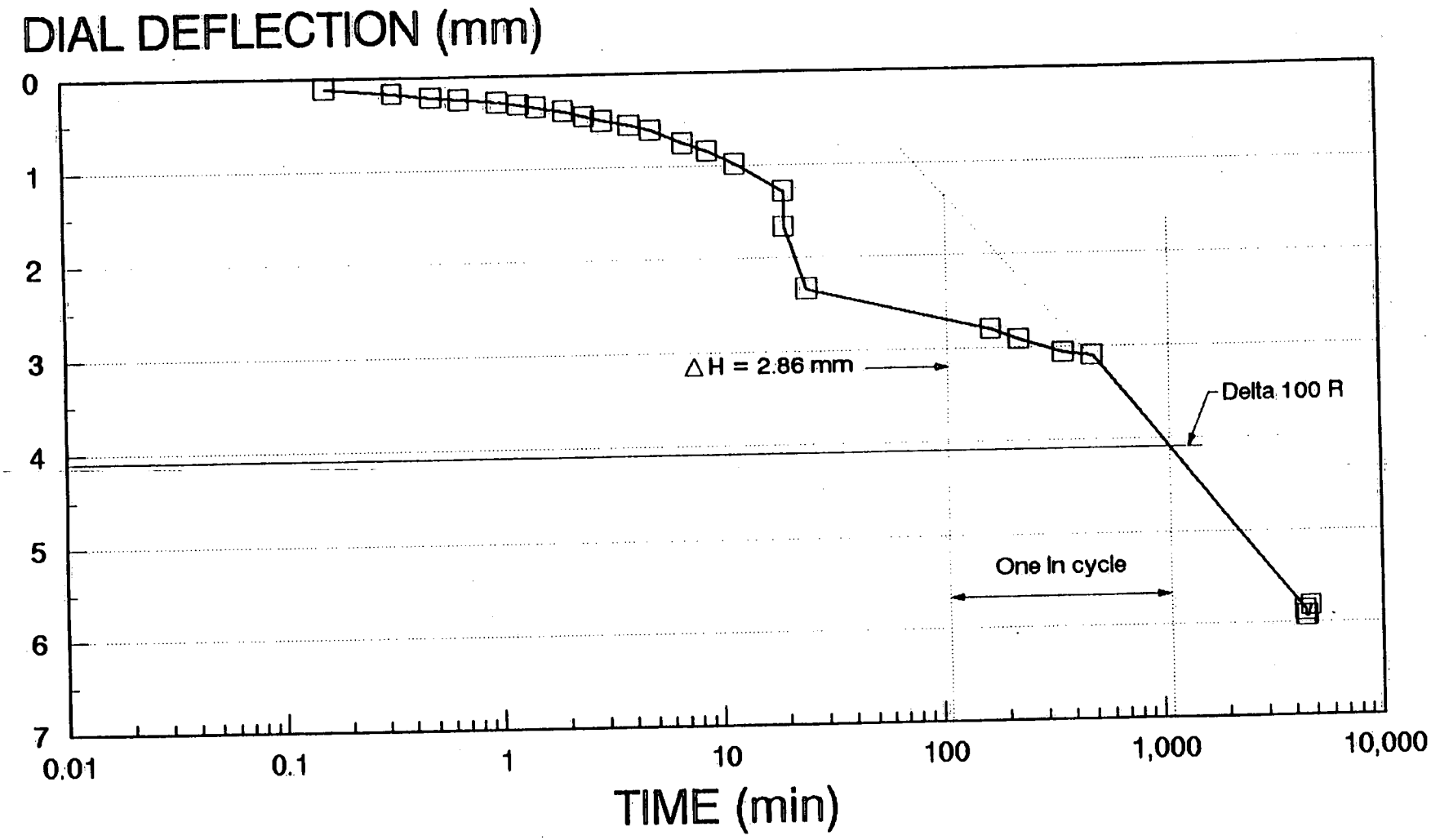

Delta 100 R = 4.13 mm

Figure 15f

SAMPLE LO-90 (320 kPa)

DIAL DEFLECTION VS. TIME

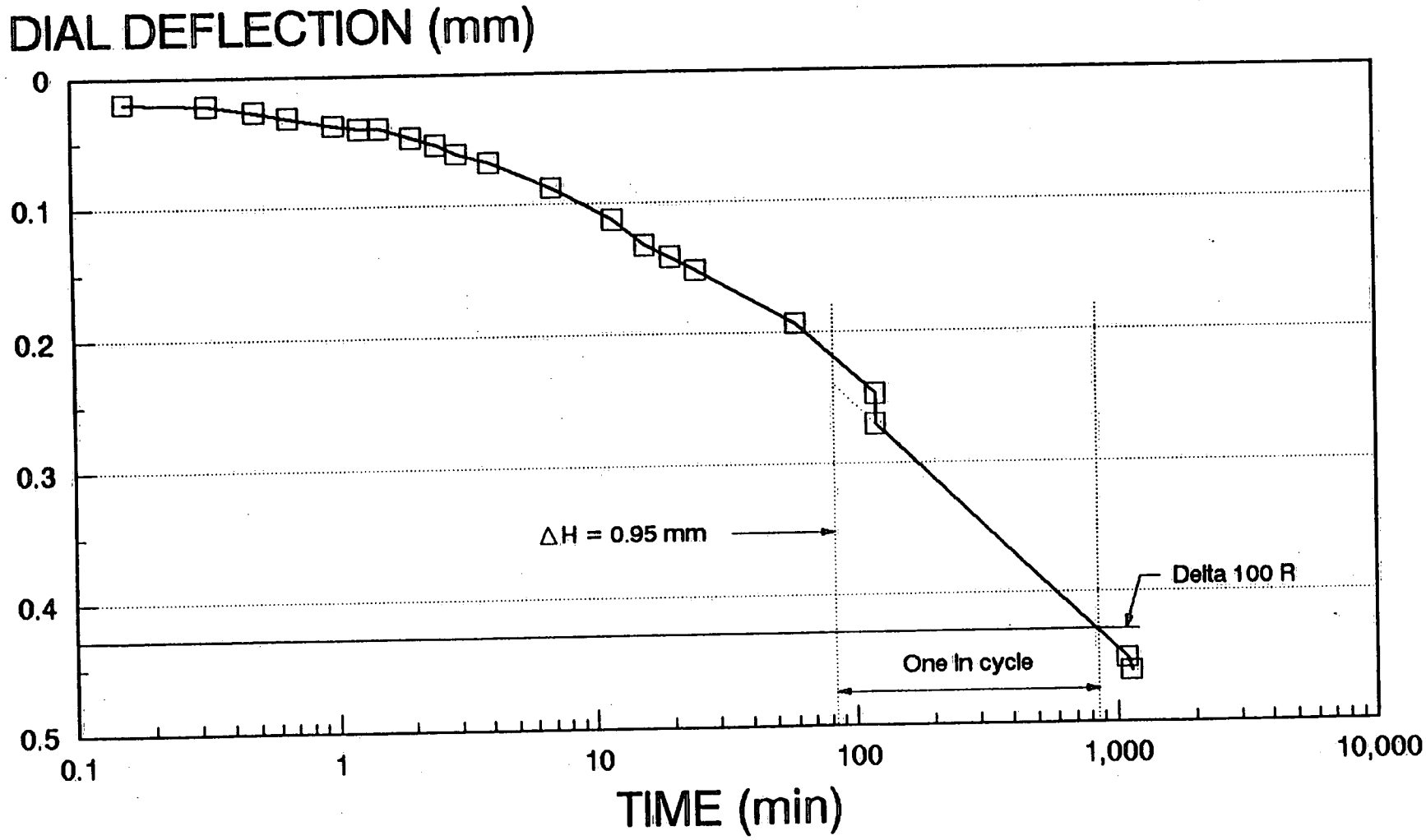

Delta 100 R = 0.429 mm

Figure 15g

SAMPLE HH-1-90 (5 kPa)

DIAL DEFLECTION VS. TIME

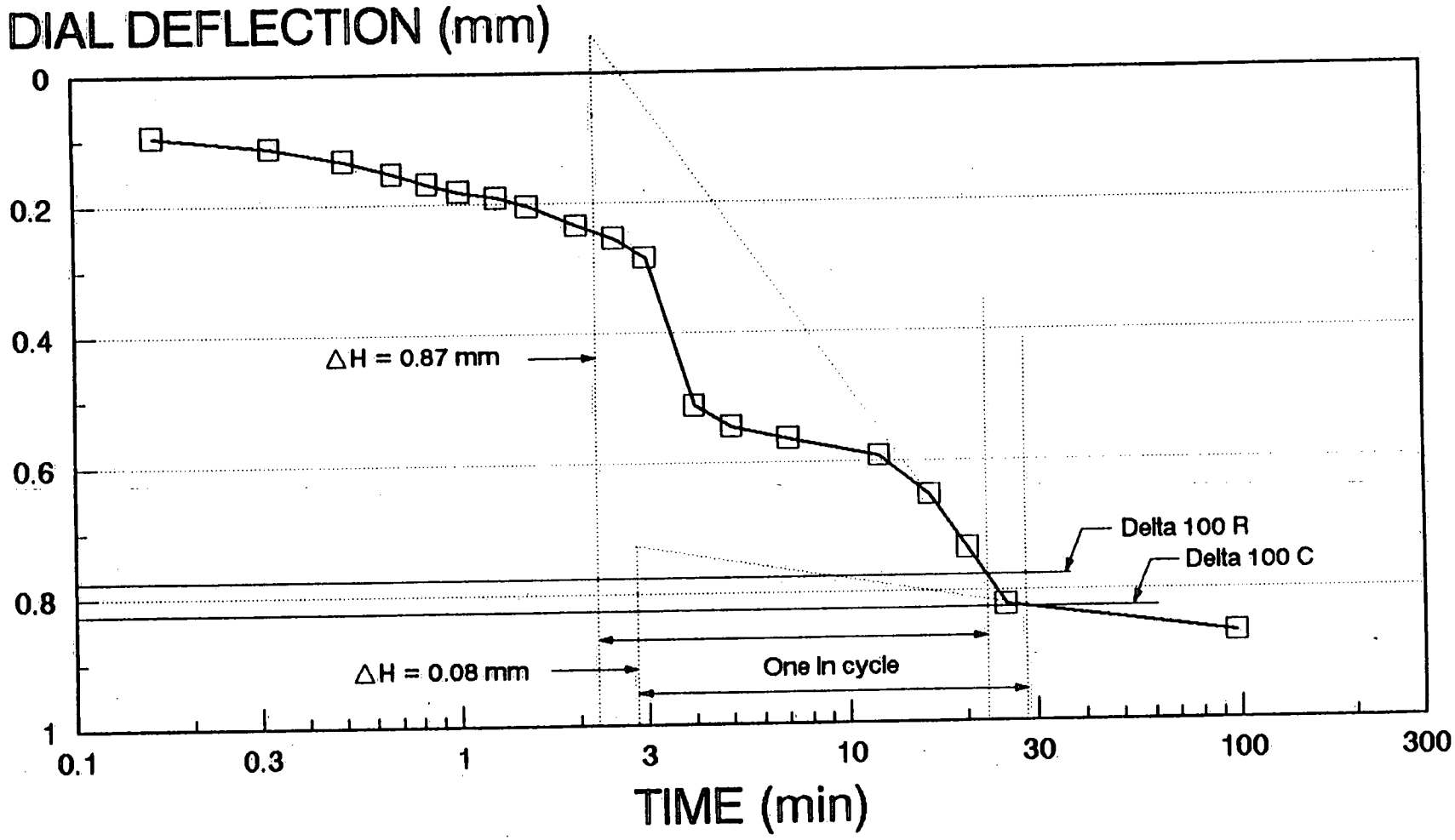

Delta 100 R = 0.78 mm
Delta 100 C = 0.82 mm

Figure 16a

SAMPLE HH-1-90 (10 kPa)

DIAL DEFLECTION VS. TIME

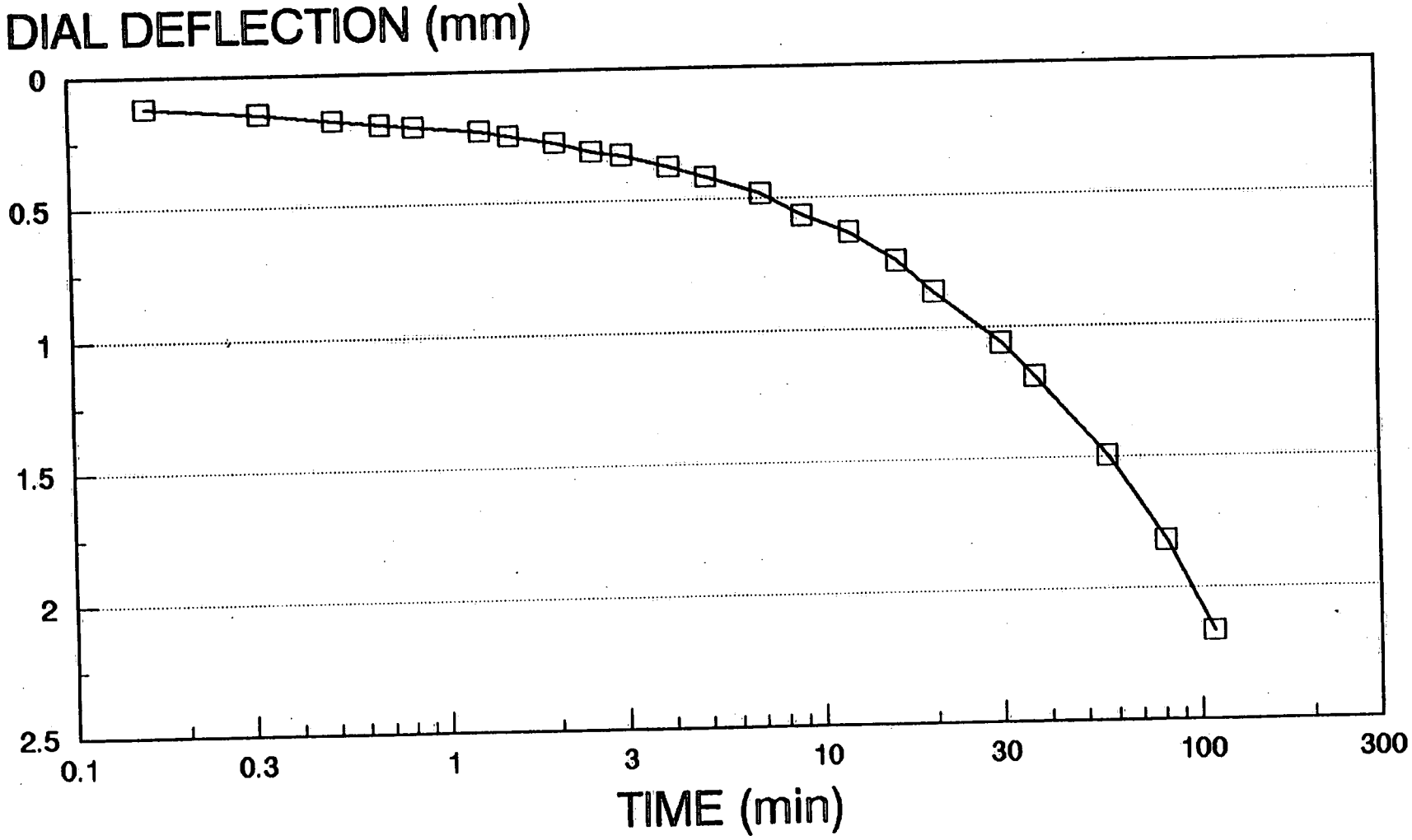

Delta 100 R = 2.65 mm (not shown)

Figure 16b

SAMPLE HH-1-90 (20 kPa)

DIAL DEFLECTION VS. TIME

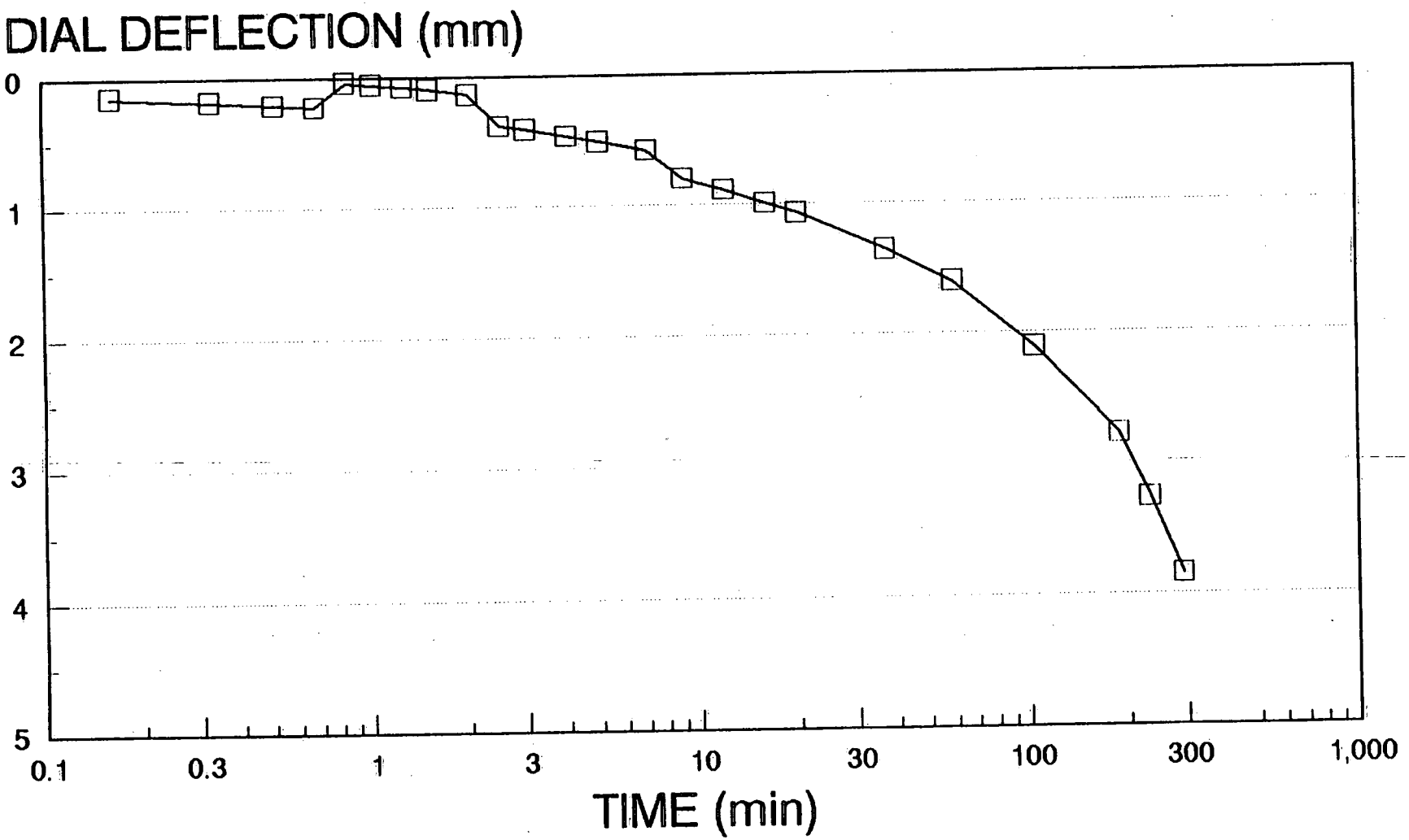

Delta 100 R = 4.51 mm (not shown)

Figure 16c

SAMPLE HH-1-90 (40 kPa)

DIAL DEFLECTION VS. TIME

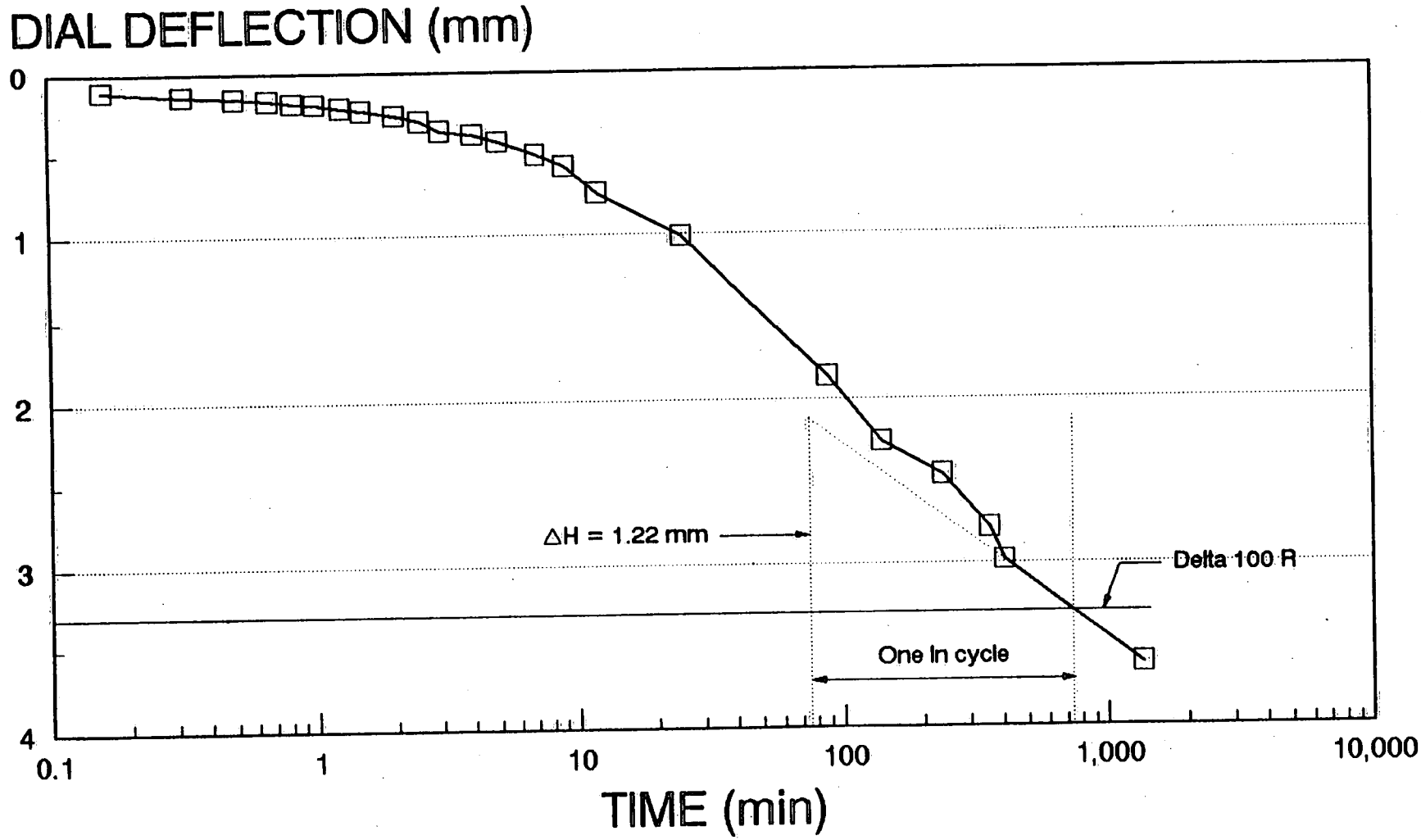

Delta 100 R = 3.46 mm

Figure 16d

SAMPLE HH-1-90 (80 kPa)

DIAL DEFLECTION VS. TIME

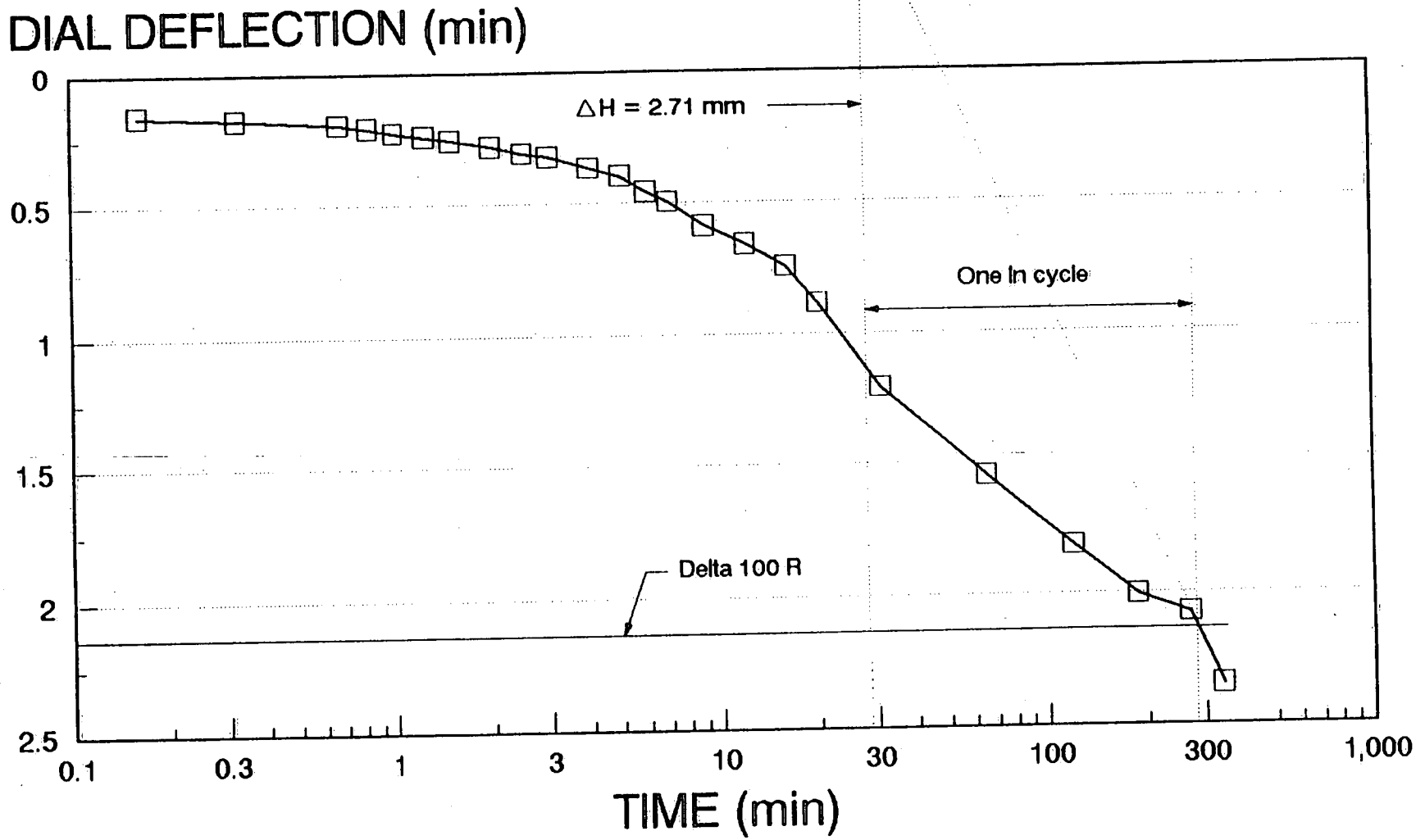

Delta 100 R = 2.17 mm

Figure 16e

SAMPLE HH-1-90 (160 kPa)

DIAL DEFLECTION VS. TIME

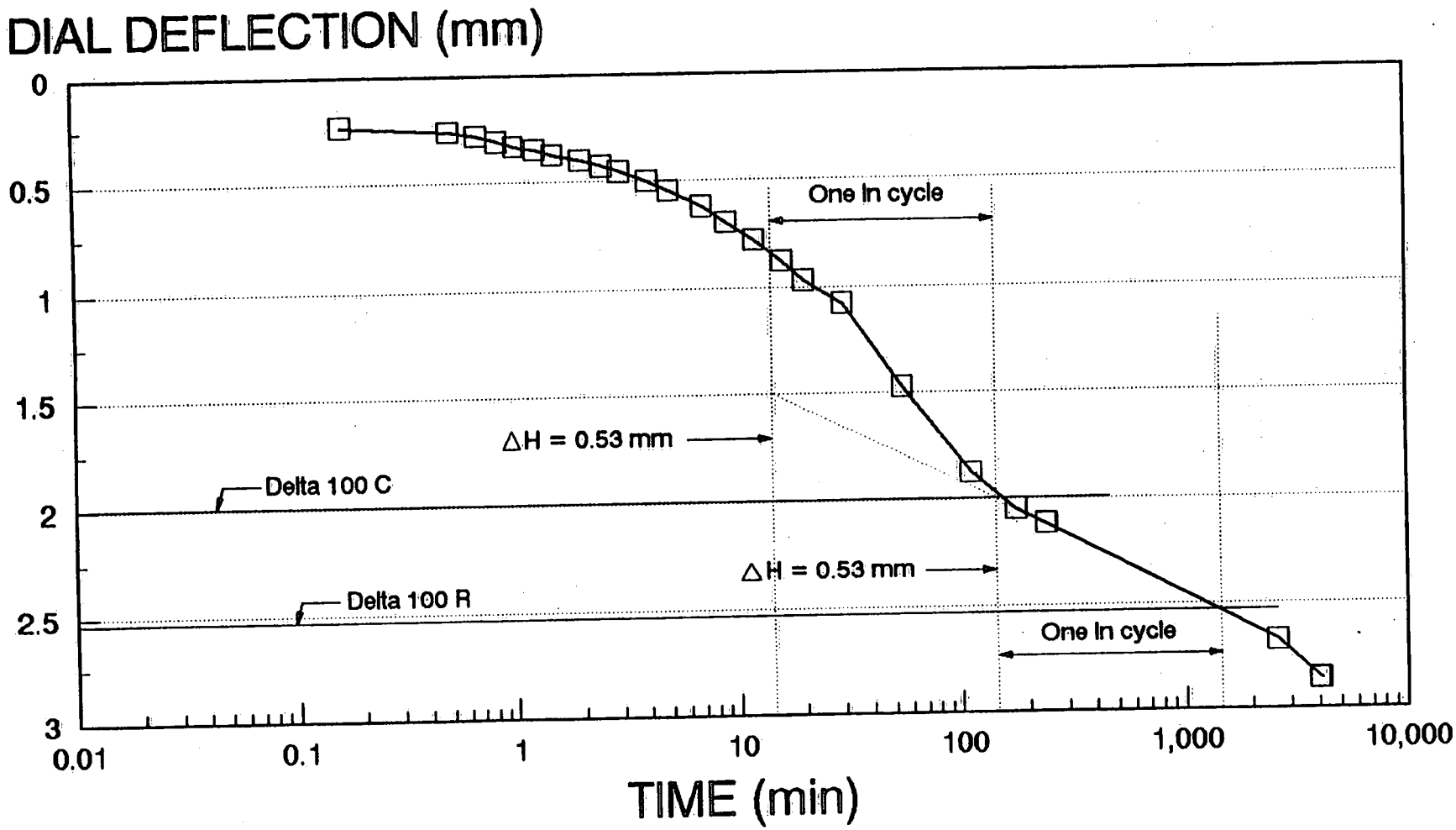

Delta 100 R = 2.52 mm
Delta 100 C = 1.99 mm

Figure 16f

SAMPLE HH-2-90 (5 kPa)

DIAL DEFLECTION VS. TIME

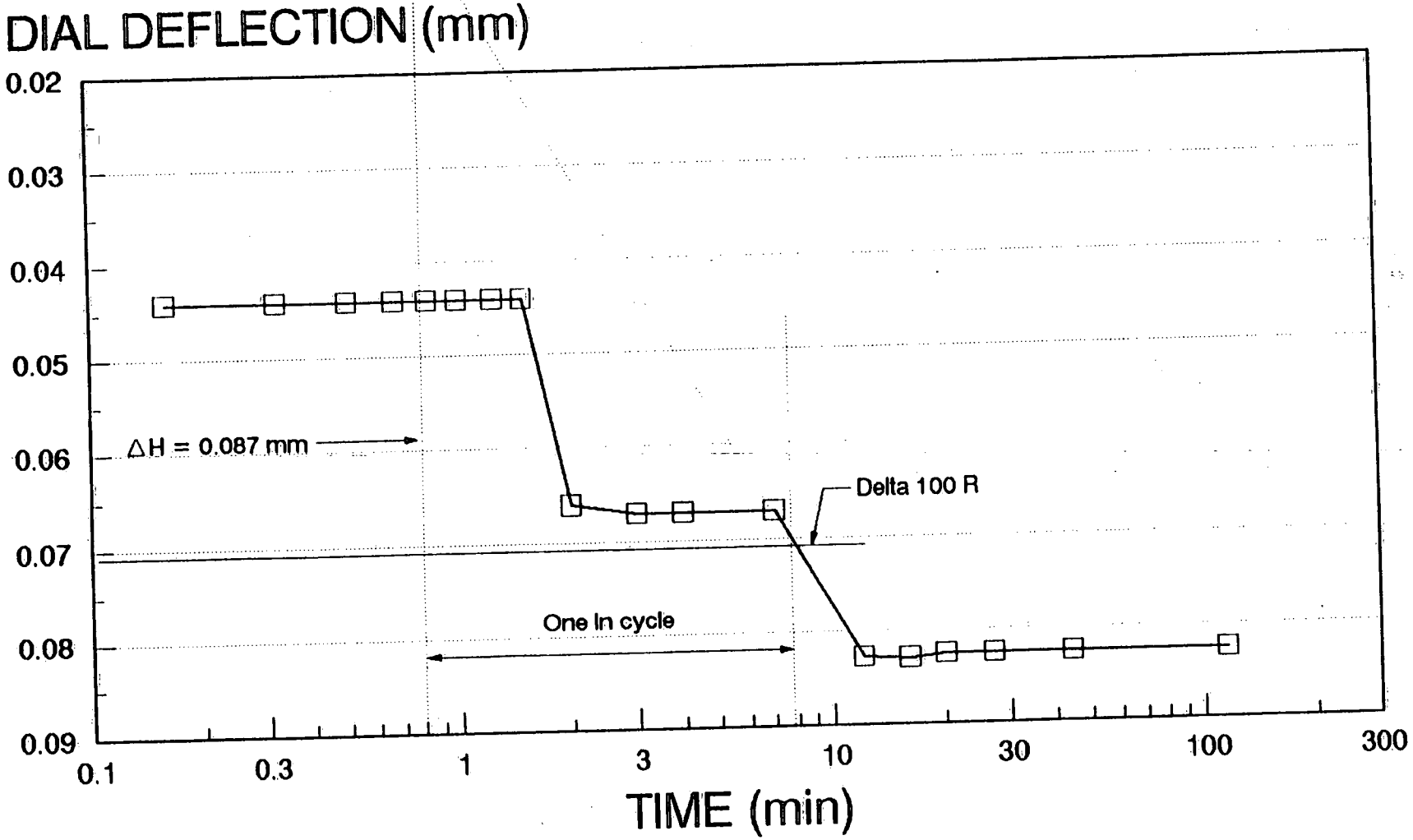

Delta 100 R = 0.071 mm

Figure 17a

SAMPLE HH-2-90 (10 kPa)

DIAL DEFLECTION VS. TIME

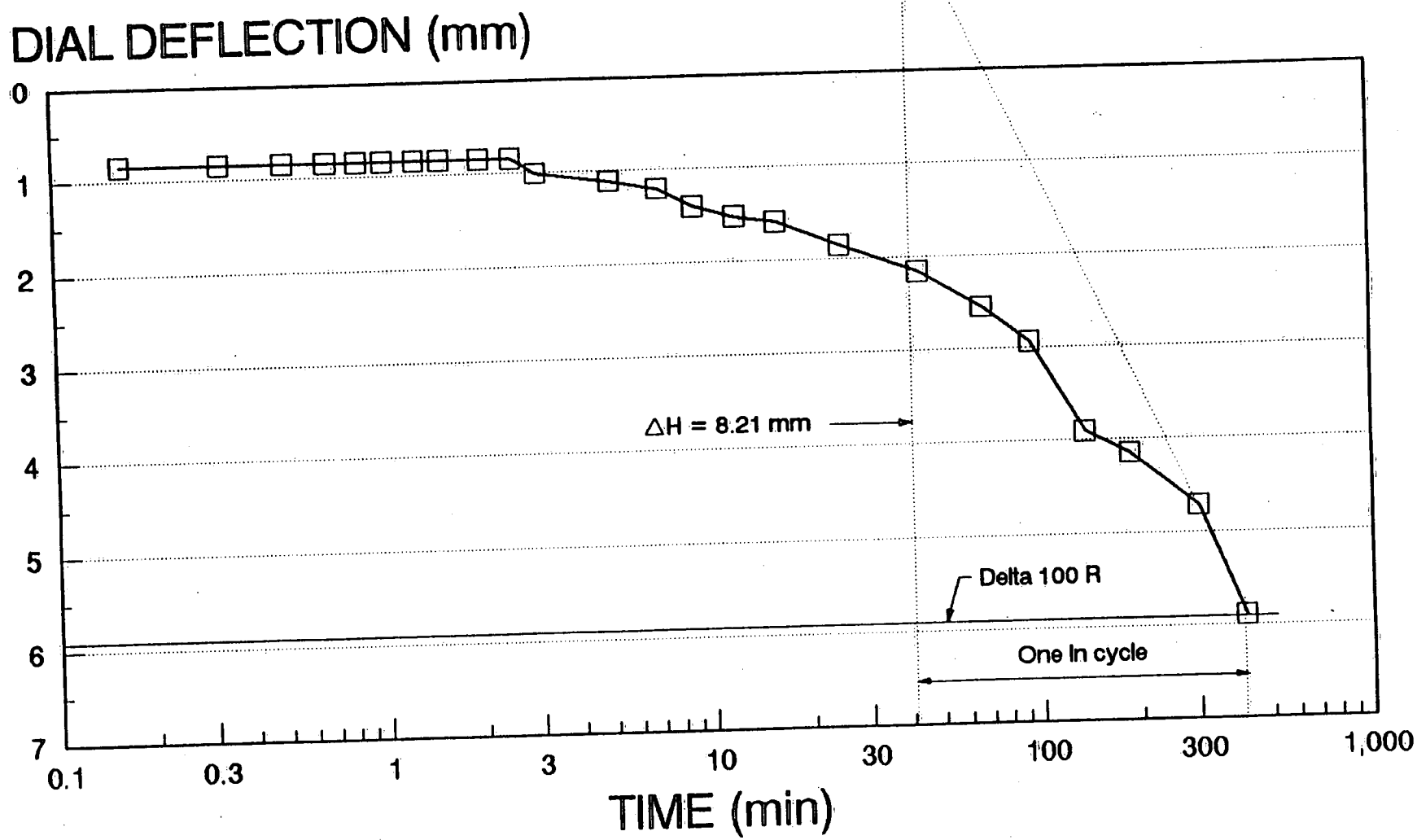

Delta 100 R = 5.91 mm

Figure 17b

SAMPLE HH-2-90 (20 kPa)

DIAL DEFLECTION VS. TIME

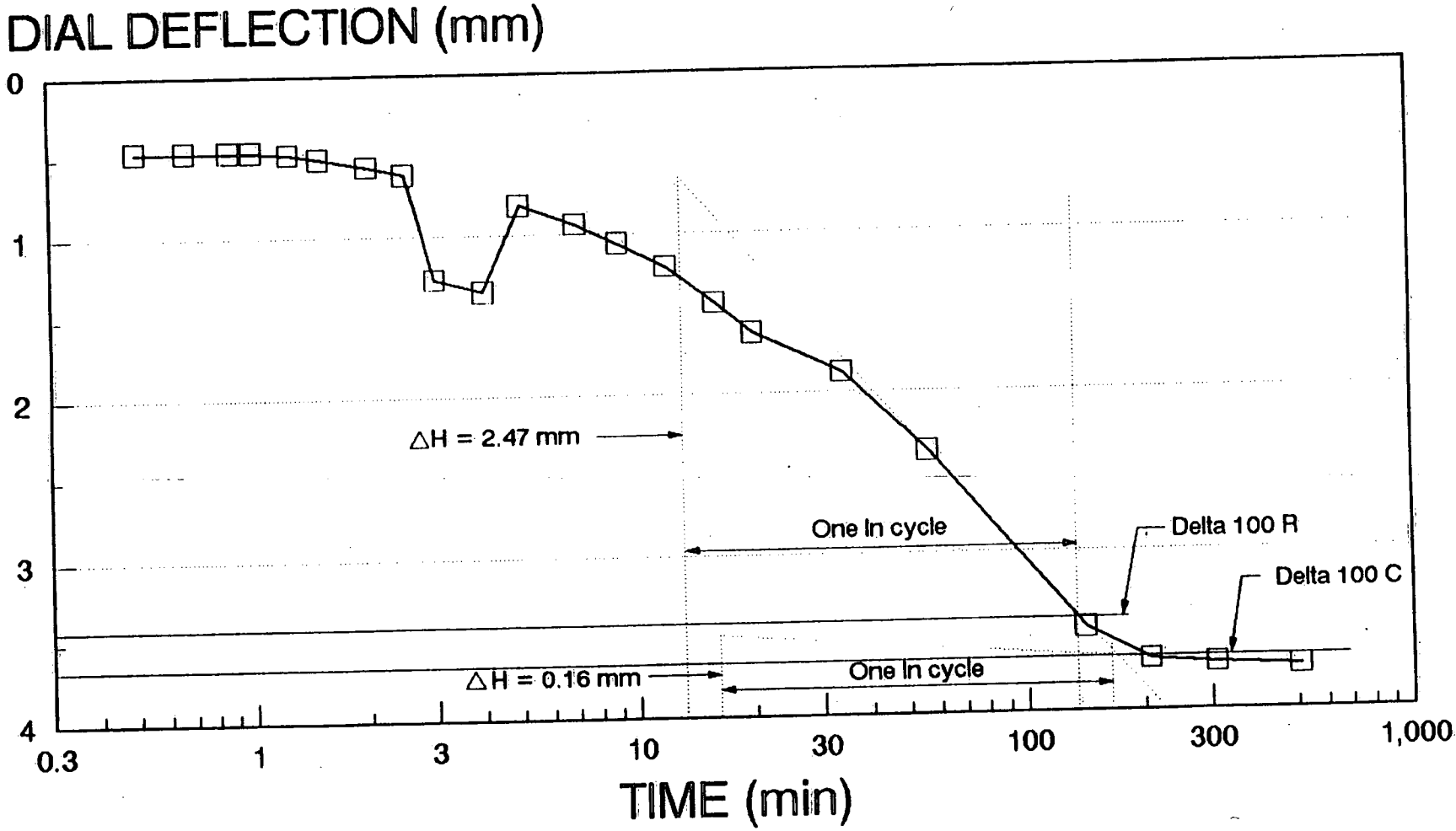

Delta 100 R = 3.46 mm
Delta 100 C = 3.65 mm

Figure 17c

SAMPLE HH-2-90 (40 kPa)

DIAL DEFLECTION VS. TIME

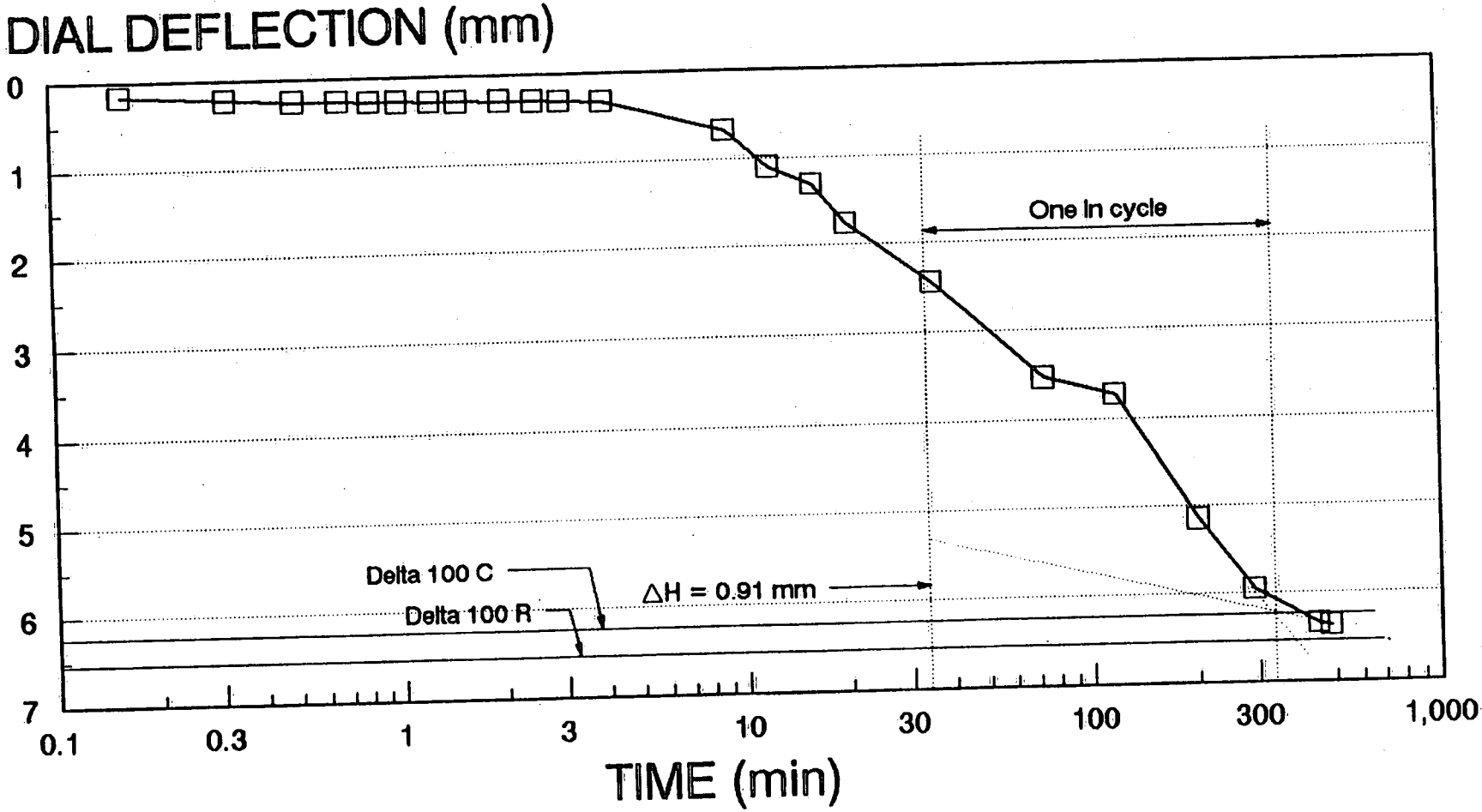

Delta 100 R = 6.53 mm
Delta 100 C = 6.30 mm

Figure 17d

SAMPLE HH-2-90 (80 kPa)

DIAL DEFLECTION VS. TIME

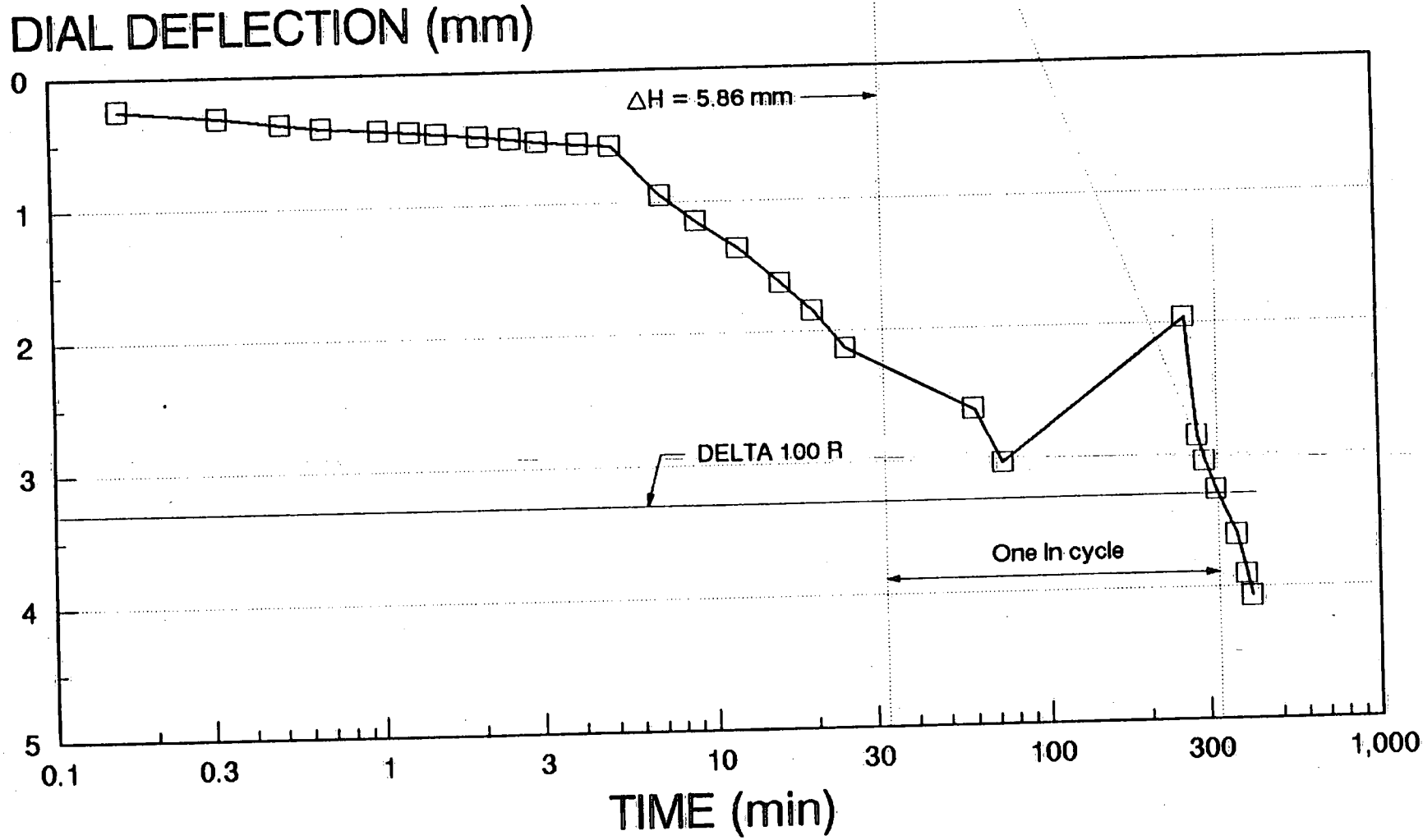

Delta 100 R = 3.28 mm

Figure 17e

SAMPLE HH-2-90 (160 kPa)

DIAL DEFLECTION VS. TIME

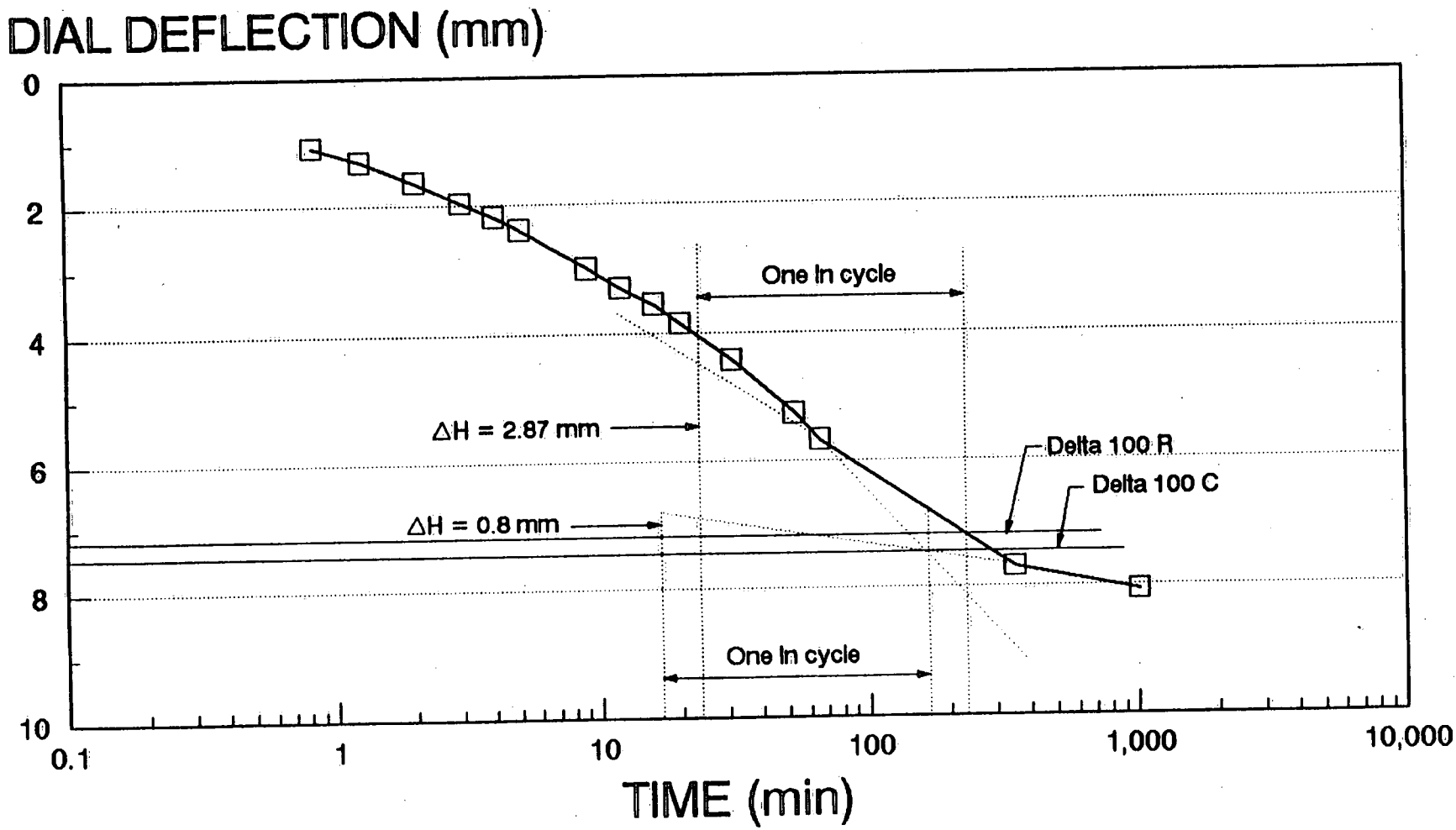

Delta 100 R = 7.13 mm
Delta 100 C = 7.36 mm

Figure 17f

SAMPLE HH-2-90 (320 kPa)

DIAL DEFLECTION VS. TIME

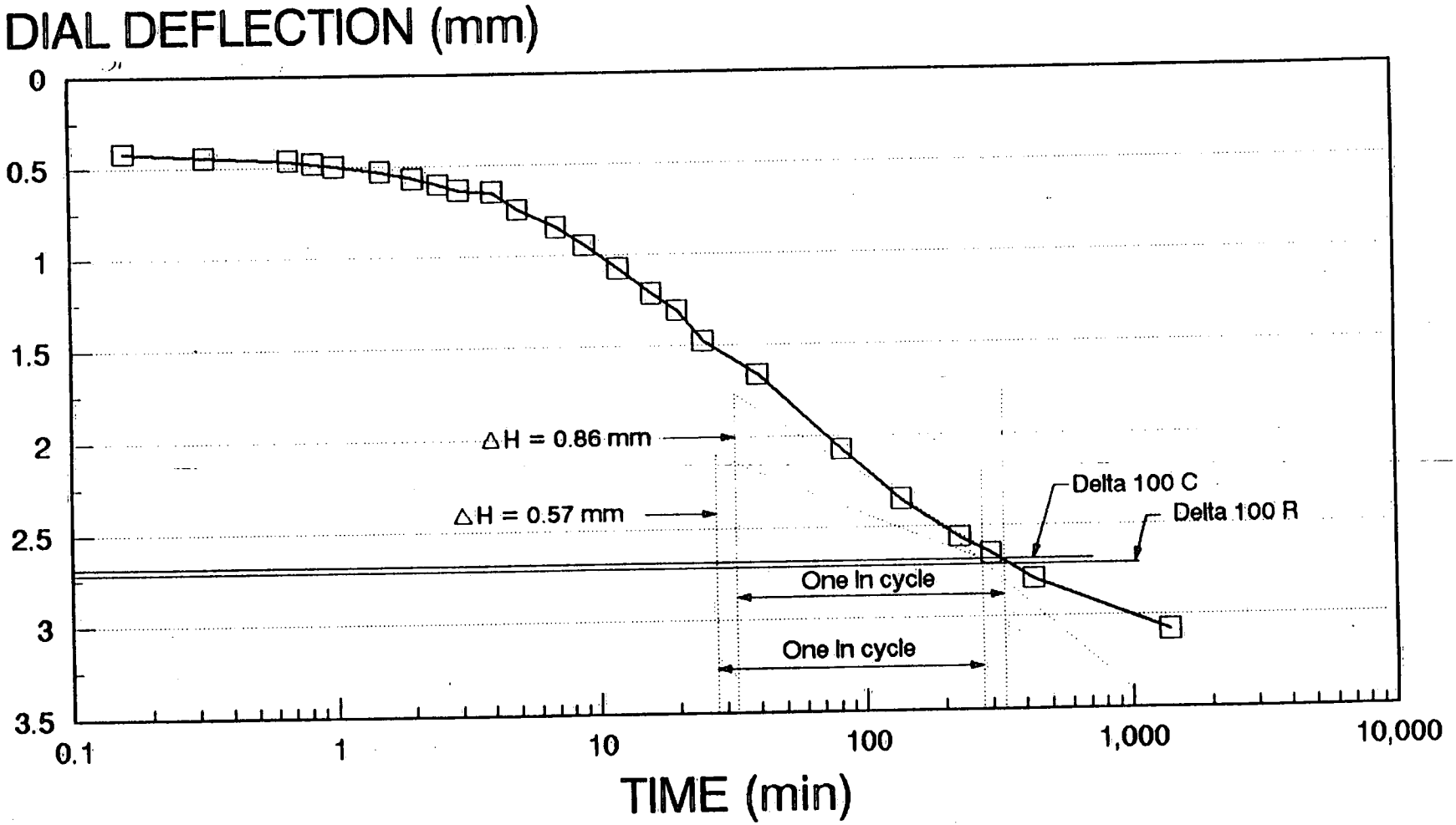

Delta 100 R = 2.72 mm
Delta 100 C = 2.70 mm

Figure 17g

HH-1-93 (5 kPa)

TEST 1, SAMPLE 1

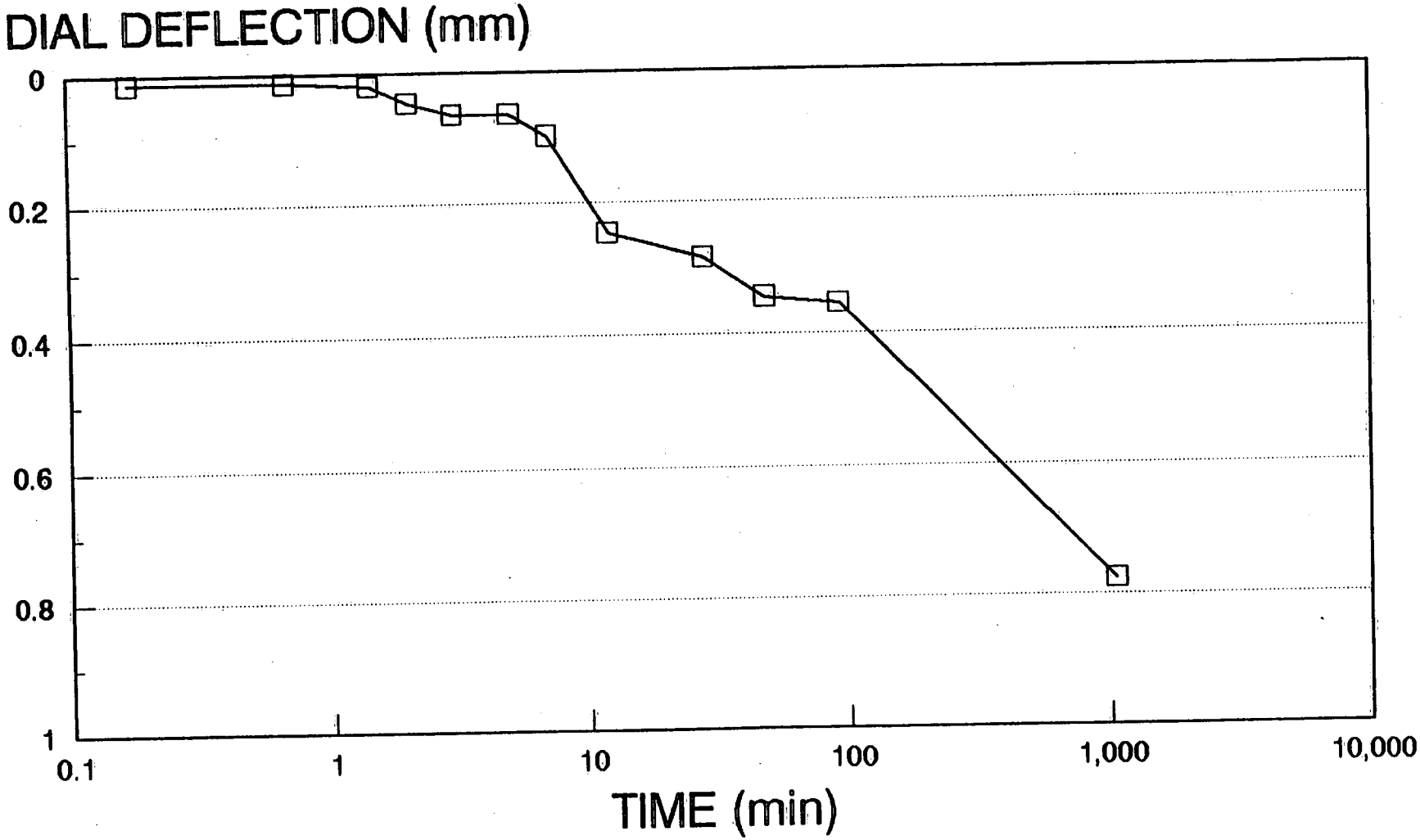

Delta 100R = 4.82 mm

Figure 18a

HH-1-93 (10 kPa)

DIAL DEFLECTION VS. TIME

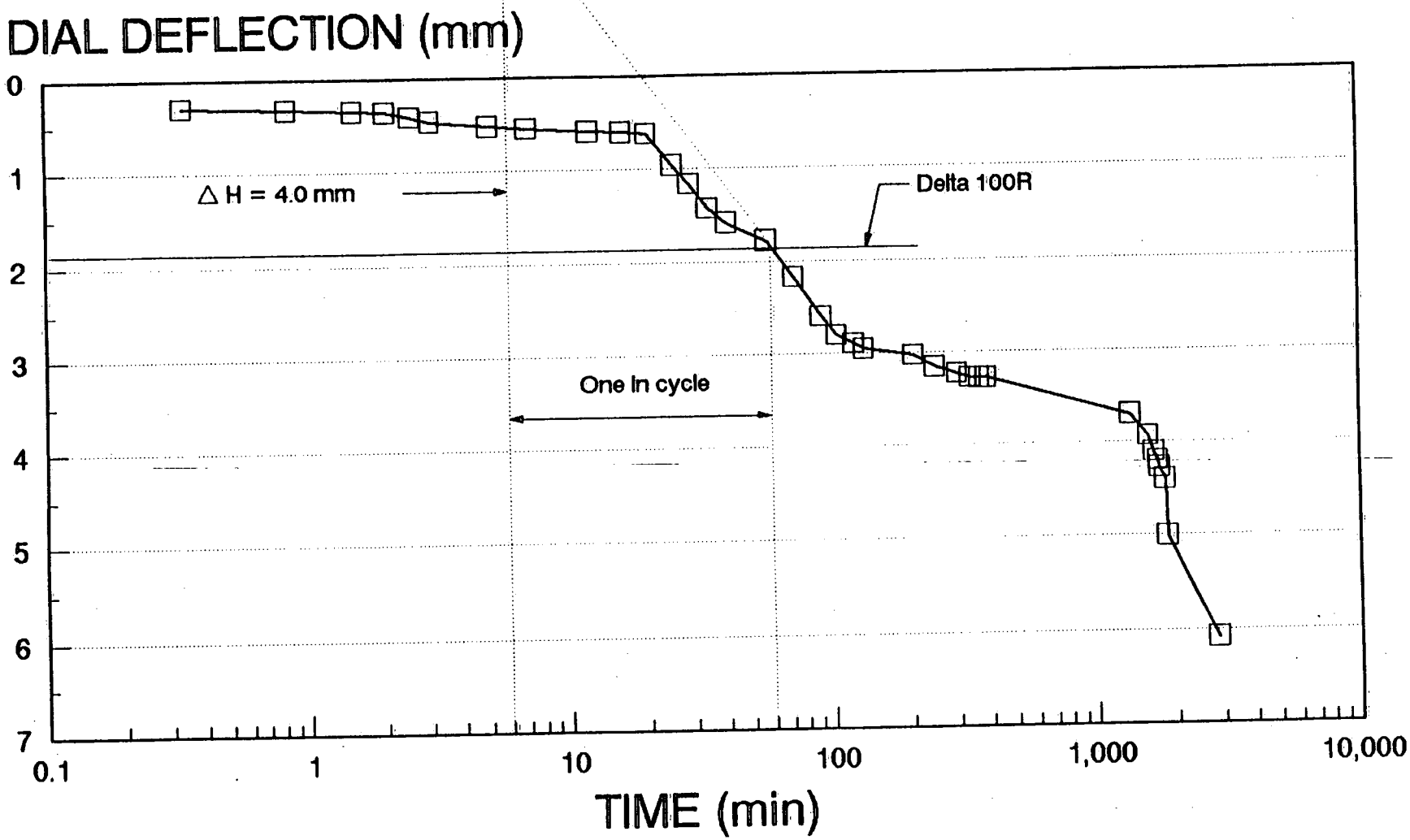

Delta 100R = 2.25 mm

Figure 18b

HH-1-93 (20 kPa)

DIAL DEFLECTION VS. TIME

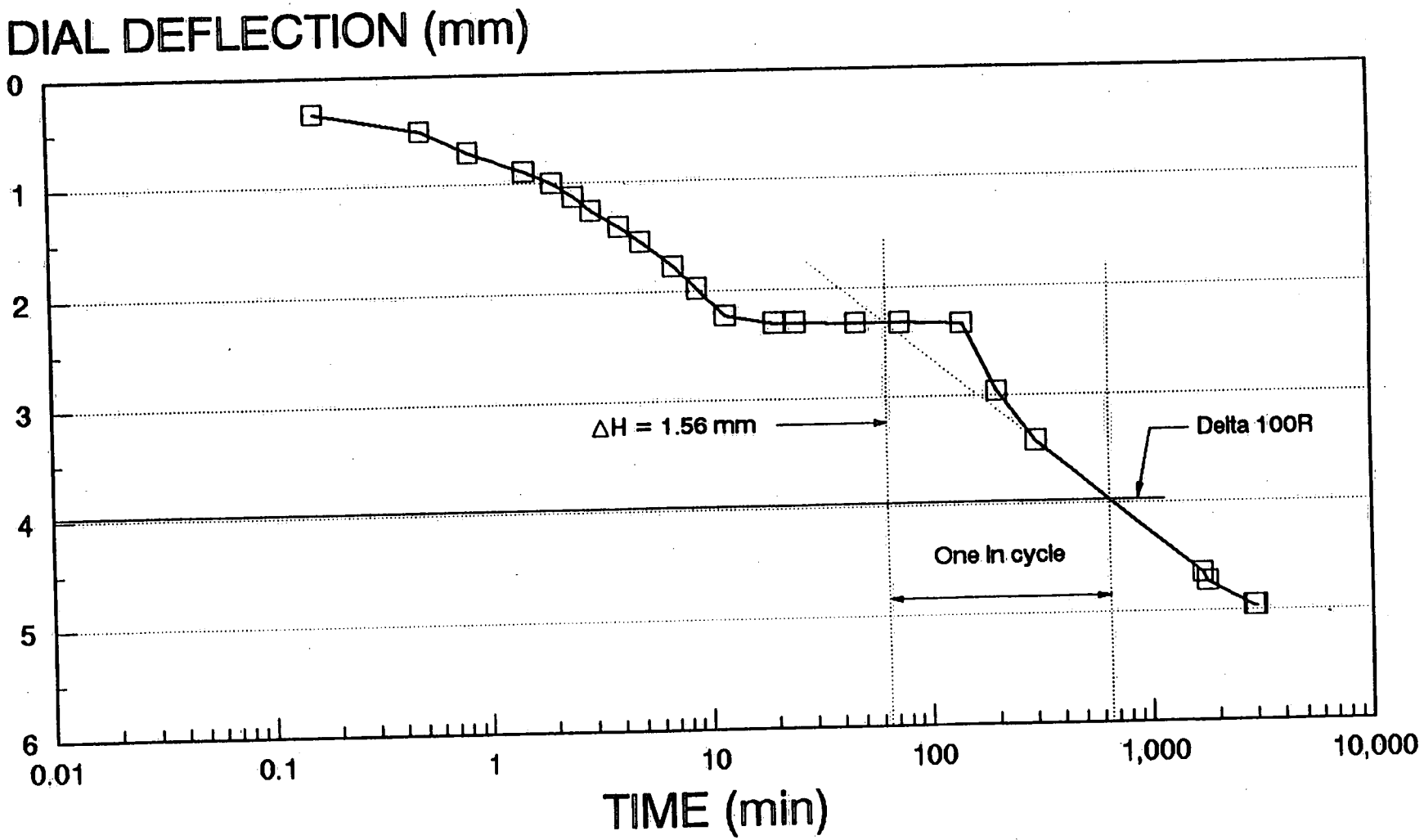

Delta 100R = 3.98 mm

Figure 18c

HH-1-93 (40 kPa)

DIAL DEFLECTION VS. TIME

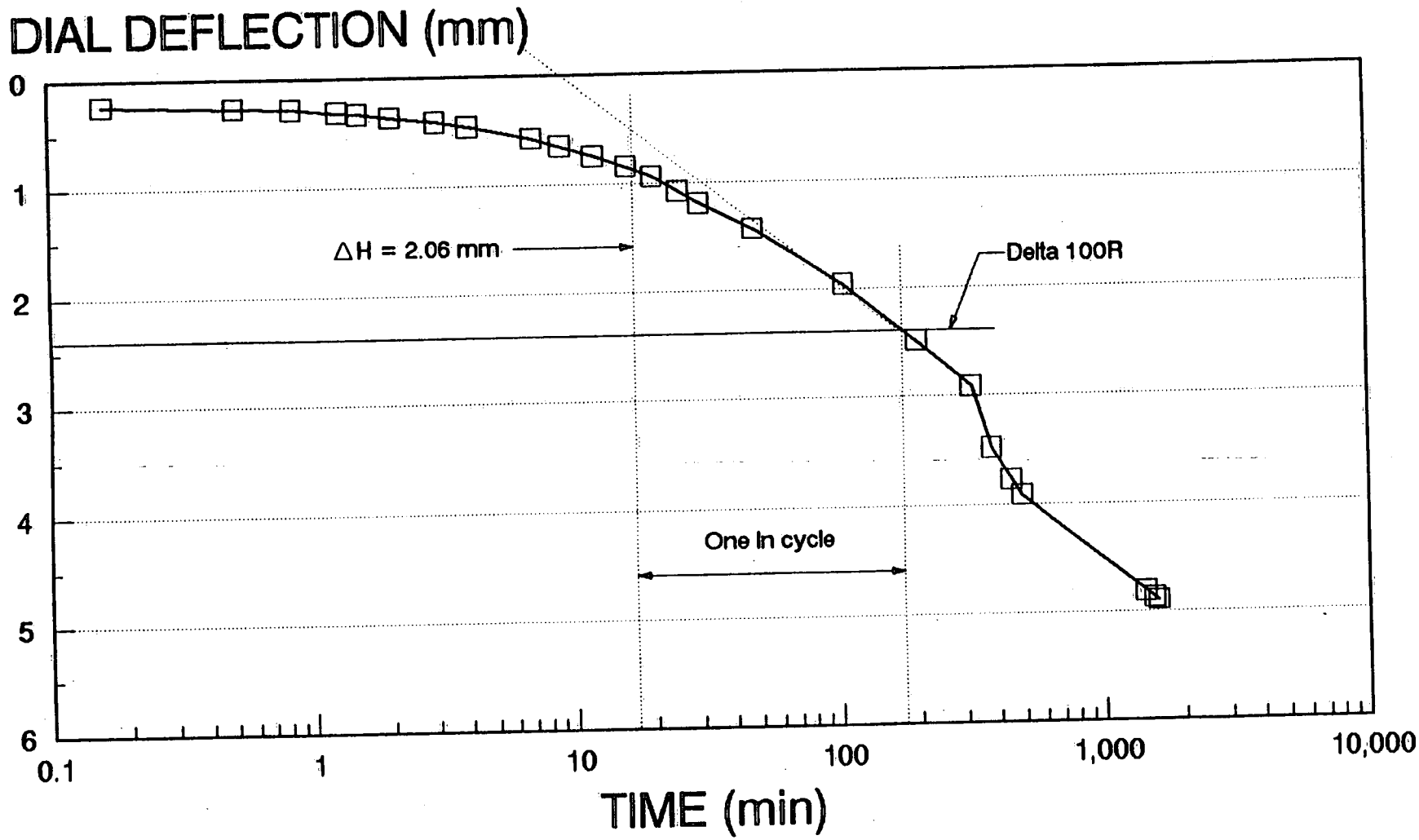

Delta 100R = 2.38 mm

Figure 18d

HH-1-93 (80 kPa)

DIAL DEFLECTION VS. TIME

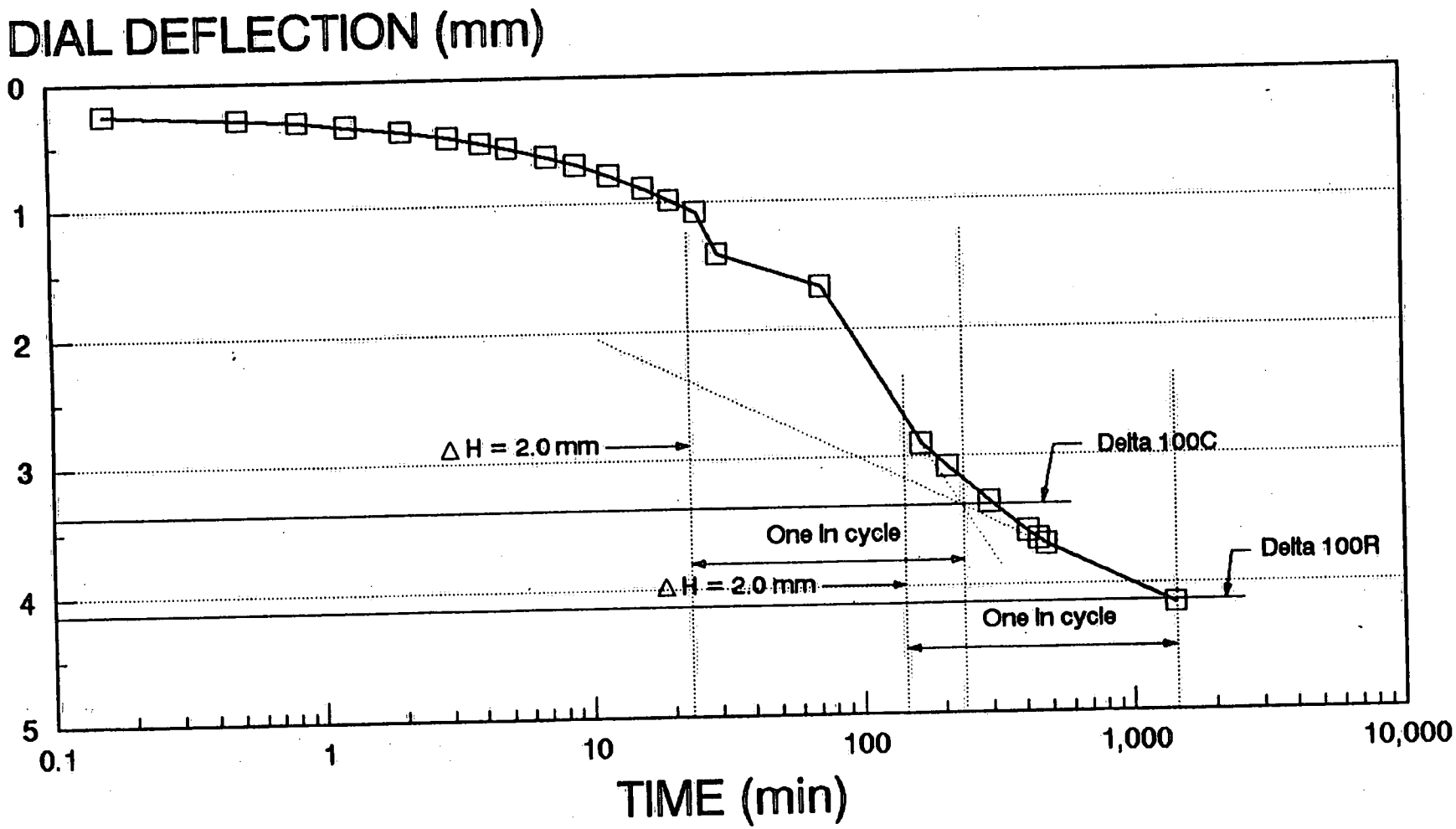

Delta 100R = 4.11 mm
Delta 100C = 3.40 mm

Figure 18e

HH-1-93 (160 kPa)

DIAL DEFLECTION VS. TIME

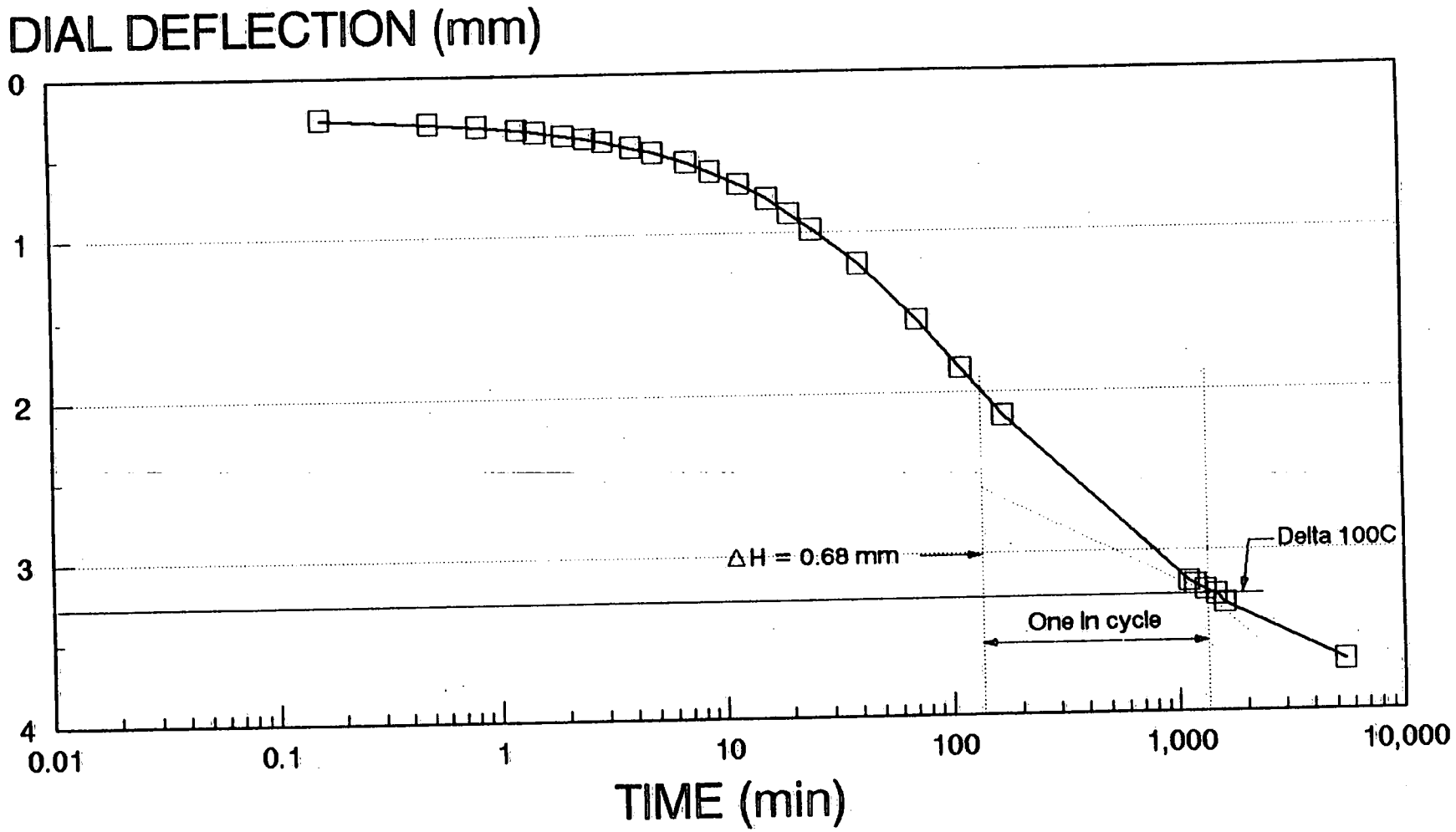

Delta 100R = 8.10 mm
Delta 100C = 3.30 mm

Figure 18f

HH-1-93 (320 kPa)

DIAL DEFLECTION VS. TIME

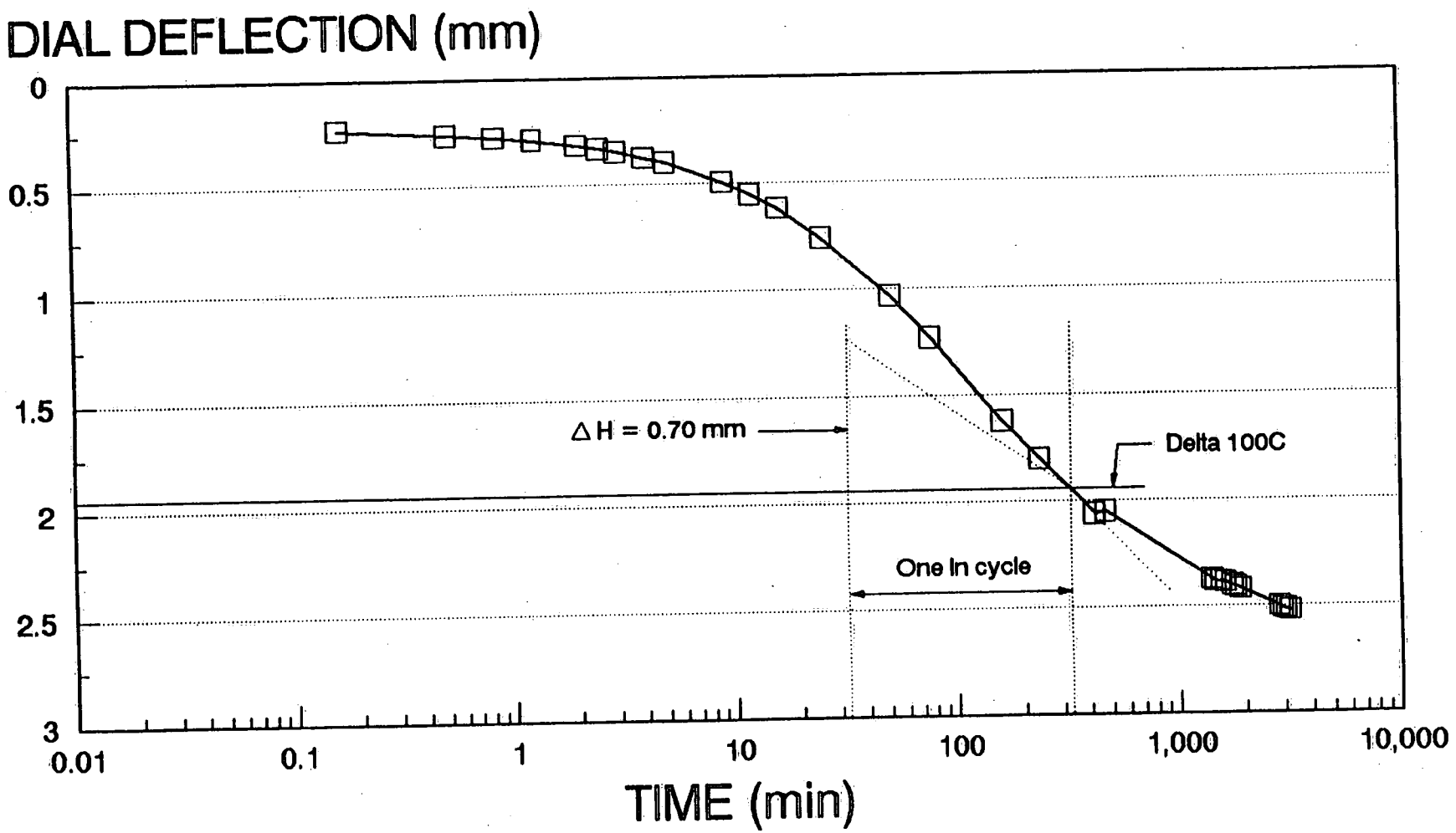

Delta 100R = 25.11 mm
Delta 100C = 1.90 mm

Figure 18g

SAMPLE LO-90

COEFF. OF CONSOLIDATION VS. PRESSURE

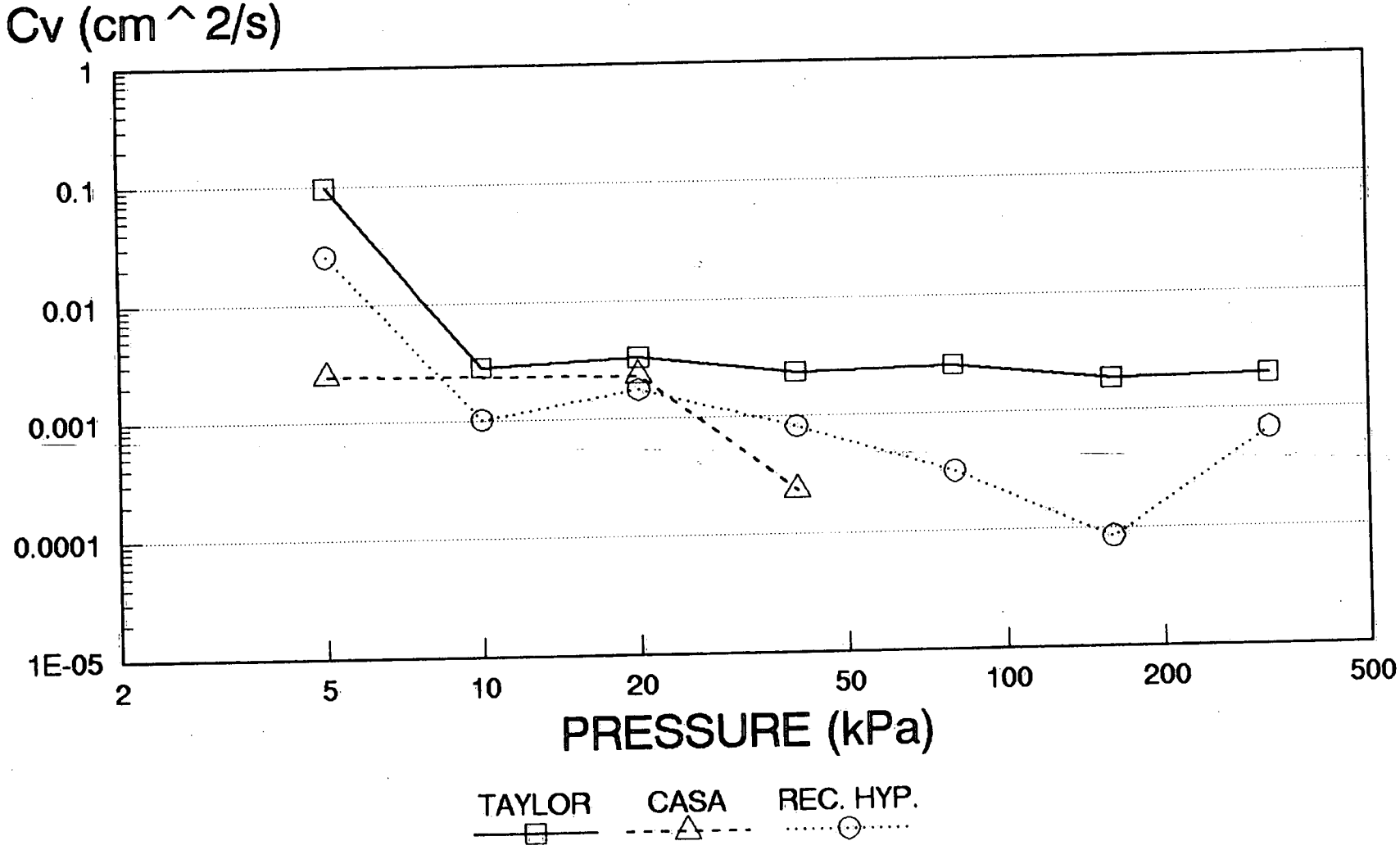

Figure 19a

SAMPLE HH-1-90

COEFF. OF CONSOLIDATION VS. PRESSURE

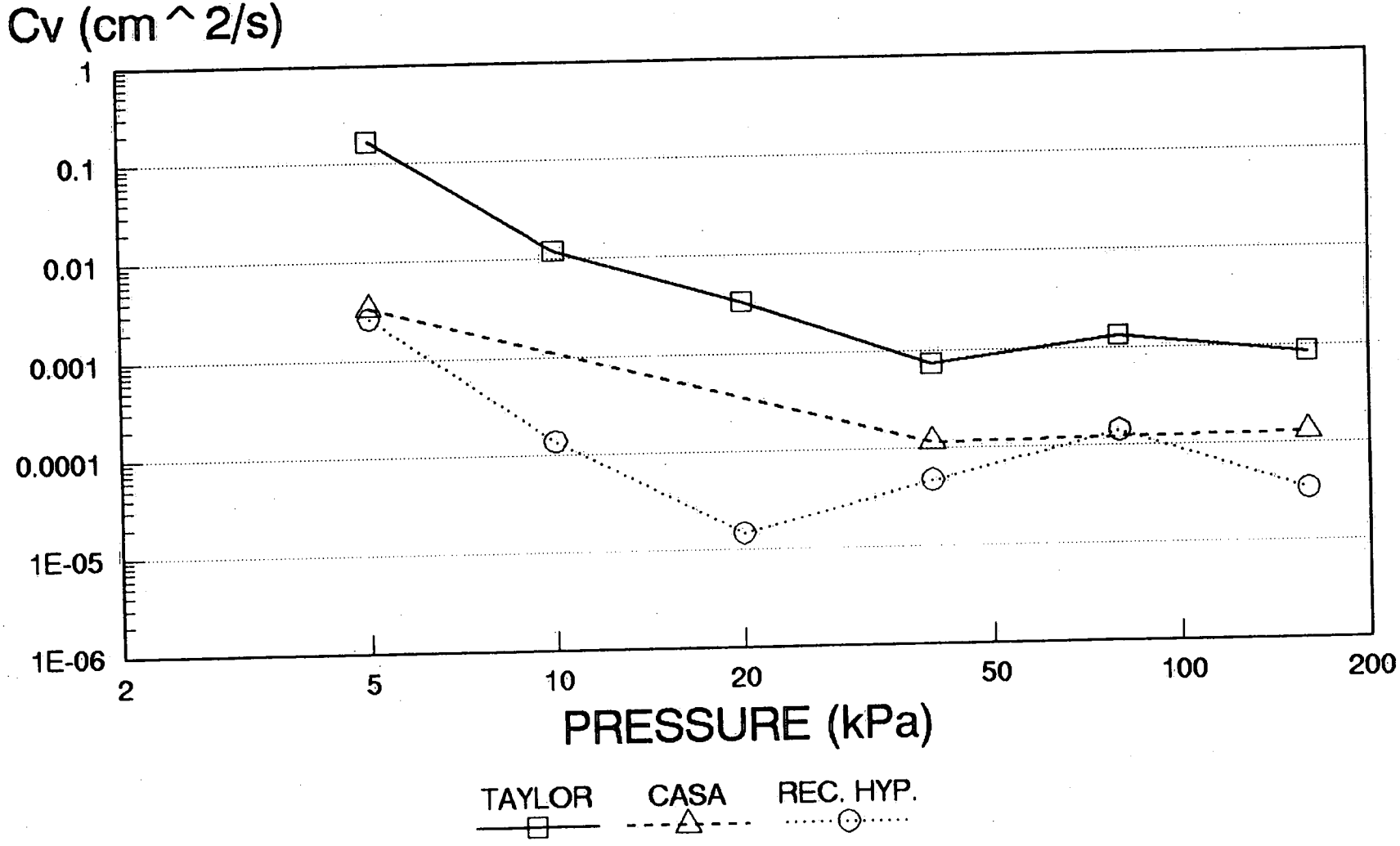

Figure 19b

SAMPLE HH-2-90

COEFF. OF CONSOLIDATION VS. PRESSURE

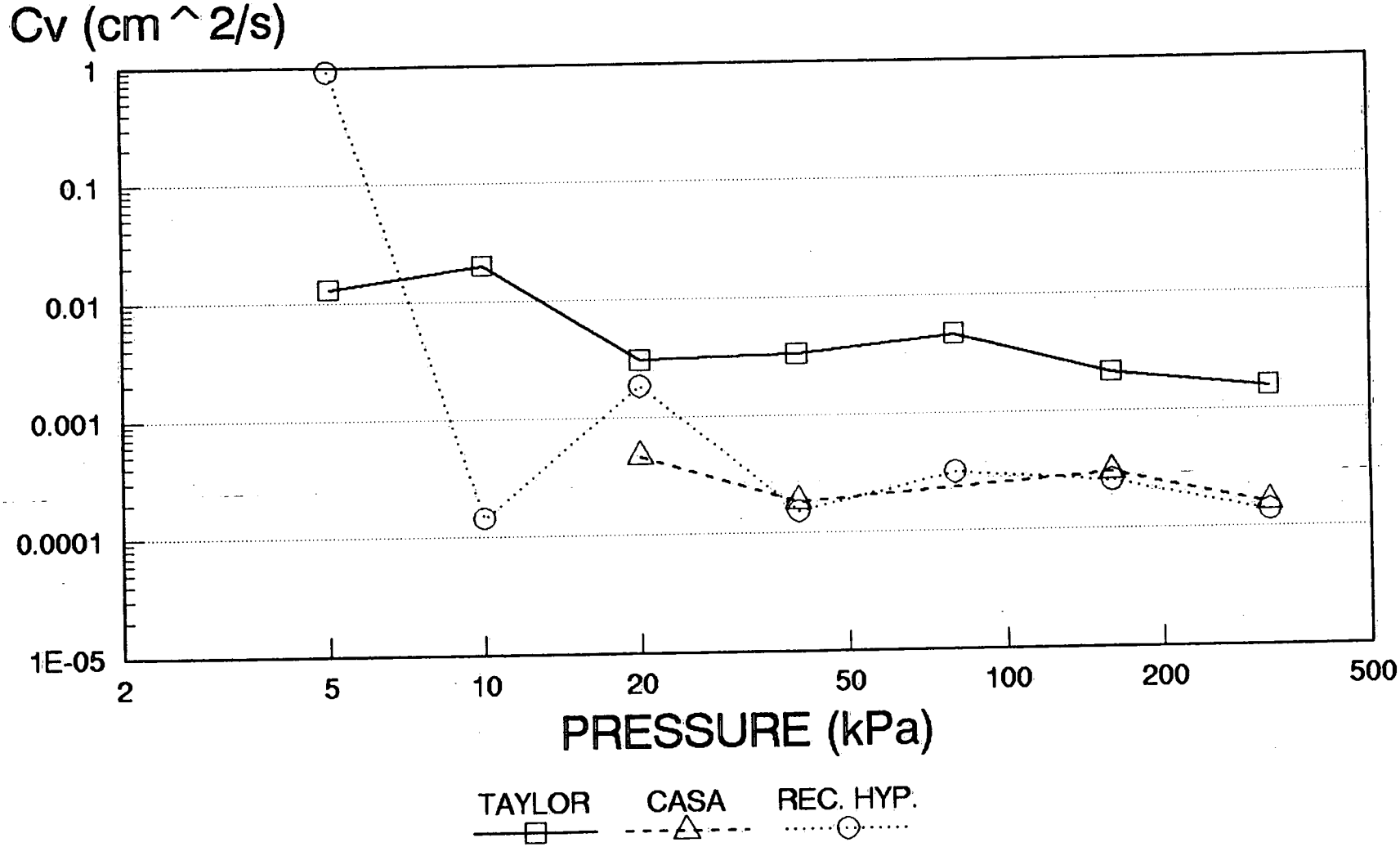

Figure 19c

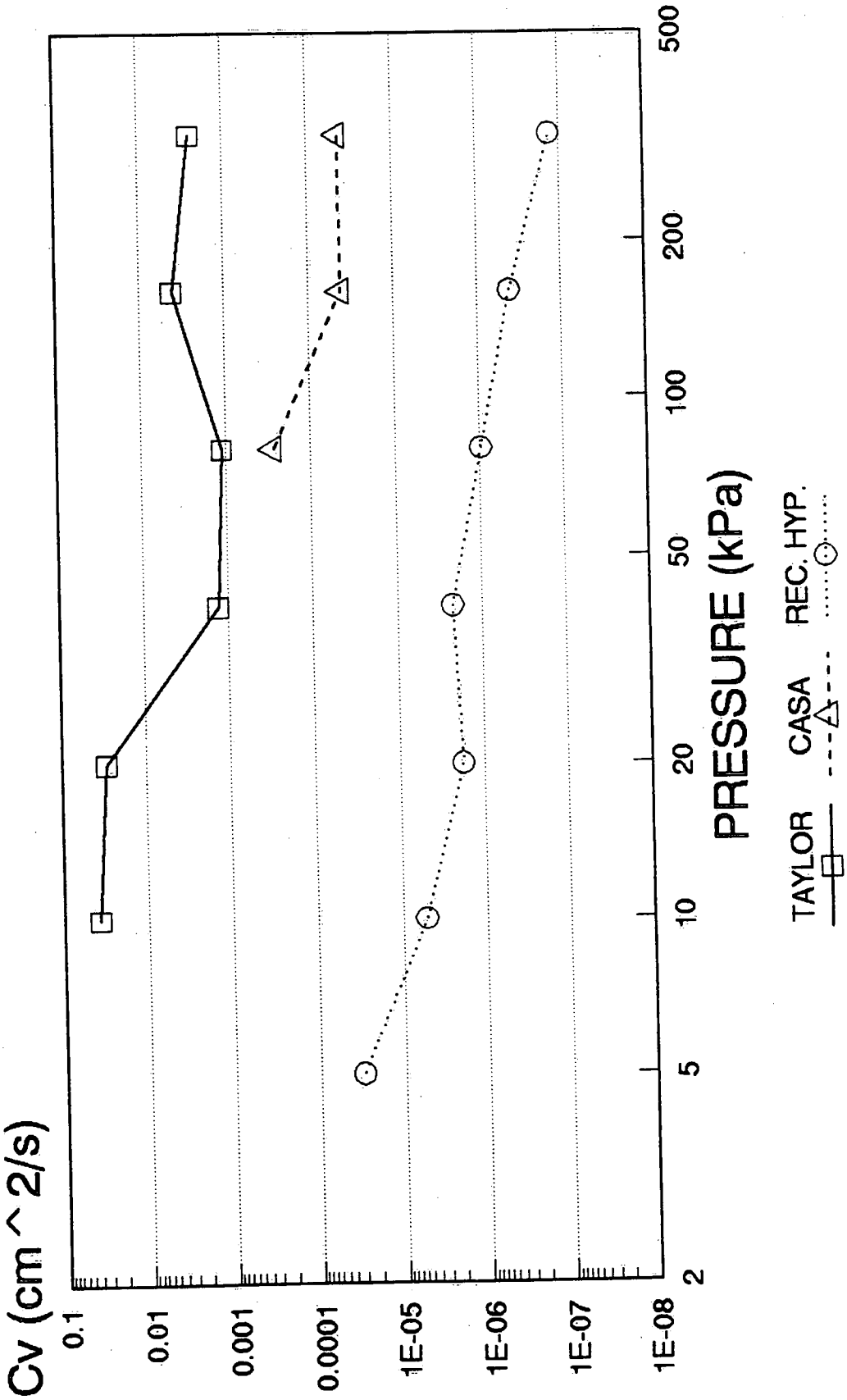
HH-1-93
COEFF. OF CONSOLIDATION VS. PRESSURE
Cv (cm^2/s)
0.1
0.01
0.001
0.0001
1E-05
1E-06
1E-07
1E-08
2
5
10
20
50
100
200
500
PRESSURE (kPa)
TAYLOR
CASA
REC. HYP.

Figure 19d

DEGREE OF CONSOLIDATION VS. TIME

TERZAGHI'S THEORY

SAMPLE HH1-93; H = 1 m

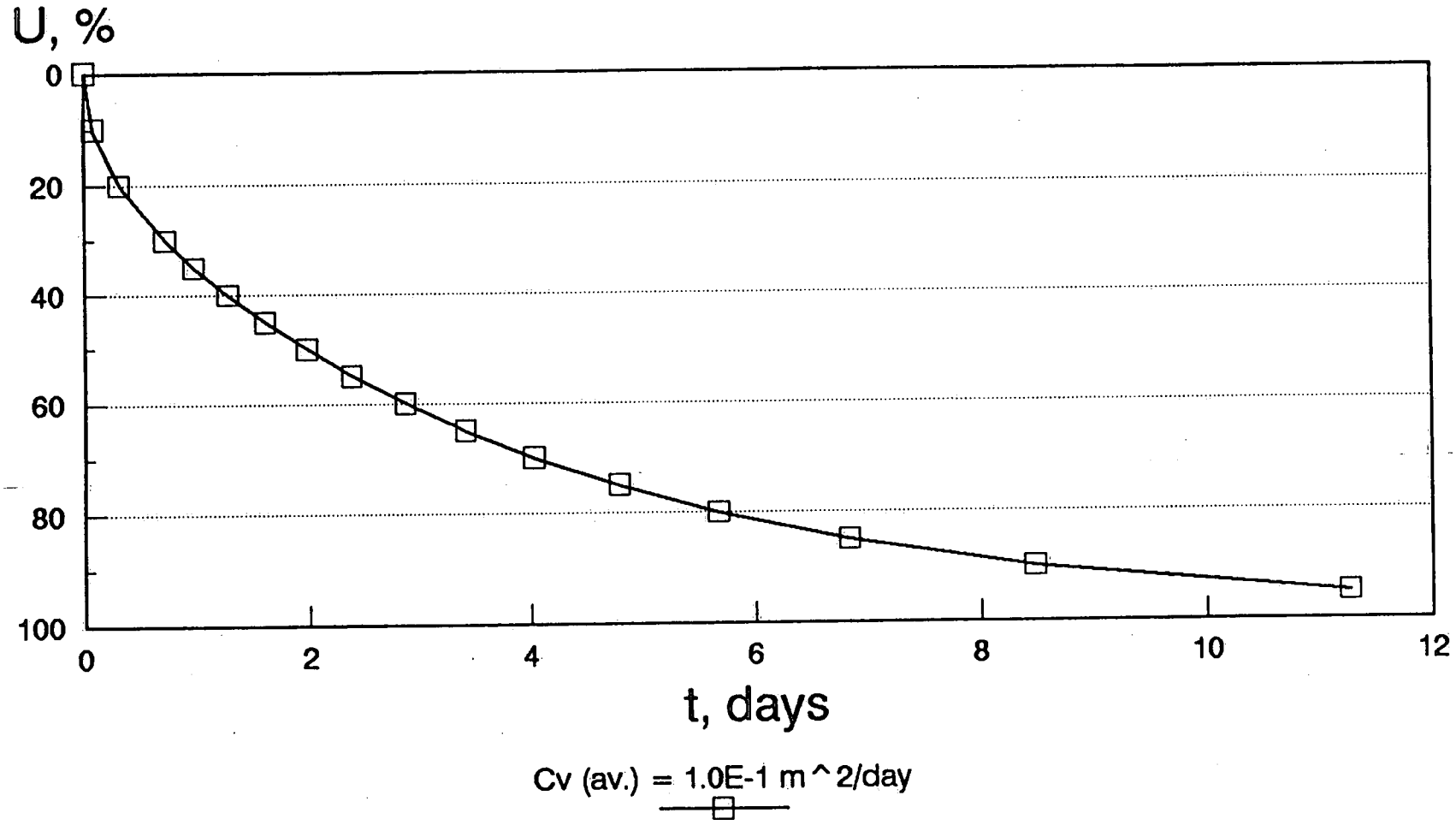

Figure 20a

DEGREE OF CONSOLIDATION VS. TIME

TERZAGHI'S THEORY

SAMPLE HH1-93; H = 2 m

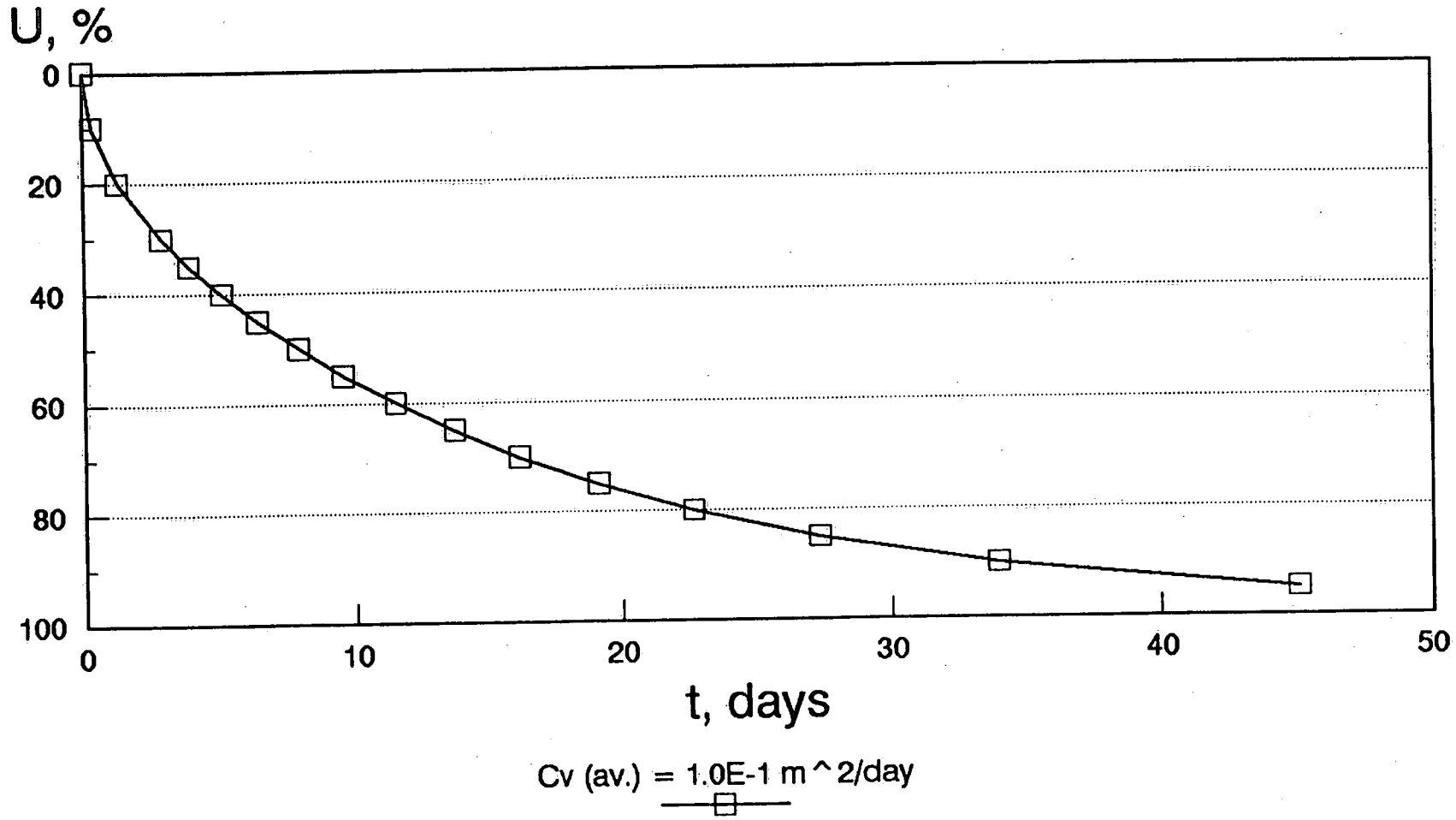

Figure 20b

DEGREE OF CONSOLIDATION VS. TIME

FINITE STRAIN THEORY

SAMPLE HH1-93; H = 1 m

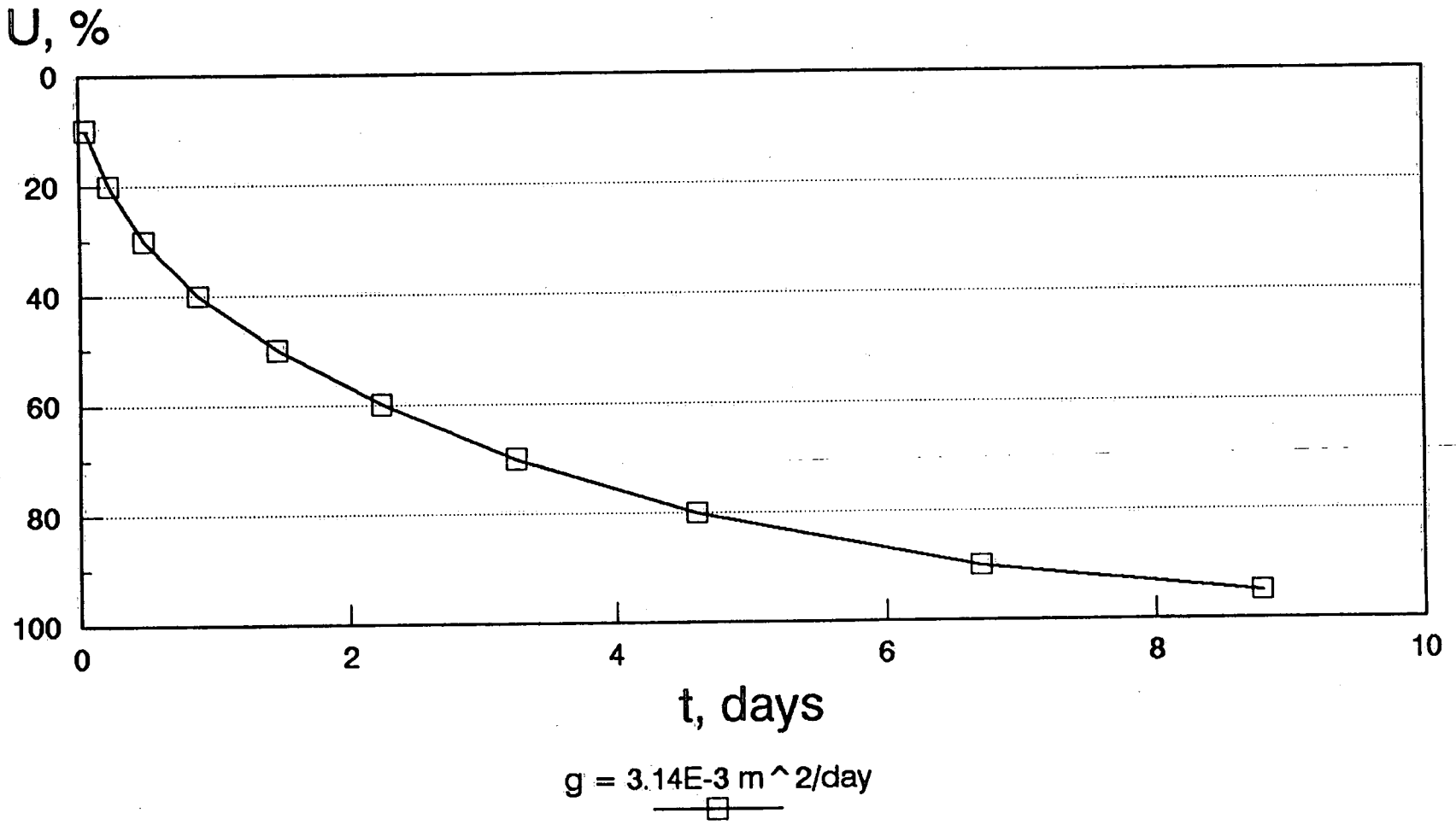

Figure 21a

DEGREE OF CONSOLIDATION VS. TIME

FINITE STRAIN THEORY

SAMPLE HH1-93; H = 2 m

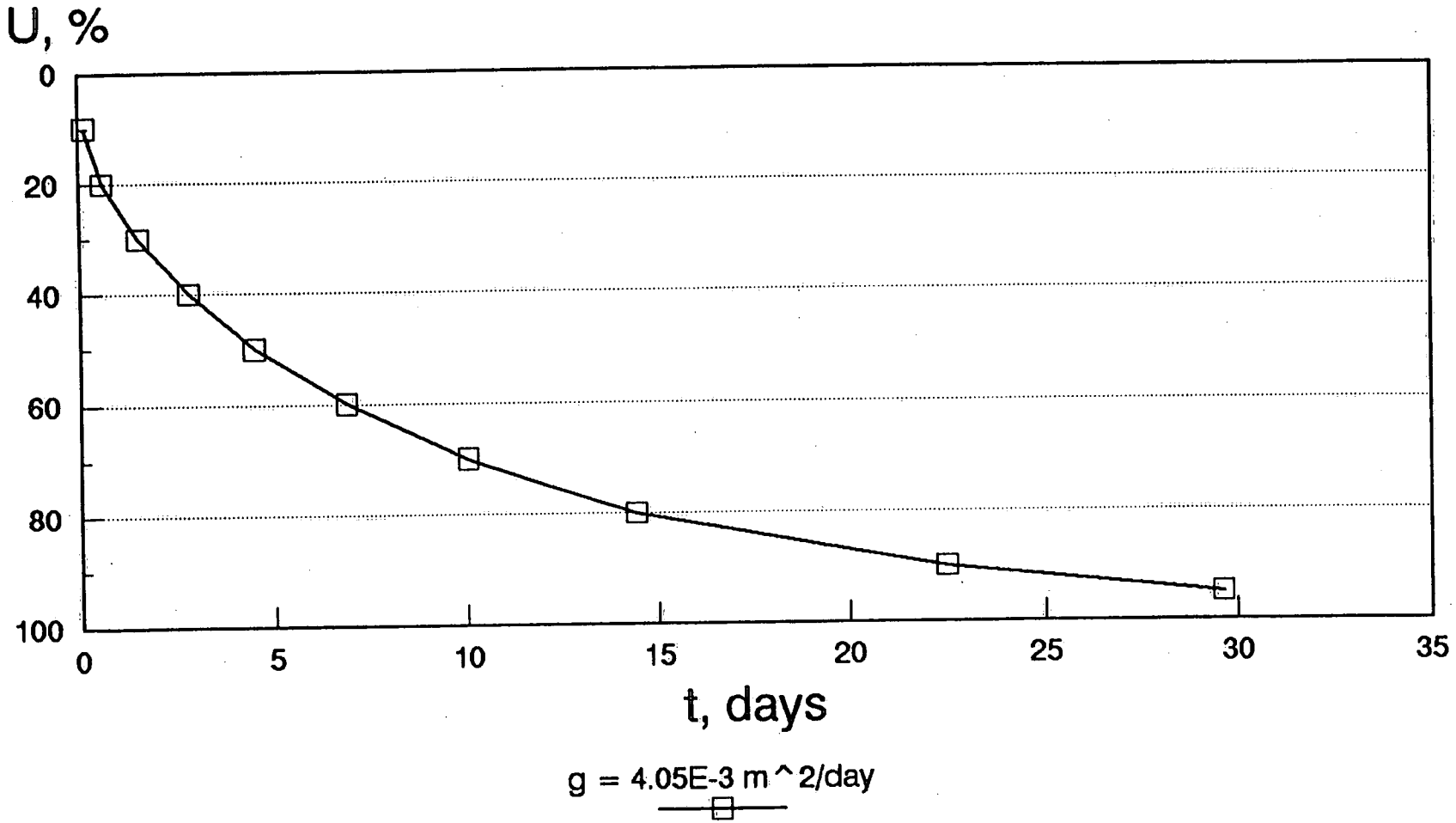

Figure 21b

SAMPLE LO-90

COEF. OF SEC. COMPRESSION VS. CONSOLID. PRESSURE

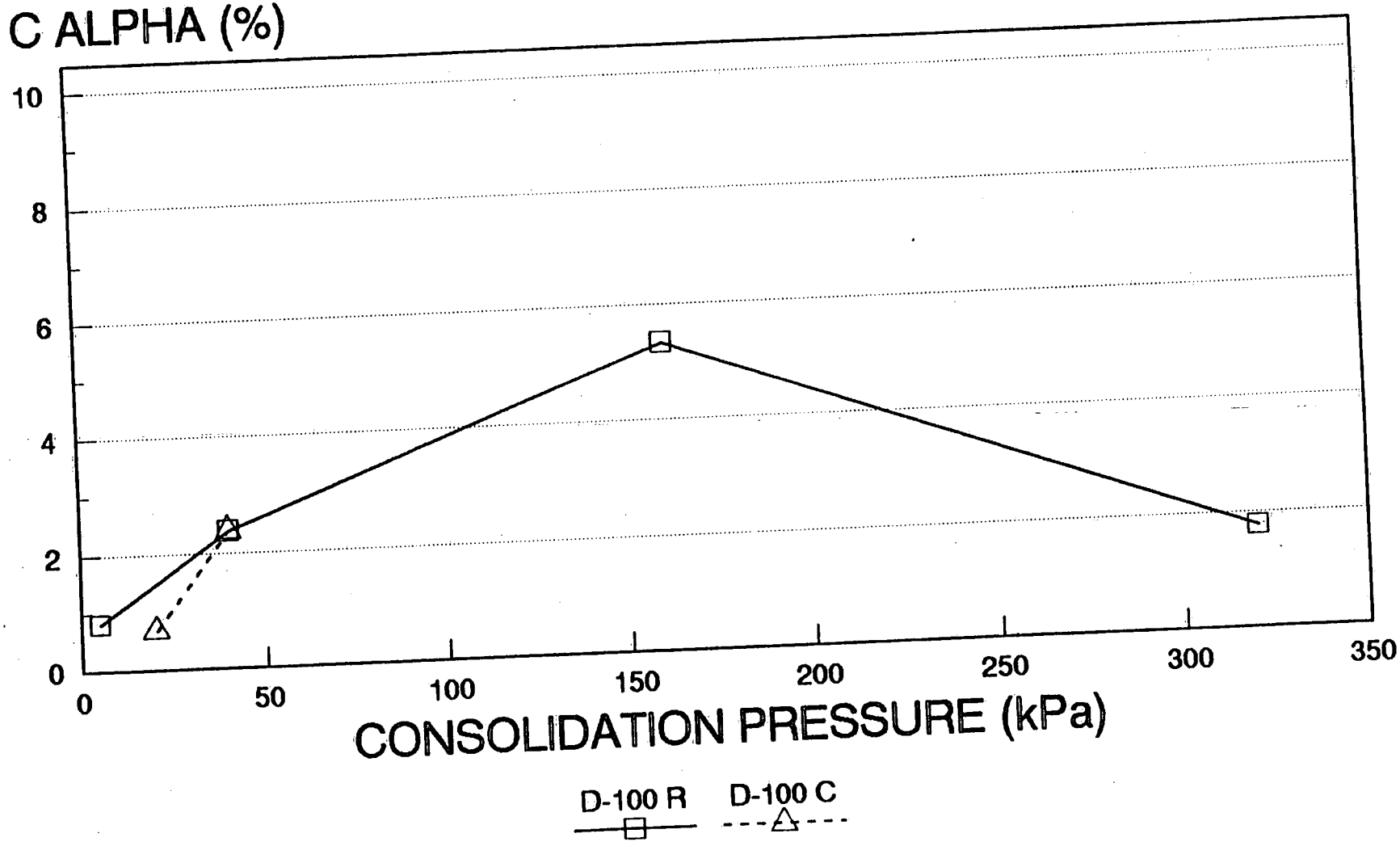

Figure 22a

SAMPLE HH-1-90

COEF. OF SEC. COMPRESSION VS. CONSOLID. PRESSURE

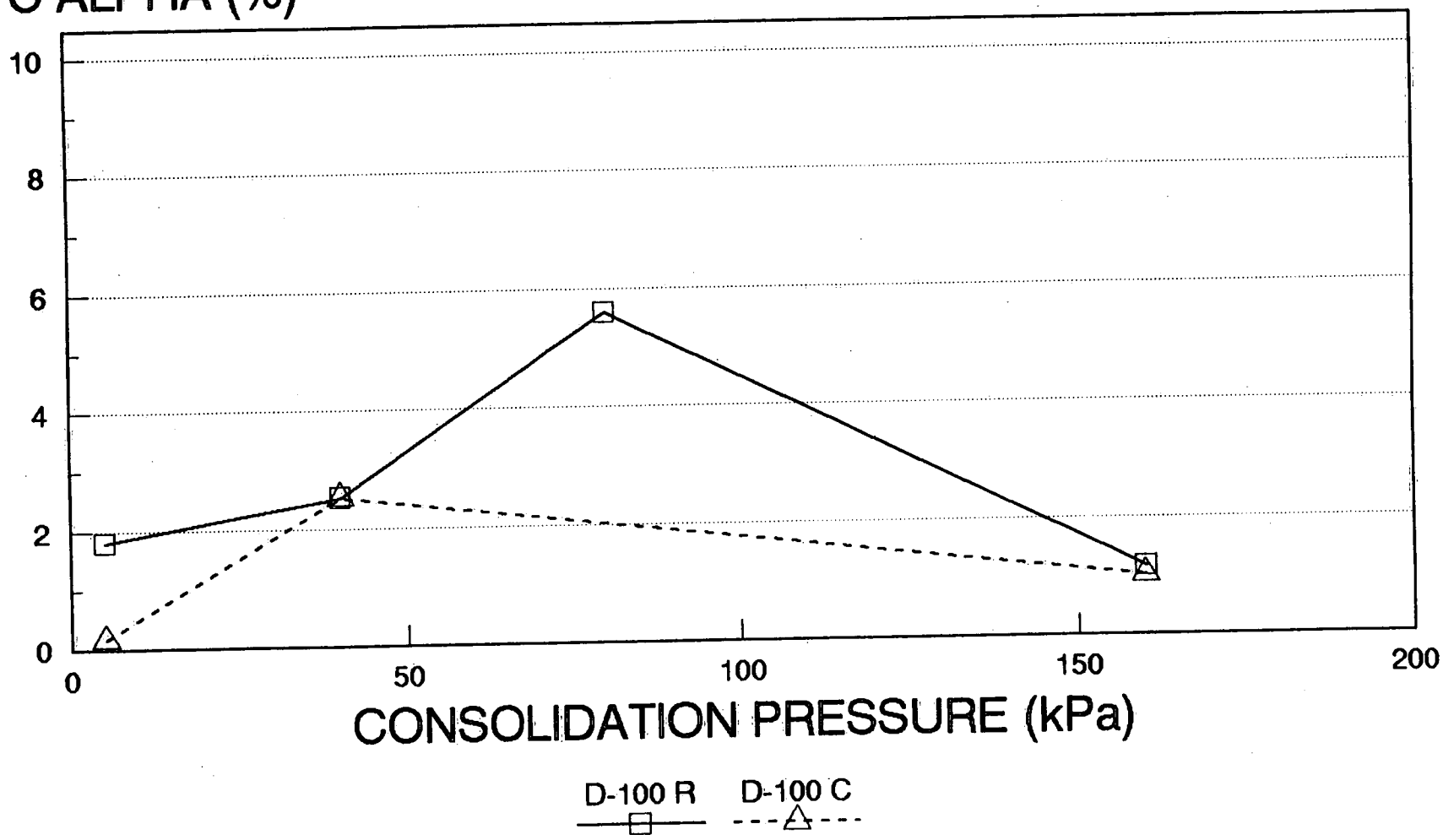

Figure 22b

SAMPLE HH-2-90

COEF. OF SEC. COMPRESSION VS. CONSOLID. PRESSURE

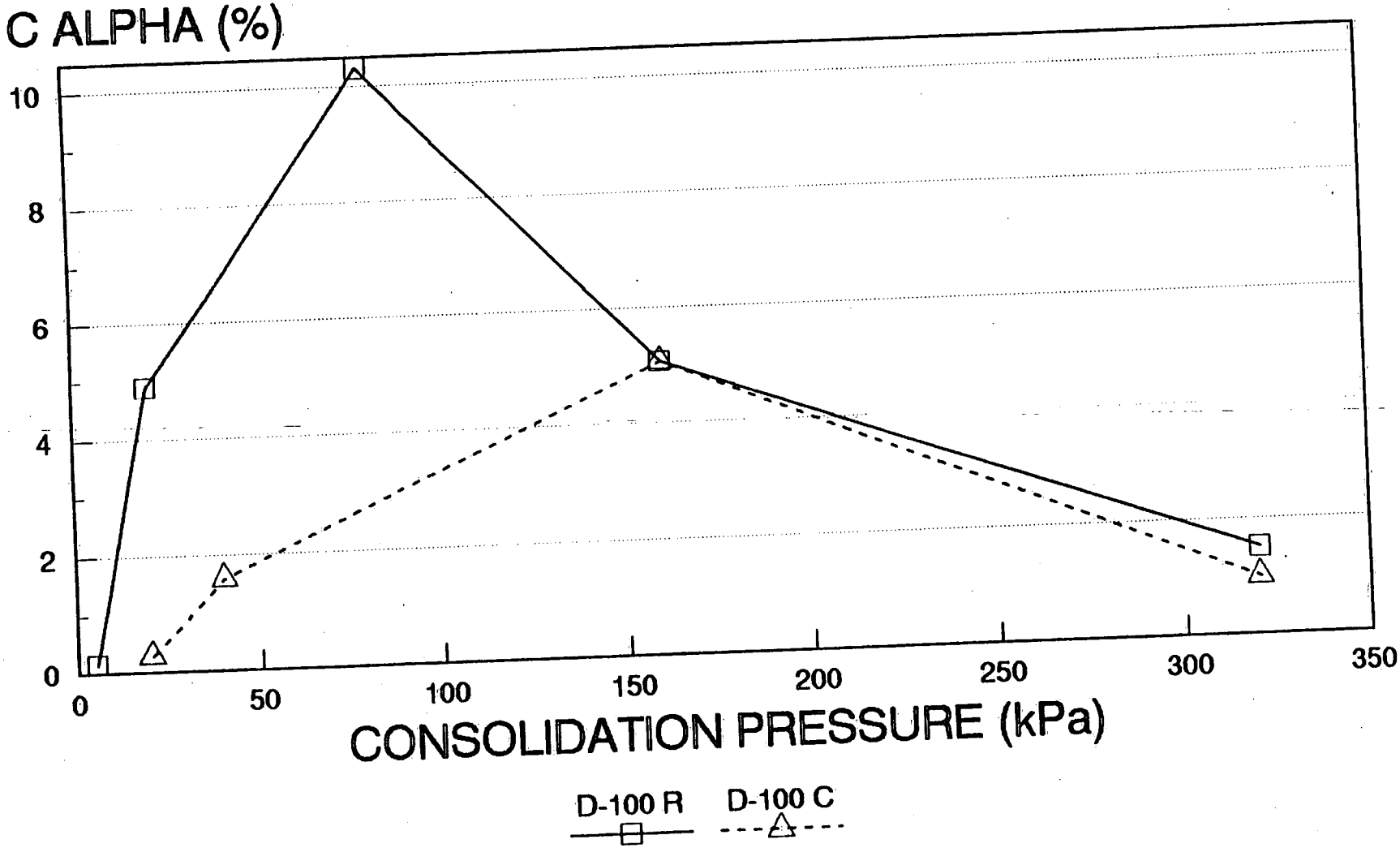

Figure 22c

SAMPLE HH-1-93

COEF. OF SEC. COMPRESSION VS. CONSOLID. PRESSURE

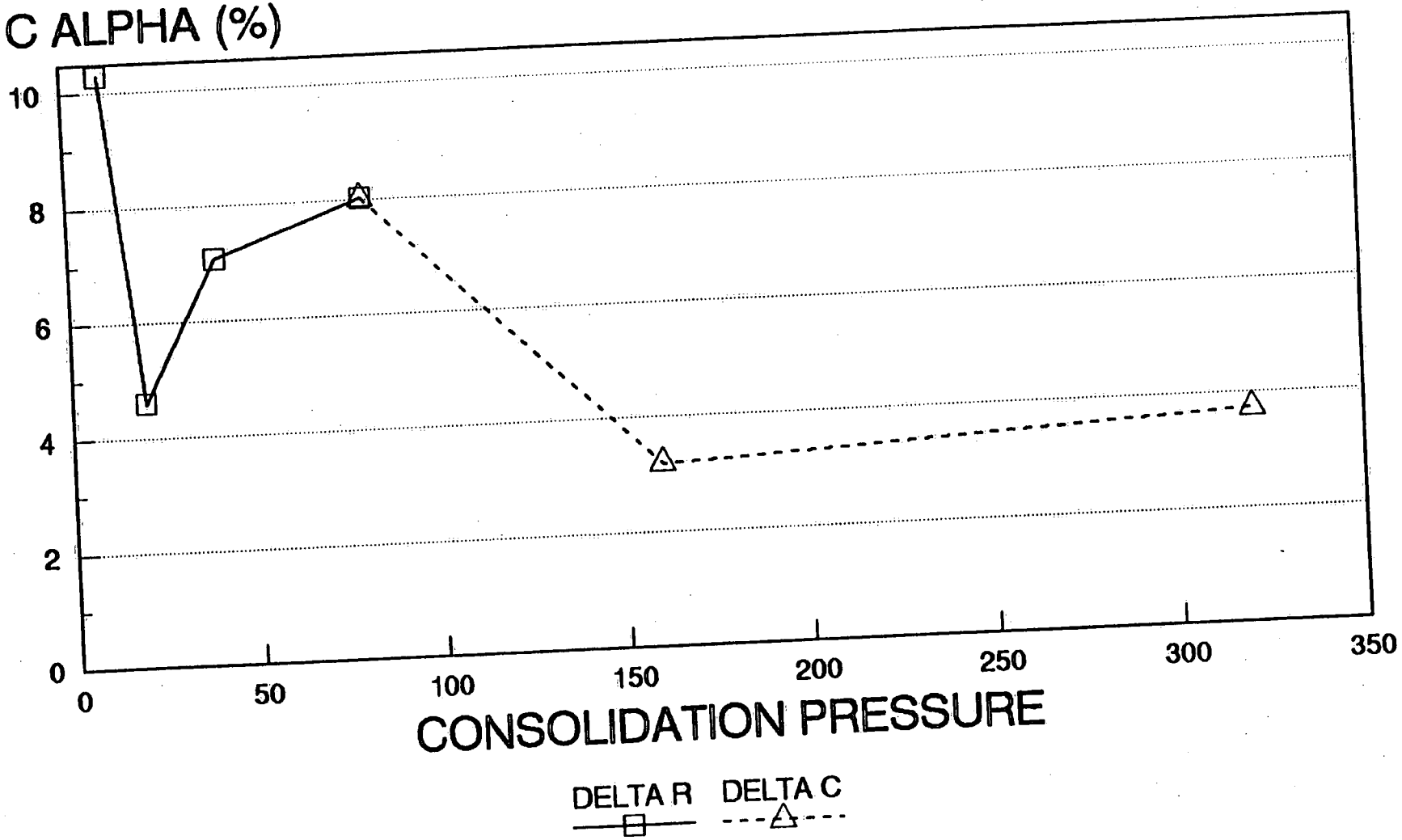

Figure 22d

ROWE CELL CREEP TEST

SAMPLE HH-1-93(C)

APPLIED PRESSURE 5 kPa

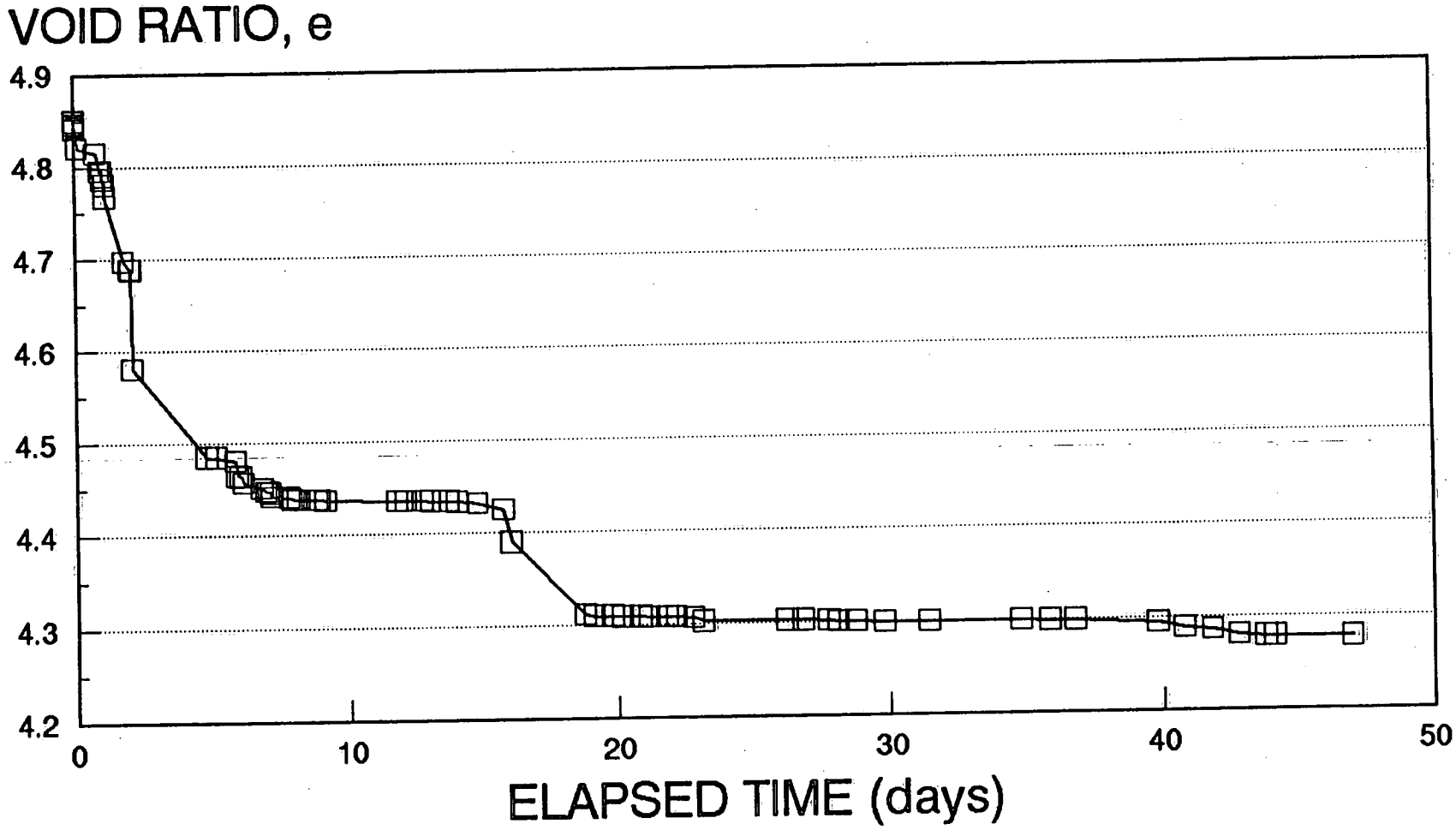

Figure 23a

ROWE CELL CREEP TEST

SAMPLE HH-1-93(C)

APPLIED PRESSURE 5 kPa

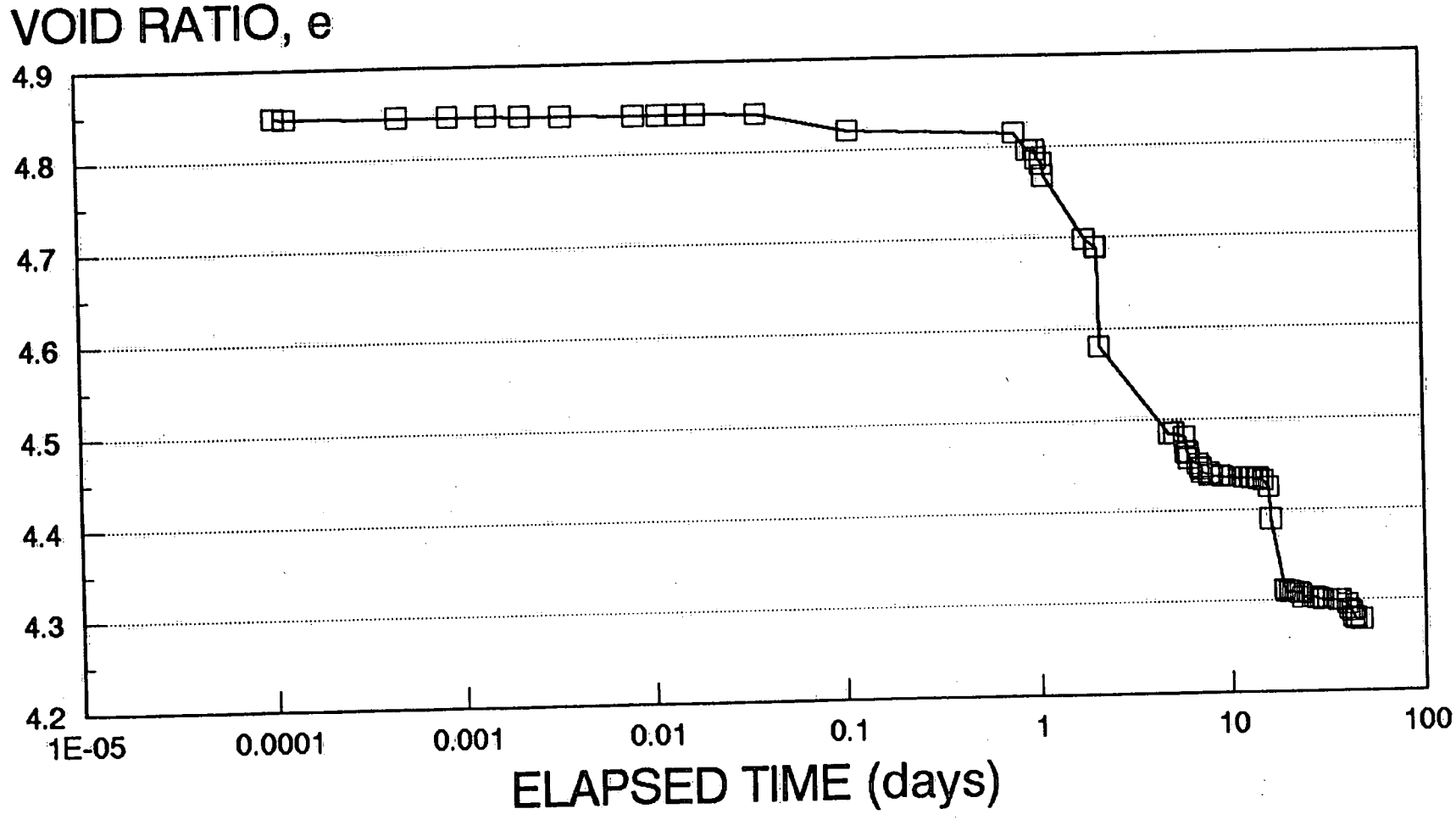

Figure 23b

ROWE CELL CREEP TEST

SAMPLE HH-1-93(C)

APPLIED PRESSURE 10 kPa

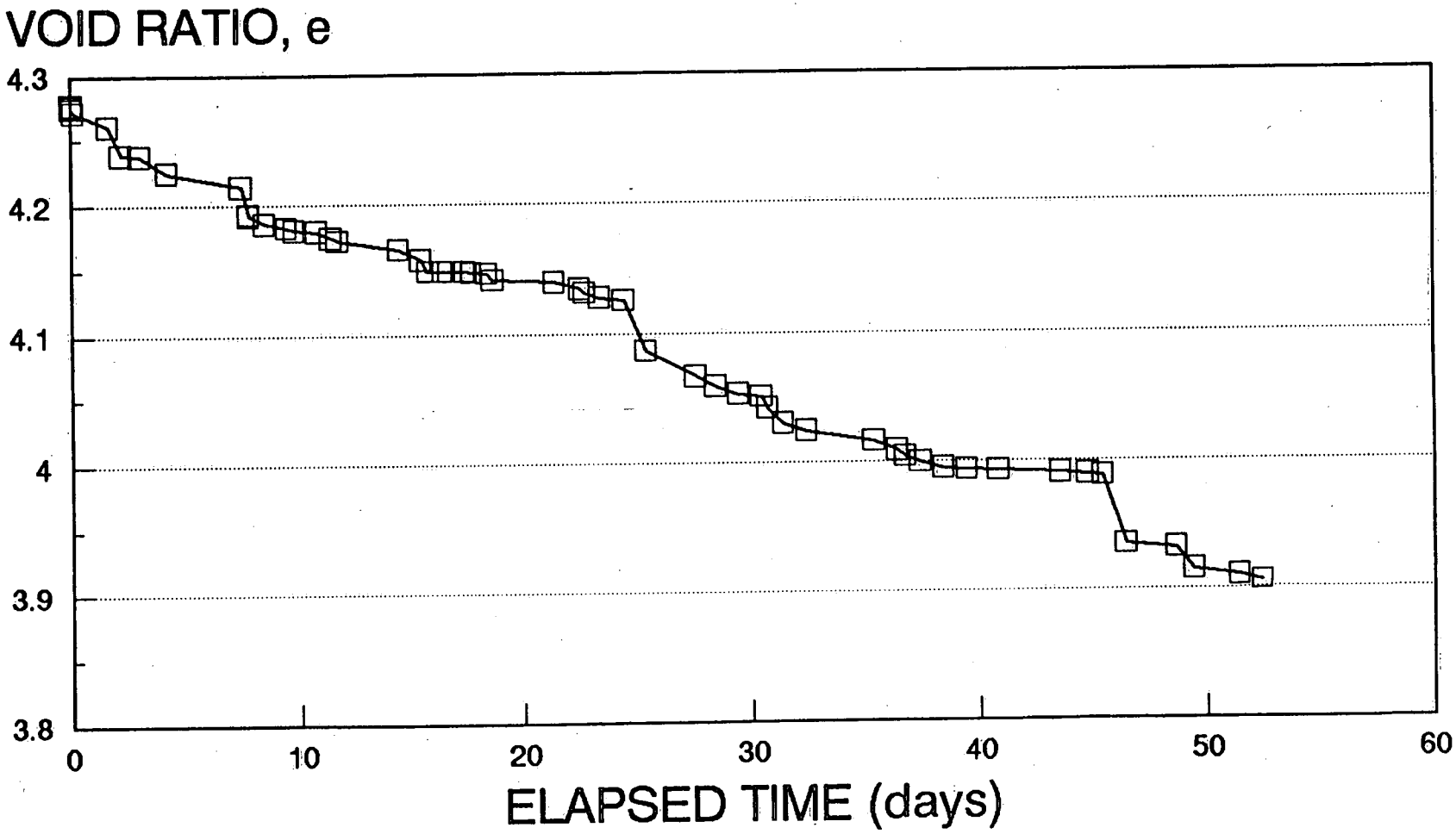

Figure 24a

ROWE CELL CREEP TEST

SAMPLE HH-1-93(C)

APPLIED PRESSURE 5 kPa

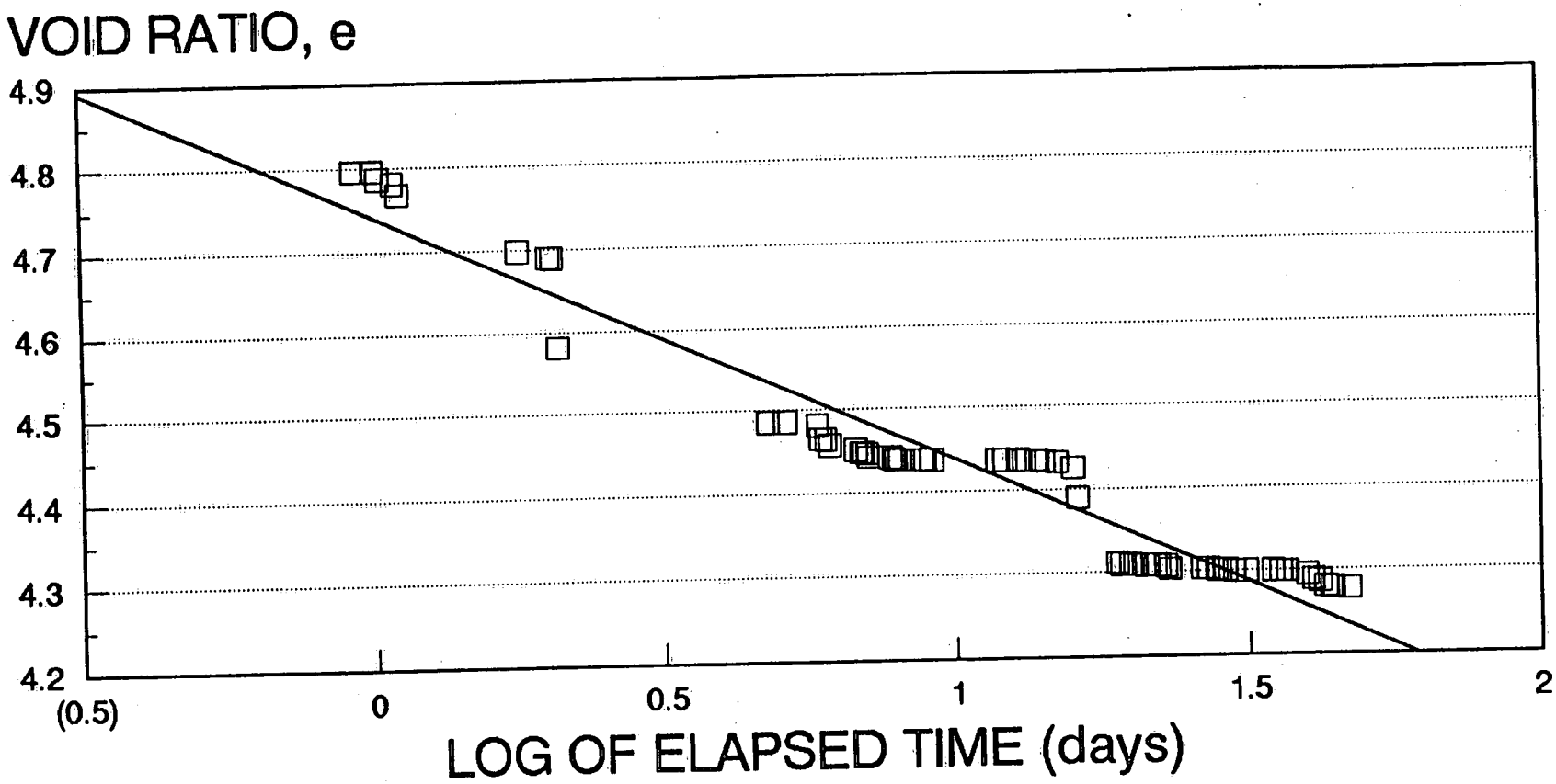

LINEAR REGRESSION:
a = 4.740927; b = -0.302462
r^2 = 0.9426191

Figure 23c

ROWE CELL CREEP TEST

SAMPLE HH-1-93(C)

APPLIED PRESSURE 10 kPa

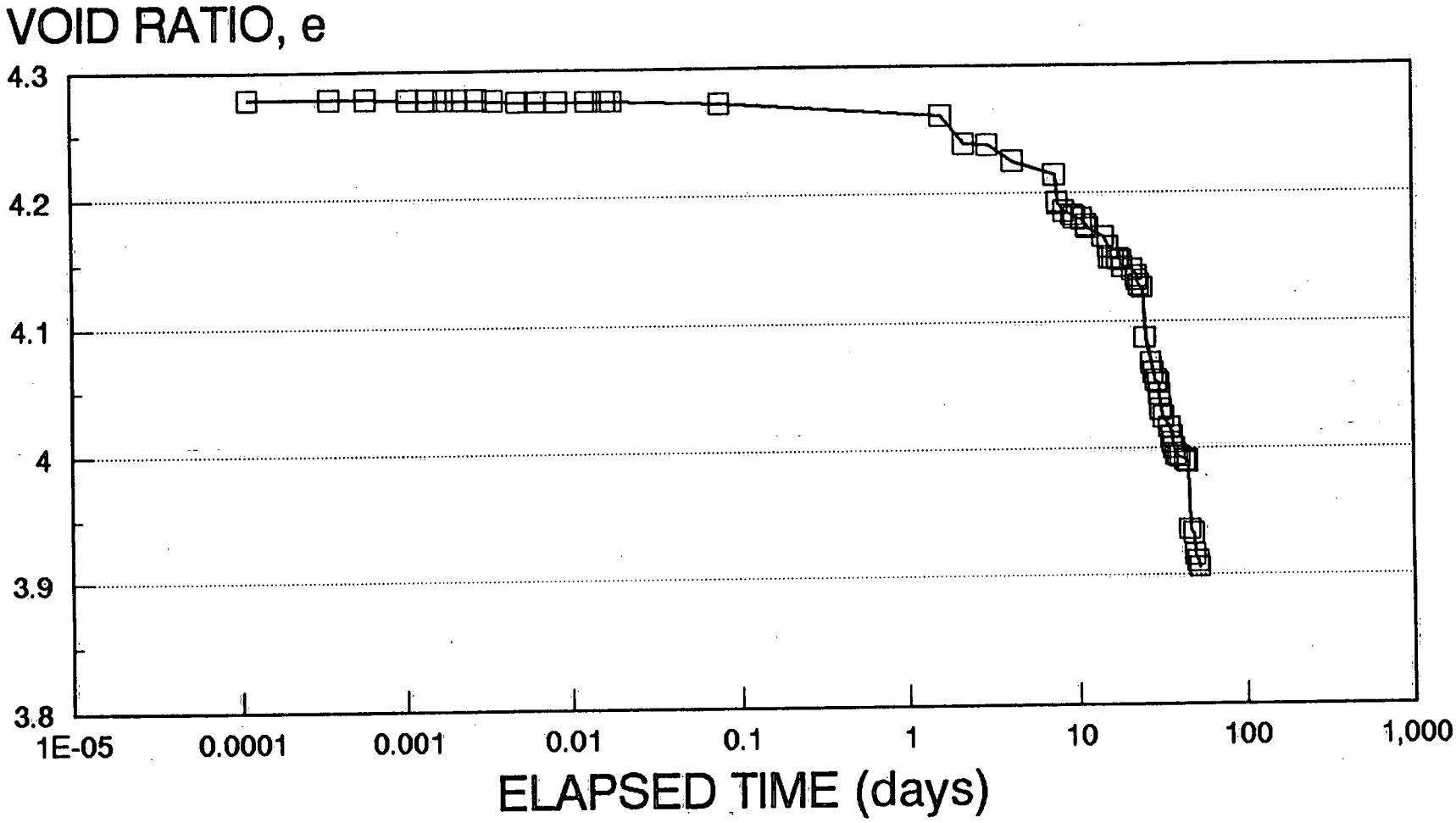

Figure 24b

ROWE CELL CREEP TEST

SAMPLE HH-1-93(C)

APPLIED PRESSURE 10 kPa

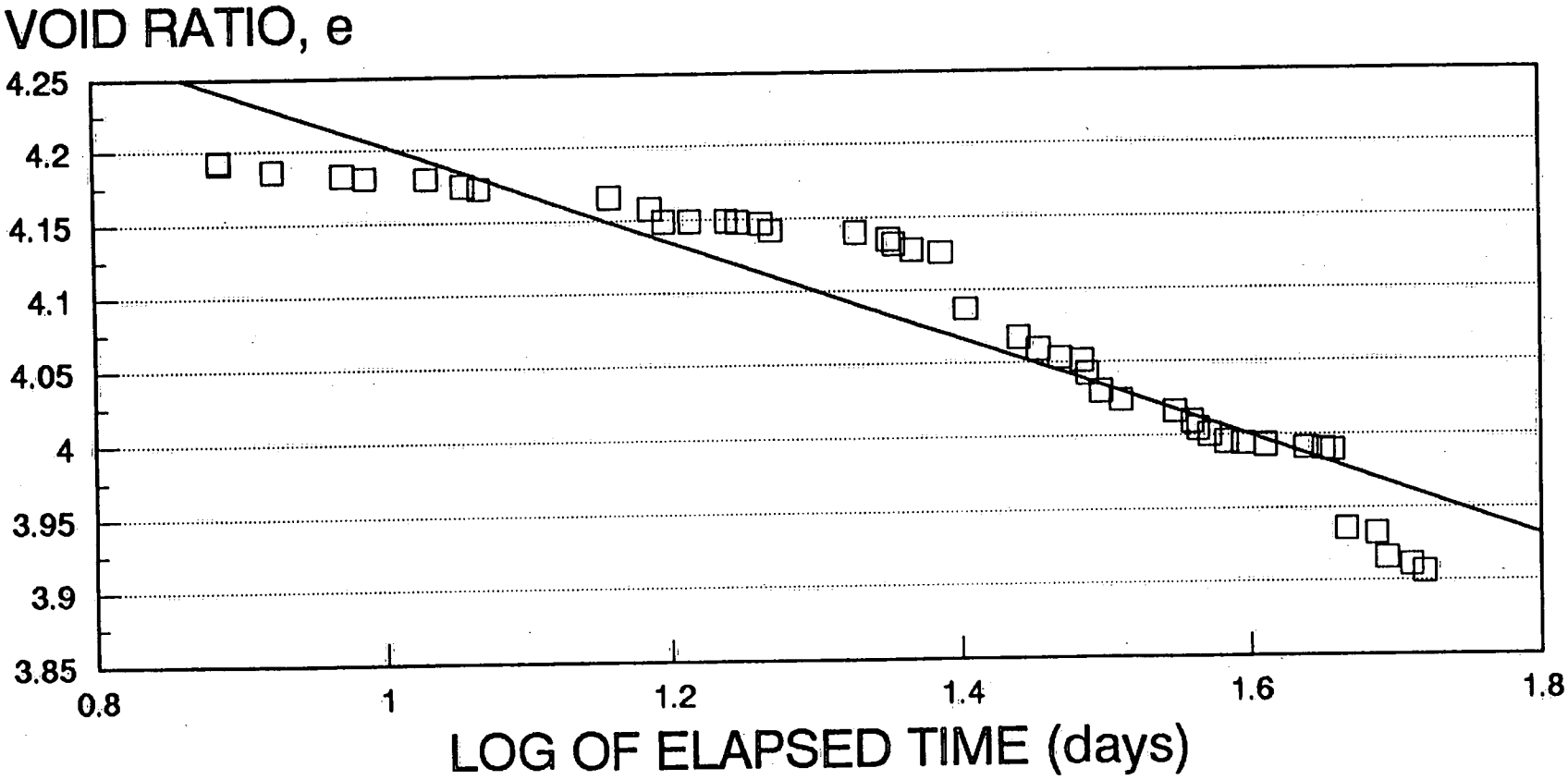

LINEAR REGRESSION:
a = 4.5410317; b = -0.338220
r^2 = 0.8892405

Figure 24C

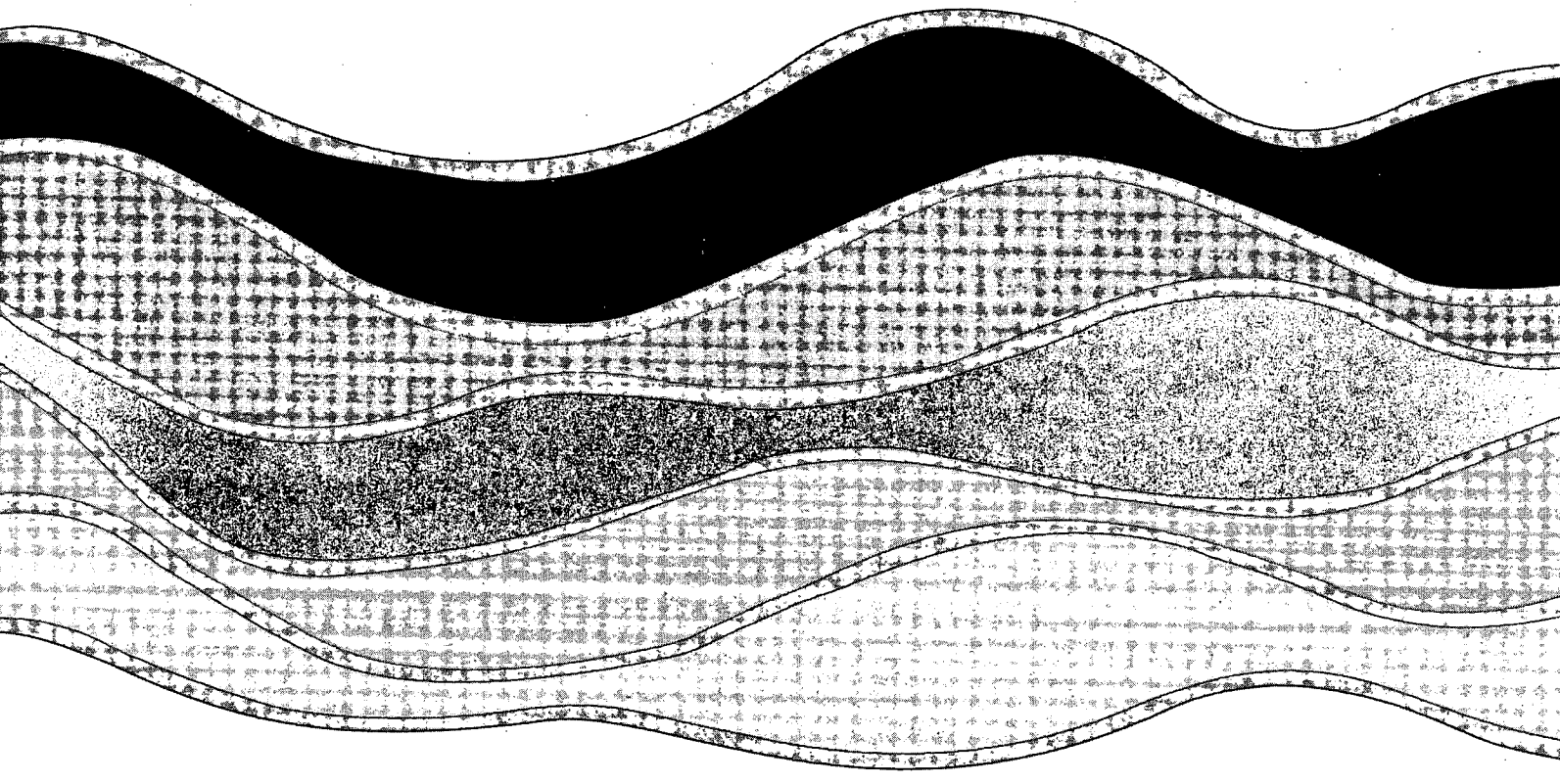

NATIONAL WATER RESEARCH INSTITUTE
P.O. BOX 5050, BURLINGTON, ONTARIO L7R 4A6

Environment Canada Environnement Canada

Canada

INSTITUT NATIONAL DE RECHERCHE SUR LES EAUX
C.P. 5050, BURLINGTON (ONTARIO) L7R 4A6

1st Impression™ Covers Item No. 03532 1/4" for 31 to 60 sheets
Avery Dennison 1-800-DENNISON